

## **INFORMATION TO USERS**

This manuscript has been reproduced from the microfilm master. UMI films the text directly from the original or copy submitted. Thus, some thesis and dissertation copies are in typewriter face, while others may be from any type of computer printer.

**The quality of this reproduction is dependent upon the quality of the copy submitted.** Broken or indistinct print, colored or poor quality illustrations and photographs, print bleedthrough, substandard margins, and improper alignment can adversely affect reproduction.

In the unlikely event that the author did not send UMI a complete manuscript and there are missing pages, these will be noted. Also, if unauthorized copyright material had to be removed, a note will indicate the deletion.

Oversize materials (e.g., maps, drawings, charts) are reproduced by sectioning the original, beginning at the upper left-hand corner and continuing from left to right in equal sections with small overlaps. Each original is also photographed in one exposure and is included in reduced form at the back of the book.

Photographs included in the original manuscript have been reproduced xerographically in this copy. Higher quality 6" x 9" black and white photographic prints are available for any photographs or illustrations appearing in this copy for an additional charge. Contact UMI directly to order.

# **UMI**

A Bell & Howell Information Company  
300 North Zeeb Road, Ann Arbor MI 48106-1346 USA  
313/761-4700 800/521-0600



**University of Alberta**

**Studies of Peroxisome Proliferator-Activated Receptors  
in Transcriptional Processes and Disease**

by

**Pamela Sarita Lagali**



**A thesis submitted to the Faculty of Graduate Studies and Research in partial fulfillment  
of the requirements for the degree of Master of Science**

**Department of Cell Biology and Anatomy**

**Edmonton, Alberta**

**Fall 1998**



National Library  
of Canada

Acquisitions and  
Bibliographic Services

395 Wellington Street  
Ottawa ON K1A 0N4  
Canada

Bibliothèque nationale  
du Canada

Acquisitions et  
services bibliographiques

395, rue Wellington  
Ottawa ON K1A 0N4  
Canada

*Your file* *Votre référence*

*Our file* *Notre référence*

The author has granted a non-exclusive licence allowing the National Library of Canada to reproduce, loan, distribute or sell copies of this thesis in microform, paper or electronic formats.

The author retains ownership of the copyright in this thesis. Neither the thesis nor substantial extracts from it may be printed or otherwise reproduced without the author's permission.

L'auteur a accordé une licence non exclusive permettant à la Bibliothèque nationale du Canada de reproduire, prêter, distribuer ou vendre des copies de cette thèse sous la forme de microfiche/film, de reproduction sur papier ou sur format électronique.

L'auteur conserve la propriété du droit d'auteur qui protège cette thèse. Ni la thèse ni des extraits substantiels de celle-ci ne doivent être imprimés ou autrement reproduits sans son autorisation.

0-612-34386-3

University of Alberta

Faculty of Graduate Studies and Research

The undersigned certify that they have read, and recommend to the Faculty of Graduate Studies and Research for acceptance, a thesis entitled ***Studies of Peroxisome Proliferator-Activated Receptors in Transcriptional Processes and Disease*** submitted by Pamela Sarita Lagali in partial fulfillment of the requirements for the degree of Master of Science.



Dr. Richard A. Rachubinski



Dr. Luis B. Agellon



Dr. Ellen K. Shibuya

Date: August 31, 1998

*"Education is an admirable thing, but it is well to remember from time to time that nothing that is worth knowing can be taught."*

*Oscar Wilde, Intentions (1891)*

## **ABSTRACT**

Peroxisome proliferator-activated receptors (PPARs) are members of the nuclear hormone receptor superfamily of transcription factors that have been implicated in a variety of physiological processes. This thesis explores the action of these regulatory proteins in biological events for which their specificity has been demonstrated. The PPAR $\alpha$  subtype is the primary mediator of the cellular response to environmental and pharmaceutical agents termed peroxisome proliferators. The mechanism by which these compounds induce transcription of peroxisomal enzymes involved in the  $\beta$ -oxidation of fatty acids is examined in Chapter 3. The PPAR $\gamma$  subtype plays a pivotal role in the differentiation of adipose cells. Assessment of PPAR $\gamma$  function in the context of congenital generalized lipodystrophy (CGL), a genetic disorder characterized by a severe absence of body fat, was the objective of the research outlined in Chapter 4. The studies described here assist to further define the modes of action of PPARs in normal biological processes and in disease states.

*For my parents  
Kokila and Sudhakar Lagali  
with much love and gratitude*



## **ACKNOWLEDGEMENTS**

First I would like to acknowledge my supervisor, Dr. Rick Rachubinski, for giving me the opportunity to pursue graduate studies in his laboratory and to work on the projects described in this thesis. I would also like to extend my gratitude to the former and current members of my supervisory committee, Dr. Colin Rasmussen, Dr. Stephen Rice, Dr. Luis Agellon, and Dr. Ellen Shibuya, for their guidance, many helpful discussions, and suggestions throughout the course of my studies.

A big thank you goes out to Eileen Reklow for her assistance with the propagation of cell cultures, especially those difficult 607s, and for sharing everything from technical expertise to benchspace to friendly conversation on a daily basis. Thanks also to the remaining members of the Rachubinski lab, both past and present, who helped to make Edmonton a home-away-from-home after the move from McMaster, who have provided me with instruction in several experimental procedures, and who have been volleyball, soccer, and softball teammates in our never-ending quests for those prized T-shirts: Gary and Kris Eitzen, Sandra Marcus, Chris Winrow, Rachel Szilard, Jennifer Smith, Altaf Kassam, Trevor Brown, Cleofe Hurtado, Vladimir Titorenko, and Melchior Evers.

Appreciation is extended to Dr. Howard Parsons at Alberta Children's Hospital in Calgary, Alberta for providing the CGL fibroblasts, culture protocols, and patient information, and to Dr. Joel Berger at Merck Research Laboratories in Rahway, New Jersey for supplying antibodies, protein samples, and valuable input.

I am indebted to my parents, Kokila and Sudhakar Lagali, and my brother Neil, for their continued love, support, and encouragement at every step along the way. I also couldn't have made it this far without the help of my good friends, Rachel Oates, Haide Razavy, and Jackie Hance. I have enjoyed our many stimulating discussions, academic and otherwise.

Finally, a very special thank you to Miguel Cabrita for his ceaseless patience, encouragement, and friendship, for the invaluable north-end getaways, for countless inspiring scientific exchanges, and for helping me to realize the importance of the journey in reaching a destination.

This work was funded in part by a Province of Alberta Graduate Fellowship and by a studentship from the Alberta Heritage Foundation for Medical Research.

## TABLE OF CONTENTS

Chapter	Page
1. INTRODUCTION	1
1.1 Overview	2
1.2 Peroxisomes	3
1.3 Peroxisomal $\beta$ -oxidation of Fatty Acids	4
1.4 Peroxisome Proliferators	5
1.5 Peroxisome Proliferator-Activated Receptors	7
1.5.1 PPAR $\alpha$	8
1.5.2 PPAR $\delta$	9
1.5.3 PPAR $\gamma$	10
1.6 Peroxisome Proliferator Response Elements	13
1.7 Convergence of Signalling Pathways	14
1.8 Focus of the Thesis	17
2. MATERIALS AND METHODS	20
2.1 Materials	21
2.1.1 Reagents and chemicals	21
2.1.2 Enzymes	23
2.1.3 Molecular size standards	23
2.1.4 Radiochemicals	23
2.1.5 Reagent kits	23
2.1.6 Plasmids	24
2.1.7 Antibodies	24
2.2 Mammalian Cell Culture Studies	24
2.2.1 Propagation of Primary Cultures and Cell Lines	24
2.2.1.1 Primary cultures	24
2.2.1.2 Cell lines	25
2.2.1.3 Passaging cells	25
2.2.1.4 Freezing cell stocks	25
2.2.2 Transient Transfections of BSC40 Cells	26
2.2.2.1 Plasmids	26
2.2.2.2 Transfections and luciferase assays	26
2.2.3 Treatment of Human Fibroblasts with PPAR $\gamma$ Activators	27
2.2.3.1 Preadipocyte differentiation protocol	27
2.2.3.2 Adipogenesis in non-determined fibroblasts protocol	28
2.3 DNA Manipulation	28
2.3.1 Transformation and Growth of Bacterial Cell Cultures	28
2.3.1.1 Transformation by heat shock	28
2.3.1.2 Transformation by electroporation	29
2.3.1.3 Selection and growth of positive transformants	30

2.3.2	Plasmid DNA Isolation	30
2.3.2.1	Small-scale isolation	30
2.3.2.2	Large-scale isolation	31
2.3.3	Genomic DNA Isolation	31
2.3.3.1	DNA isolation from cultured mammalian cells	31
2.3.3.2	DNA isolation from blood samples	32
2.3.4	Quantitation of DNA Samples	32
2.3.5	Agarose Gel Electrophoresis	33
2.3.6	Restriction Endonuclease Digestion	33
2.3.7	Generation of Blunt-Ended DNA for Subcloning	34
2.3.7.1	Blunt-ending restriction endonuclease-digested DNA fragments	34
2.3.7.2	Blunt-ending PCR and RACE products	34
2.3.8	Purification of DNA Fragments	35
2.3.9	Concentration of DNA Samples	35
2.3.10	Subcloning DNA Fragments	35
2.3.10.1	Vectors	35
2.3.10.2	Ligation of complementary cohesive termini	36
2.3.10.3	Ligation of blunt-ended DNA	36
2.3.11	Labelling of DNA Probes	36
2.3.11.1	End-labelling oligonucleotide probes	
2.3.11.2	Random primer labelling of DNA probes	37
2.3.11.3	Purification and quantitation of labelled probes	37
2.3.12	Southern Blot Analysis	37
2.3.12.1	Hybridization with oligonucleotide probes	38
2.3.12.2	Hybridization with DNA fragments as probes	38
2.3.12.3	Hybridization with a $\beta$ -actin control probe	39
2.3.13	Oligonucleotide Synthesis	39
2.3.14	Polymerase Chain Reactions	40
2.3.14.1	Reaction composition and cycling parameters	40
2.3.14.2	Analysis of PCR products	41
2.3.15	DNA Sequencing	41
2.3.15.1	Manual sequencing	41
2.3.15.2	Automated sequencing	42
2.3.15.3	DNA sequence analysis	42
2.4	Library Screening	42
2.4.1	Library Screening by Hybridization	42
2.4.1.1	Plating phage	43
2.4.1.2	Plaque lifts	43
2.4.1.3	Detection of positive phage plaques	43
2.4.1.4	Phage purification	44
2.4.1.5	Harvesting positive phage clones	44
2.4.1.6	DNA isolation from plate lysates	45
2.4.1.7	Analysis of positive phage DNA	45

2.4.2	Library Screening by PCR	45
2.4.2.1	Screening plasmid libraries	45
2.4.2.2	Screening phage libraries	45
2.4.2.3	Screening with single-sided specificity PCR	46
2.5	RNA Manipulation	46
2.5.1	Isolation and Quantitation of Total RNA	46
2.5.2	Isolation of Poly(A) <sup>+</sup> RNA	47
2.5.3	Reverse Transcription - Polymerase Chain Reaction (RT-PCR)	47
2.5.3.1	Preparation of primed templates	47
2.5.3.2	Reverse transcription	48
2.5.3.3	cDNA purification	48
2.5.3.4	PCR amplification of cDNA	49
2.5.4	Rapid Amplification of cDNA Ends (RACE)	49
2.5.4.1	5' RACE	50
2.5.4.2	3' RACE	51
2.5.5	Northern Blot Analysis	51
2.5.5.1	Assessment of RNA transfer efficiency	52
2.5.5.2	Hybridization with radiolabelled DNA probes	52
2.5.5.3	Stripping and reprobing blots	53
2.5.5.4	Quantitative analysis of hybridization signals by densitometry	53
2.5.5.5	Multiple tissue Northern blot	53
2.6	Protein Analysis	54
2.6.1	Preparation of Protein Samples	54
2.6.1.1	Protein extracts of cultured cells	54
2.6.1.2	<i>In vitro</i> transcribed/translated protein samples	54
2.6.2	Quantitation of Protein Samples	54
2.6.3	Concentration of Protein Samples	55
2.6.4	Sodium Dodecyl Sulfate - Polyacrylamide Gel Electrophoresis (SDS-PAGE)	55
2.6.5	Western Blot Analysis	56
2.6.5.1	Transfer of proteins to nitrocellulose	56
2.6.5.2	Immunoblotting	56
2.6.5.3	Stripping and reprobing blots	57
2.6.6	Antibody Production	57
2.6.6.1	Antigen preparation	57
2.6.6.2	Immunization of rabbits	58
2.6.6.3	Serum sampling and analysis	58
3.	PROMOTER ANALYSIS OF THE PEROXISOMAL 3-KETOACYL-CoA THIOLEASE B GENE FOR THE IDENTIFICATION OF A PPRE	63
3.1	Introduction	64
3.2	Results	65
3.2.1	Testing promoter regions 1 kb and 2 kb upstream of the rat thiolase B coding sequence for PPRE activity	65

3.2.2 Attempts to isolate further upstream sequences within the rat thiolase B gene promoter	66
3.3 Discussion	67
4. INVESTIGATING THE INVOLVEMENT OF PPAR $\gamma$ IN CONGENITAL GENERALIZED LIPODYSTROPHY	84
4.1 Introduction	85
4.1.1 Adipogenesis	85
4.1.2 Congenital Generalized Lipodystrophy	88
4.2 Results	90
4.2.1 Clinical Report	90
4.2.2 Cloning of mPPAR $\gamma$ 2 cDNA	90
4.2.3 Detection of an aberrant hPPAR $\gamma$ mRNA species in CGL human fibroblasts	91
4.2.4 Analysis of hPPAR $\gamma$ message levels in normal and CGL human fibroblasts	94
4.2.5 Analysis of hPPAR $\gamma$ protein in normal and CGL fibroblasts by immunoblotting	95
4.2.6 Treatment of normal and CGL primary fibroblasts with PPAR $\gamma$ activators	96
4.2.7 Detection of an aberrant hPPAR $\gamma$ sequence in genomic DNA from the CGL patient and the patient's father	97
4.3 Discussion	98
5. SUMMARY AND CONCLUSIONS	145
6. BIBLIOGRAPHY	149

## LIST OF TABLES

<b>Table</b>		<b>Page</b>
Table 2.1	Properties of antibodies used for immunoblot analyses	60
Table 2.2	Synthetic oligonucleotides used for PCR, RACE, and DNA sequencing	61-62
Table 4.1	Oligonucleotide primer sets used for hPPAR $\gamma$ exon and $\beta$ -actin fragment amplification from genomic DNA samples	140

## LIST OF FIGURES

Figure		Page
Figure 1.1	The peroxisomal straight-chain fatty acid $\beta$ -oxidation pathway	19
Figure 3.1	Partial map of the rat peroxisomal 3-ketoacyl-CoA thiolase B gene promoter region	73
Figure 3.2	Promoter sequences within the 1-kb region found upstream of the rat peroxisomal 3-ketoacyl-CoA thiolase B gene do not confer wy-14,643-responsiveness	75
Figure 3.3	Promoter sequences within the 2-kb region found upstream of the rat peroxisomal 3-ketoacyl-CoA thiolase B gene do not confer wy-14,643-responsiveness	77
Figure 3.4	No distinct rat peroxisomal 3-ketoacyl-CoA thiolase B gene upstream regions are isolated from rat genomic DNA by Southern blotting	79
Figure 3.5	DNA from isolated rat liver genomic library phage clones hybridizes with Probe 1 but not with Probe 2	81
Figure 3.6	No amplification products are obtained in PCRs of DNA from isolated rat liver genomic library phage clones using rat peroxisomal 3-ketoacyl-CoA thiolase B gene upstream region-specific primers	83
Figure 4.1	Interactions among transcription factors in the control of adipocyte differentiation	111
Figure 4.2	Isolation of mPPAR $\gamma$ 2 cDNA from a 14-day mouse whole embryo cDNA library	113
Figure 4.3	An internal fragment of hPPAR $\gamma$ can be amplified from RNA of normal human fibroblasts and CGL fibroblasts	115
Figure 4.4	Nucleotide sequence of the 5' RACE product obtained from RNA of CGL fibroblasts encoding an aberrant form of hPPAR $\gamma$	117
Figure 4.5	Distinct signals corresponding to the unknown 5' sequence of the hybrid RACE product do not appear on Southern blots of human genomic DNA from normal fibroblasts or from blood samples of CGL-associated individuals	119
Figure 4.6	The hybrid RACE product sequence is found in genomic DNA from normal and CGL human fibroblasts	121

<b>Figure 4.7</b>	<b>The unknown 5' sequence of the hybrid RACE product consists of normal hPPAR<math>\gamma</math> intron DNA</b>	<b>123</b>
<b>Figure 4.8</b>	<b>The hybrid RACE product sequence is detected in poly(A)<sup>+</sup> RNA pools from normal and CGL human fibroblasts</b>	<b>125</b>
<b>Figure 4.9</b>	<b>Human PPAR<math>\gamma</math> message is specifically detected in a variety of human tissues using a hPPAR<math>\gamma</math> cDNA fragment probe</b>	<b>127</b>
<b>Figure 4.10</b>	<b>Human PPAR<math>\gamma</math> message is found in normal human fibroblasts while is virtually undetectable in CGL fibroblasts</b>	<b>129</b>
<b>Figure 4.11</b>	<b>Densitometric analysis of hPPAR<math>\gamma</math> mRNA levels in normal and CGL fibroblasts detected by Northern blotting</b>	<b>131</b>
<b>Figure 4.12</b>	<b>Specificity test for rabbit serum containing antibodies raised against a hPPAR<math>\gamma</math> synthetic peptide</b>	<b>133</b>
<b>Figure 4.13</b>	<b>Rabbit polyclonal antibodies raised against a hPPAR<math>\gamma</math>-specific synthetic peptide do not recognize human PPAR<math>\gamma</math> protein</b>	<b>135</b>
<b>Figure 4.14</b>	<b>Detection of hPPAR<math>\gamma</math> protein in extracts of normal human fibroblasts and CGL cells</b>	<b>137</b>
<b>Figure 4.15</b>	<b>Treatment of normal or CGL fibroblasts with PPAR<math>\gamma</math> activators does not induce hPPAR<math>\gamma</math> expression</b>	<b>139</b>
<b>Figure 4.16</b>	<b>PCR amplification of hPPAR<math>\gamma</math> exons from genomic DNA samples</b>	<b>142</b>
<b>Figure 4.17</b>	<b>Amplification of an aberrant hPPAR<math>\gamma</math> exon 2 sequence from genomic DNA of the CGL patient and the patient's father</b>	<b>144</b>



## LIST OF ABBREVIATIONS

A	adenosine
ACS	aqueous counting scintillant
ADD1/SREBP1	adipocyte determination and differentiation factor 1/ sterol response element binding protein 1
AMP	adenosine monophosphate
amp	ampicillin
AOx	fatty acyl-CoA oxidase
aP2	adipocyte P2 fatty acid binding protein
ARF6	adipocyte regulatory factor 6
ATP	adenosine triphosphate
BLAST	basic local alignment search tool
bp	base pair
BSA	bovine serum albumin
bZIP	basic region/leucine zipper
C	cytidine
C/EBP	CAATT/enhancer binding protein
cDNA	complimentary DNA
CDTA	trans-1,2-diaminocyclohexane-N,N,N',N'-tetraacetic acid
CGL	congenital generalized lipodystrophy
CIP	calf intestinal alkaline phosphatase
cm	centimetre
cpm	counts per minute
CPS	carbamoyl phosphate synthetase
°C	degree(s) celcius
15-d-PGJ <sub>2</sub>	15-deoxy- $\Delta^{12,14}$ -prostaglandin J <sub>2</sub>
DCC	dextran-coated charcoal
dATP	deoxyadenosine-5'-triphosphate
dCTP	deoxycytidine-5'-triphosphate
DEPC	diethylpyrocarbonate
DMEM	Dulbecco's Modified Eagles Medium
DMF	N,N-dimethylformamide
DMSO	dimethyl sulfoxide
DNA	deoxyribonucleic acid
dNTPs	deoxyribonucleoside triphosphates
DR	direct repeat
DTT	dithiothreitol
ECL	enhanced chemiluminescence
ECM	extracellular matrix
EDTA	ethylenediaminetetraacetic acid
ER	estrogen receptor
ETYA	5,8,11,14-eicosatetraynoic acid
FAAR	fatty acid-activated receptor
FABP	fatty acid binding protein
FAD	flavin adenine dinucleotide (oxidized)
FADH <sub>2</sub>	flavin adenine dinucleotide (reduced)
G	guanosine
GLUT4	insulin dependent glucose transporter
GR	glucocorticoid receptor

GTG	genetic technology grade
8(S)-HETE	8(S)-hydroxyeicosatetraenoic acid
HD	enoyl-CoA hydratase/3-hydroxyacyl-CoA dehydrogenase
HDL	high density lipoprotein
HEPES	N-2-hydroxyethylpiperazine-N'-2-ethane sulfonic acid
HNF-4	hepatocyte nuclear factor 4
hNUC1	human NUC1
hPPAR	human peroxisome proliferator-activated receptor
HRE	hormone response element
HRP	horseradish peroxidase
HSFB	primary human skin fibroblasts
I	inosine
IMDM	Iscoe's Modified Dulbecco's Medium
in Hg	inches mercury
J	joule
k $\Omega$	kiloohm
kb	kilobase
kDa	kiloDalton
KLH	keyhole limpet hemocyanin
kV	kilovolt
L	litre
LB	Luria-Bertani
LDL	low density lipoprotein
luc	luciferase
LXR	liver X receptor
$\mu$ Ci	microcurie
$\mu$ F	microfarad
$\mu$ g	microgram
$\mu$ L	microlitre
$\mu$ M	micromolar
M	molar
MEM	Minimum Essential Medium
mg	milligram
MIX	methylisobutylxanthine
mL	millilitre
mm	millimetre
mM	millimolar
mmol	millimole
MOPS	morpholino propane sulfonic acid
MPC	magnetic particle concentrator
mPPAR	mouse peroxisome proliferator-activated receptor
mRNA	messenger RNA
N	normal
NAD <sup>+</sup>	nicotinamide adenine dinucleotide (oxidized)
NADH	nicotinamide adenine dinucleotide (reduced)
NCBI	National Center for Biotechnology Information
ng	nanogram
NIDDM	non-insulin dependent diabetes mellitus
nmol	nanomole
NP-40	nonidet P-40

NSAID	non-steroidal anti-inflammatory drug
ob	obese gene
OD	optical density
oxLDL	oxidized low density lipoprotein
PBS	phosphate buffered saline
PCR	polymerase chain reaction
PEG	polyethylene glycol
pfu	plaque-forming units
PI	pre-immune serum
pmol	picomole
PMSF	phenylmethylsulfonyl fluoride
PPAR	peroxisome proliferator-activated receptor
PPRE	peroxisome proliferator response element
R	purine
RACE	rapid amplification of cDNA ends
RAR	retinoic acid receptor
RNA	ribonucleic acid
RNase	ribonuclease
RNasin	ribonuclease inhibitor
RT-PCR	reverse transcription - polymerase chain reaction
RXR	9- <i>cis</i> retinoic acid receptor
RZR/ROR	retinoid Z receptor/retinoid-related orphan receptor
SDS	sodium dodecyl sulfate
SDS-PAGE	sodium dodecyl sulfate - polyacrylamide gel electrophoresis
SSC	sodium chloride, tri-sodium citrate buffer
T	thymidine
TBST	tris-buffered saline + Tween 20
TCA	tricarboxylic acid
T <sub>d</sub>	dissociation temperature
TdT	terminal deoxynucleotidyltransferase
TE	Tris-HCl/EDTA
TEMED	N,N,N',N'-tetramethyl-ethylenediamine
ThB	thiolase B
T <sub>m</sub>	melting temperature
TNF	tumor necrosis factor
TPP	thiolase B promoter probe
Tris	tris(hydroxymethyl)aminomethane
TR	thyroid hormone receptor
TUP	thiolase B upstream primer
U	unit
U	uridine
uv	ultraviolet
v	volume
V	volt
VDR	vitamin D receptor
VLDL	very low density lipoprotein
w	weight
X-gal	5-bromo-4-chloro-3-indolyl-β-D-galactoside
Y	pyrimidine

## **Chapter 1**

### **Introduction**

## 1.1 OVERVIEW

The survival of all species is dependent on the ability to adapt to changes in the requirement for and availability of energy. Efficient regulation of fuel metabolism in response to both internal and environmental stimuli is essential for maintaining overall energy balance. The metabolic processes involved in fuel consumption and storage are controlled by signal relay systems that translate information pertaining to hormonal and nutritional status into rapid cellular responses serving the physiological needs of the organism. Characterization of these signalling pathways is crucial to our understanding of both normal biological function and the mechanisms underlying the development of metabolic disorders.

Regulation of transcription is a common mode of controlling gene expression in response to changing cellular conditions. The ability of different regulatory proteins to recognize specific target genes provides a means for selective modulation of gene expression. Peroxisome proliferator-activated receptors (PPARs) are a class of signal transducing proteins that function as transcription factors in the control of a variety of genes involved in lipid metabolism and homeostasis (reviewed in Lemberger *et al.*, 1996). These regulatory proteins are able to specifically modulate the expression of target genes via binding to sequence-specific DNA elements found in the promoter regions of these genes. The resulting protein-DNA interaction enables contacts to be made with other regulatory proteins and ultimately the basal transcriptional machinery, thereby influencing the initiation of transcription and subsequently the rate of messenger RNA production (reviewed in Torchia *et al.*, 1998).

Since their discovery, PPARs have been implicated in the regulation of an ever-increasing number of genes and biochemical processes. Different PPAR subtypes appear to be specialized for distinct functions, exhibiting differential tissue distribution (Jones *et al.*, 1995; Braissant *et al.*, 1996; Tugwood *et al.*, 1996) and ligand sensitivities (Yu *et al.*, 1995; Forman *et al.*, 1997a; Kliewer *et al.*, 1997), and selectively controlling the transcription of different target genes (Juge-Aubry *et al.*, 1997). This thesis explores the involvement of different PPAR subfamily members, specifically PPAR $\alpha$  and PPAR $\gamma$ , in the processes for which they have been shown to be specialized. The PPAR $\alpha$  subtype is the primary transcription factor mediating the pleiotropic cellular responses to chemical agents termed peroxisome proliferators, including the transcriptional activation of genes encoding the enzymes catalyzing peroxisomal fatty acid  $\beta$ -oxidation (Lee *et al.*,

1995). The PPAR $\gamma$  subtype is believed to be the master regulator of adipose cell differentiation (reviewed in Spiegelman and Flier, 1996, and Spiegelman, 1998). Activating ligands for PPARs include a broad range of compounds such as various natural fatty acids, fatty acid metabolites, and synthetic hypolipidemic drugs (Forman *et al.*, 1997a; Kliewer *et al.*, 1997). Selectivity of these compounds for the individual PPAR subtypes demonstrates a potential mechanism whereby organisms can maintain equilibrium between fatty acid breakdown (through PPAR $\alpha$  activation) and storage (through PPAR $\gamma$  activation).

It is evident that the PPARs play a central role in coordinating several aspects of fuel metabolism and energy homeostasis. Studies such as those described here assist to further delineate the precise molecular actions of these regulatory proteins under varying physiological conditions and in disease states.

## 1.2 PEROXISOMES

Peroxisomes are roughly spherical subcellular organelles bound by a single unit membrane and contain a fine granular matrix as well as a paracrystalline core in some cell types. By definition, they contain at least one oxidase that produces H<sub>2</sub>O<sub>2</sub> and catalase to decompose the H<sub>2</sub>O<sub>2</sub> (de Duve and Baudhuin, 1966). Peroxisomes belong to the microbody family of organelles, along with the glyoxysomes of plants and the glycosomes of Trypanosomes, and are found widely distributed within most eukaryotic cells.

A variety of biochemical processes have been localized to peroxisomes, dependent on the organism and cell type in which they are found. Peroxisomes play an important role in lipid metabolism, with over half of the enzymes identified in peroxisomes participating in catabolic and anabolic processes involving lipids (Reddy and Mannaerts, 1994). They have been implicated in cholesterol synthesis and metabolism (Thompson *et al.*, 1987; Krisans, 1992), bile acid formation (Krisans *et al.*, 1985; Pedersen *et al.*, 1993), plasmalogen biosynthesis (Hajra and Bishop, 1982), methanol oxidation (van der Klei *et al.*, 1991), purine metabolism (Yeldandi *et al.*, 1996), ether lipid synthesis (van den Bosch *et al.*, 1992), the degradation of prostaglandins (Diczfalusy and Alexson, 1988) and leukotrienes (Jedlitschky *et al.*, 1991), and most notably the  $\beta$ -oxidation of fatty acids (Lazarow and de Duve, 1976). The critical importance of peroxisomes for normal development and physiology is illustrated by the

incidence of a myriad of severe human disorders which are characterized by deficient or dysfunctional peroxisomes (Moser, 1993).

### 1.3 PEROXISOMAL $\beta$ -OXIDATION OF FATTY ACIDS

The process of fatty acid  $\beta$ -oxidation within cells is distributed between the mitochondria and the peroxisome. The oxidation of medium-, long-, and very long-chain fatty acids between 10 and 30 carbon atoms in length is localized to peroxisomes, while mitochondria preferentially oxidize short-, medium-, and long-chain fatty acids up to 18 carbon atoms in length (Tolbert, 1981; Mannaerts and Debeer, 1982). The enzymatic reactions involved in the peroxisomal and mitochondrial pathways are similar, however the enzymes themselves are totally distinct with different molecular and catalytic properties, and are encoded by completely different sets of genes that are differentially regulated (Tolbert, 1981; Hashimoto, 1982; Lazarow and Fujiki, 1985). The distribution of these two  $\beta$ -oxidation systems within different organelles enables their differential response to various physiological and biochemical conditions. As such, the peroxisomal pathway has been shown to be inducible, reliant upon high circulating lipid levels or the administration of chemical agents known as peroxisome proliferators (Lazarow and de Duve, 1976; Mannaerts and Debeer, 1982; Osmundsen, 1982), while the mitochondrial system is constitutive and comparatively inert to these compounds (Hashimoto, 1982; reviewed in Osumi and Hashimoto, 1984).

In addition, it has recently been demonstrated that different pathways exist in peroxisomes for the metabolism of straight-chain and branched-chain fatty acids (Mannaerts and Van Veldhoven, 1996; Wanders *et al.*, 1997). The enzymes involved in the two distinct peroxisomal pathways are encoded by different genes and have different substrate specificities (Mannaerts and Van Veldhoven, 1996; Antonenkov *et al.*, 1997). Whether there is a difference between the responsiveness of these two pathways to peroxisome proliferators has yet to be fully examined. However, expression of the prostanoyl-CoA oxidase enzyme catalyzing the first step in 2-methyl-branched fatty acid  $\beta$ -oxidation was shown to be unaffected by the treatment of rats with these compounds (Van Veldhoven *et al.*, 1991).

The sequence of reactions involved in the peroxisomal  $\beta$ -oxidation of straight-chain fatty acids is shown in Figure 1.1.

## 1.4 PEROXISOME PROLIFERATORS

Peroxisome proliferators are a structurally diverse class of chemicals whose members include a broad spectrum of synthetic and naturally occurring compounds, such as herbicides, phthalate ester plasticizers, industrial solvents, several fatty acids and steroids, analgesics, and a number of hypolipidemic drugs used clinically to lower cholesterol and triglyceride levels as a treatment for coronary heart disease (for reviews see Reddy and Lalwani, 1983; Moody *et al.*, 1991). Peroxisome proliferators exhibit very little obvious structural similarity; the only apparent shared chemical features are a lipophilic backbone and a carboxylic acid moiety, conferring upon these compounds the characteristics of amphipathic acids. Exposure of rodents to peroxisome proliferators elicits a number of pleiotropic responses, including a dramatic increase in the size, number, and metabolic capacity of peroxisomes (Lock *et al.*, 1989). As well, a wide range of hepatic changes occur in rats and mice following administration of a variety of these xenobiotics (reviewed in Reddy and Chu, 1996). In addition, the transcription of several genes involved in lipid transport and metabolism are induced, including those encoding liver fatty acid-binding protein (Kaikaus *et al.*, 1993), and the microsomal cytochrome P450IVA family of enzymes involved in the  $\omega$ -hydroxylation of fatty acids (Sharma *et al.*, 1989; Muerhoff *et al.*, 1992). In particular, there is a marked induction of the genes encoding the three enzymes catalyzing the reactions of the peroxisomal straight-chain fatty acid  $\beta$ -oxidation spiral: fatty acyl-CoA oxidase (AOx), enoyl-CoA hydratase/3-hydroxyacyl-CoA dehydrogenase bifunctional enzyme (HD), and 3-ketoacyl-CoA thiolase (Lazarow *et al.*, 1982; Hashimoto, 1982). The coordinated transcriptional induction of these genes results in an increase in corresponding mRNA and enzyme levels (Reddy *et al.*, 1986; Osumi *et al.*, 1990), and in overall peroxisomal  $\beta$ -oxidation activity (Lazarow and de Duve, 1976; Lazarow, 1977). Regulation of mitochondrial fatty acid oxidative enzymes by peroxisome proliferators has also been observed (Gulick *et al.*, 1994; Aoyama *et al.*, 1998).

The phenomenon of peroxisome proliferation has been documented for a variety of species. Rats and mice appear to be the most responsive species, while variable susceptibility to the proliferation of peroxisomes and increases in peroxisomal enzyme activities in response to treatment with hypolipidemic agents has been observed in the livers of cats, dogs, hamsters, chickens, pigeons, and monkeys (Reddy *et al.*, 1984a; Gray and de la Iglesia, 1984). Conflicting evidence exists as to the effects of



peroxisome proliferators in humans. Cultured human liver cells appear to be nonresponsive to these compounds, as demonstrated by a number of studies (Hanefeld *et al.*, 1983; Hertz *et al.*, 1987; Blaaboer *et al.*, 1990). However, analysis of human hepatocytes transplanted into athymic nude mice shows proliferation of peroxisomes in response to proliferator treatment in some studies (Reddy *et al.*, 1984b; Reddy and Chu, 1996), while no effect on the number or enzymatic activity of peroxisomes is observed in other studies (Hertz *et al.*, 1987). Long-term administration of hypolipidemic drugs to patients undergoing treatment for hyperlipidemia does not appear to stimulate peroxisome proliferation (Cameron *et al.*, 1996), however an increase in the number of peroxisomes and the induction of peroxisomal enzymes as a result of human exposure to phthalate ester plasticizers has been reported (Ganning *et al.*, 1984).

It has been widely demonstrated that a number of peroxisome proliferators can induce the development of liver tumors in rodents (Reddy *et al.*, 1976; Reddy *et al.*, 1980; Reddy and Lalwani, 1983; Rao and Reddy, 1987). It is now well established that all of these agents are potentially carcinogenic, with a strong correlation existing between peroxisome proliferation as an early effect in the liver and hepatocarcinogenicity following chronic exposure (Ashby *et al.*, 1994). It is believed that tumorigenesis is most likely induced upon the production of secondary oxidative damage resulting from increased hydrogen peroxide generated by the upregulated  $\beta$ -oxidation pathway. Peroxisome proliferators themselves are nonmutagenic in that they do not bind to and damage DNA directly, as demonstrated in several mutagenesis assays (Warren *et al.*, 1980; Glauert *et al.*, 1984; Gupta *et al.*, 1985). However, induction of chromosomal aberrations apparently independent of significant peroxisome induction has been observed in rat, hamster, and human hepatocytes upon treatment with certain peroxisome proliferators at particular doses, demonstrating the genotoxic potential of these compounds or their metabolites (Hwang *et al.*, 1993; Reisenbichler *et al.*, 1993; Tsutsui *et al.*, 1983).

The detailed mechanism by which peroxisome proliferators bring about the observed cellular responses and induce hepatic tumors is not well understood. Given the widespread use of chemicals classified as peroxisome proliferators, their beneficial effects in the treatment of coronary heart disease, as well as their deleterious effects on liver morphology and in tumorigenesis, it is of great importance to elucidate the molecular mechanisms of action of these agents in order to evaluate their potential health risks to humans.

## 1.5 PEROXISOME PROLIFERATOR-ACTIVATED RECEPTORS

Mediating the peroxisome proliferative response are members of the nuclear hormone receptor superfamily of transcription factors termed peroxisome proliferator-activated receptors (PPARs) (Issemann and Green, 1990). Similar to other members of the superfamily, PPARs are proteins that consist of distinct structural domains to which specific functions have been ascribed (reviewed in Tsai and O'Malley, 1994, and Lemberger *et al.*, 1996). The amino-terminal A/B domain is highly variable among different nuclear receptors and harbors a transactivation function. The DNA-binding C domain displays the greatest sequence conservation among members of the superfamily and consists of two zinc finger motifs that are responsible for DNA recognition and dimerization. The D domain is less conserved, serving as a flexible hinge region connecting domains C and E. The E domain is the largest and most functionally complex of all the modular domains, containing ligand-binding, transactivation, dimerization, nuclear localization, and intermolecular silencing regions. A short carboxy-terminal F domain also exists, for which no specific function has as of yet been identified.

PPARs belong to a subgroup of nuclear hormone receptors to which receptors including those for all-*trans* retinoic acid (RAR), thyroid hormone (TR), and vitamin D<sub>3</sub> (VDR) have been assigned based on the high degree of homology exhibited by their DNA- and ligand-binding domains (Laudet *et al.*, 1992; Laudet, 1997). Members of this subgroup bind to their cognate DNA sequences as heterodimers with isoforms of the receptor for 9-*cis* retinoic acid (RXRs) (reviewed in Glass, 1994).

PPARs represent a subfamily of the nuclear hormone receptor superfamily which are structurally related to one another though are distinct in their patterns of expression, ligand specificities, and physiological actions (reviewed in Lemberger *et al.*, 1996). Initially characterized as mediators of the cellular response to peroxisome proliferators (Issemann and Green, 1990), multiple isoforms of these receptors have been cloned from a number of species and have been demonstrated to participate in a variety of metabolic and physiological processes. Sequence conservation among the members of this receptor subfamily identified to date predicts the existence of three different PPAR subtypes: PPAR $\alpha$ , PPAR $\delta$  (also referred to as PPAR $\beta$ , NUC1, or FAAR), and PPAR $\gamma$ .

All PPARs by definition can be activated by peroxisome proliferators, however individual isoforms exhibit differences in responsiveness to a variety of these chemicals

as well as to certain natural fatty acids and fatty acid metabolites (reviewed in Lemberger *et al.*, 1996). The diversity of compounds that are able to function as PPAR activators initially led to the hypothesis that stimulation of receptor activity occurs through an indirect mechanism rather than as a consequence of direct binding of these agents to PPARs (Issemann and Green, 1990; Göttlicher *et al.*, 1992). Through various *in vitro* binding assays, it has recently been demonstrated that a number of structurally dissimilar peroxisome proliferators, several fatty acids, and metabolites of fatty acids known as eicosanoids are *bona fide* ligands for PPARs (Forman *et al.*, 1997a; Kliewer *et al.*, 1997; Krey *et al.*, 1997). This ability of PPARs to accommodate a wide range of molecular structures as ligands yet exhibit preferences for activation of the individual isoforms is reflected by the divergence observed in the ligand-binding domain among the various PPAR subtypes, and is unique to this subfamily of nuclear hormone receptors (Lemberger *et al.*, 1996). There are some compounds that are capable of inducing transactivation through responsive DNA elements but do not demonstrate an ability to bind any of the PPARs (Krey *et al.*, 1997), suggesting the existence of alternate mechanisms mediating PPAR activation in such instances. These may include conversion of the activator to a natural ligand through metabolic pathways, stimulation of processes that result in production of the endogenous ligand, or post-translational modification and activation of PPARs resulting from the induction of signal transduction cascades.

### 1.5.1 PPAR $\alpha$

PPAR $\alpha$  is the primary mediator of the effects of peroxisome proliferators, as indicated by studies of PPAR $\alpha$ -knockout mice (Lee *et al.*, 1995; Peters *et al.*, 1997; Aoyama *et al.*, 1997). PPAR $\alpha$  is predominantly expressed in liver, kidney, heart, intestine, and brown adipose tissue, consistent with reported sites of peroxisome proliferator-induced changes and the high rates of fatty acid oxidation characteristic of these tissues (Kliewer *et al.*, 1994; Braissant *et al.*, 1996; Reddy and Chu, 1996). In addition, several constitutive metabolic processes are controlled by this PPAR subtype, including lipoprotein metabolism (Peters *et al.*, 1997) and mitochondrial fatty acid catabolism (Aoyama *et al.*, 1998). PPAR $\alpha$  is involved in modulation of the entire oxidative pathway at several levels, including uptake, activation, and oxidation of fatty acids in peroxisomes, microsomes, and mitochondria, as well as in ketogenesis (reviewed in Lemberger *et al.*, 1996). The identification of a growing number of both

peroxisomal and non-peroxisomal target genes involved in lipolytic pathways demonstrates the fundamental role of PPAR $\alpha$  in maintaining lipid homeostasis.

The hypolipidemic drugs wy-14,643 and 5,8,11,14-eicosatetraenoic acid (ETYA), a synthetic arachidonic acid analog, are peroxisome proliferators that have been shown to bind directly to PPAR $\alpha$  (Devchand *et al.*, 1996; Krey *et al.*, 1997). A recent study of AOX null mice indicates that acyl-CoA molecules and other natural substrates of AOX serve as the biological ligands for PPAR $\alpha$  that mediate spontaneous peroxisome proliferation, induction of PPAR $\alpha$ -regulated genes, and hepatocarcinogenesis *in vivo* (Fan *et al.*, 1998). The naturally occurring proinflammatory eicosanoids leukotriene B<sub>4</sub> and 8(S)-hydroxyeicosatetraenoic acid (8(S)-HETE) have also been identified as high-affinity PPAR $\alpha$  ligands (Devchand *et al.*, 1996; Forman *et al.*, 1997a; Kliewer *et al.*, 1997; Krey *et al.*, 1997), and additional activators of this receptor include several non-steroidal anti-inflammatory drugs (NSAIDs) (Lehmann *et al.*, 1997a), thereby implicating this receptor in the control of immune responses. This is consistent with reports of PPAR $\alpha$  expression in tissues of the immune system (Braissant *et al.*, 1996). Evidence for the involvement of the PPAR $\alpha$  subtype in adipogenesis (Brun *et al.*, 1996) and in the suppression of apoptosis (Roberts *et al.*, 1998) has also been documented.

### 1.5.2 PPAR $\delta$

At present, the precise function of the PPAR $\delta$  subtype is not known, however information on its tissue distribution, ligand specificity, and distinction from other PPARs provides clues as to its biological significance.

In contrast to the other subtypes, PPAR $\delta$  expression is abundant and widespread in both embryonic and adult tissues, possibly reflecting a general "housekeeping" role during development and in different organs (Kliewer *et al.*, 1994; Braissant *et al.*, 1996; Braissant and Wahli, 1998). Prominent expression of PPAR $\delta$  has been detected in a variety of regions of the brain and in different cell types found in the central nervous system, while the other PPAR subtypes are present in much lower abundance within these tissues (Xing *et al.*, 1995; Cullingford *et al.*, 1998). Recent studies show specific expression of the PPAR $\delta$  subtype in immature oligodendrocytes and an increase in oligodendrocyte number upon treatment with PPAR activators, suggesting a role for this PPAR subfamily member in neural cell differentiation (Granneman *et al.*, 1998).

It has also been observed that mPPAR $\delta$  and hNUC1 isoforms are able to act as dominant negative repressors of PPAR $\alpha$ -mediated responsiveness to peroxisome proliferators (Kliwer *et al.*, 1994; Jow and Mukherjee, 1995). Repression by hNUC1 was observed to occur through sequestration of a limiting factor required for PPAR $\alpha$  function (Jow and Mukherjee, 1995). These findings suggest that regulation of the activity of PPAR $\alpha$  may be a role for the PPAR $\delta$  isoform in tissues where both receptors are expressed. The observation that PPAR $\alpha$  and PPAR $\delta$  possess overlapping ligand specificities (Forman *et al.*, 1997a; Krey *et al.*, 1997) indicates their involvement in similar physiological processes. As for the PPAR $\alpha$  subtype (Bogazzi *et al.*, 1994; Juge-Aubry *et al.*, 1995), inhibition of ligand-dependent activation of the thyroid hormone receptor, TR, has also been demonstrated for PPAR $\delta$ , implicating it in the regulation of multiple metabolic pathways (Jow and Mukherjee, 1995).

### 1.5.3 PPAR $\gamma$

Two isoforms of PPAR $\gamma$  have been cloned from a variety of species, and are designated PPAR $\gamma$ 1 and PPAR $\gamma$ 2 (Zhu *et al.*, 1993; Tontonoz *et al.*, 1994a; Greene *et al.*, 1995; Elbrecht *et al.*, 1996; Sundvold *et al.*, 1997). Analysis of the structural organization of the mouse and human PPAR $\gamma$  genes indicates that the two isoforms are derived from alternative promoter usage and differential splicing of a single gene (Zhu *et al.*, 1995; Fajas *et al.*, 1997). The PPAR $\gamma$ 2 transcript encodes an additional 30 amino acids (28 amino acids for hPPAR $\gamma$ 2) amino-terminal to the start codon of PPAR $\gamma$ 1, and each isoform has a different 5' untranslated sequence. The remainder of the coding region for the two PPAR $\gamma$  isoforms is identical. Recently, the existence of a third PPAR $\gamma$ , designated PPAR $\gamma$ 3, has been reported (Fajas *et al.*, 1998; Ricote *et al.*, 1998b). This newly identified species is transcribed from a different promoter of the PPAR $\gamma$  gene than those directing expression of PPAR $\gamma$ 1 and PPAR $\gamma$ 2 transcripts, and encodes a protein identical to PPAR $\gamma$ 1 (Fajas *et al.*, 1998; Ricote *et al.*, 1998b). Determination of whether distinct or overlapping functions are attributed to PPAR $\gamma$ 3 *vis à vis* the other two PPAR $\gamma$  isoforms awaits its cloning and further characterization.

The tissue-specific expression of the extensively studied PPAR $\gamma$  isoforms is indicative of the functions that have been ascribed to this PPAR family member. Abundant and restricted expression of PPAR $\gamma$ 2 in adipose tissue is in accordance with the finding that this transcription factor plays a pivotal role in adipogenesis (Tontonoz *et*

*et al.*, 1994a-c; Fajas *et al.*, 1997; Vidal-Puig *et al.*, 1997). Several studies have now established PPAR $\gamma$  as a central regulator of fat cell differentiation (reviewed in Fajas *et al.*, 1998, and Spiegelman, 1998). The more widely expressed PPAR $\gamma$ 1 isoform, particularly in human tissues, suggests additional biological roles for this nuclear hormone receptor (Tugwood *et al.*, 1996; Fajas *et al.*, 1997). The discovery of a variety of ligands for the PPAR $\gamma$  subtype also indicates its involvement in a number of physiological processes.

The stimulatory effect of PPAR $\gamma$  on adipose tissue development naturally led to the hypothesis that the activity of this receptor may contribute to the progression of obesity. Indeed, an elevation in PPAR $\gamma$  expression is observed in several rodent models of obesity (Vidal-Puig *et al.*, 1996; Hallakou *et al.*, 1997) and in obese patients (Park *et al.*, 1997). In addition, expression of the obese (*ob*) gene product, leptin, a hormone secreted by adipose cells that reduces food intake, increases energy expenditure, and induces weight loss (Halaas *et al.*, 1995; Pelleymounter *et al.*, 1995), is downregulated upon PPAR $\gamma$  activation (Kallen and Lazar, 1996; De Vos *et al.*, 1996; Hollenberg *et al.*, 1997). Signalling through this transcription factor therefore influences the regulation of body weight and potentially the etiology of energy balance disorders.

The first demonstration of a high affinity ligand for members of the PPAR orphan receptor family was observed in the discovery of selective activation of both PPAR $\gamma$  isoforms as a result of direct binding to thiazolidinediones, a class of antidiabetic agents known to promote adipocyte differentiation (Lehmann *et al.*, 1995). Binding of these compounds to PPAR $\gamma$  and the resultant effect on transcriptional induction correlate with their antidiabetic activities in insulin-resistant mice (Berger *et al.*, 1996). Moreover, PPAR $\gamma$  expression has been detected in skeletal muscle and liver (Vidal-Puig *et al.*, 1997; Mukherjee *et al.*, 1997; Park *et al.*, 1997; Kruszynska *et al.*, 1998), the major sites of insulin-stimulated glucose uptake, and tissues in which the effects of thiazolidinediones have been described (Hofman *et al.*, 1991; Kobayashi *et al.*, 1992; Hofman *et al.*, 1992). These findings implicate this receptor in the regulation of systemic insulin sensitivity and possibly the pathogenesis of non-insulin dependent diabetes mellitus (NIDDM) (reviewed in Spiegelman, 1998).

Direct binding of several hypolipidemic drugs to PPAR $\gamma$  has been demonstrated, as has been observed for the other PPAR subtypes, consistent with the role of this

nuclear receptor subfamily in regulating the transcription of enzymes involved in lipid metabolism and clearance (Kliwer *et al.*, 1997; Krey *et al.*, 1997).

Expression of PPAR $\gamma$  in the spleen, particularly in lymphocyte proliferating centers, as well as in bone marrow, suggests that this PPAR subtype, like PPAR $\alpha$ , may be biologically functional in the immune system (Greene *et al.*, 1995; Gimble *et al.*, 1996; Braissant *et al.*, 1996; Elbrecht *et al.*, 1996). PPAR $\gamma$  levels are higher in activated macrophages compared to resting macrophages, and this transcription factor downregulates several genes associated with inflammation, providing a mechanism to control the magnitude and duration of inflammatory responses (Ricote *et al.*, 1998a). Inflammatory cytokine production is also inhibited by PPAR $\gamma$  activation in monocytes, providing another means by which immune responses can be suppressed through the action of this receptor (Jiang *et al.*, 1998). These observations, coupled with the identification of a number of NSAIDs as PPAR $\gamma$  agonists, explain the likely mode of action of such drugs in the treatment of conditions such as rheumatoid arthritis (Lehmann *et al.*, 1997a).

In addition to synthetic pharmaceuticals, a variety of naturally occurring compounds have been designated as PPAR $\gamma$  ligands, including the prostaglandin metabolite, 15-deoxy- $\Delta^{12,14}$ -PGJ<sub>2</sub> (15-d-PGJ<sub>2</sub>), and different fatty acids (Forman *et al.*, 1995; Kliwer *et al.*, 1995; Krey *et al.*, 1997). These biological molecules have similar effects on PPAR $\gamma$  activation and corresponding downstream events as those described for the aforementioned therapeutic drugs.

PPAR $\gamma$  has also been implicated in a signalling pathway regulating the conversion of monocytes to specialized cholesterol-laden macrophages termed foam cells, whose aggregation leads to the formation of atherosclerotic plaques (Tontonoz *et al.*, 1998; Nagy *et al.*, 1998; Ricote *et al.*, 1998b). The differentiation process is stimulated by exposure of monocytes to oxidized low density lipoproteins (oxLDL) and involves the activation of specific sets of genes, uptake of the oxLDL particles, and changes in lipid metabolism (reviewed in Steinberg *et al.*, 1989). OxLDL lipid components themselves are PPAR $\gamma$  ligands and function to regulate foam cell gene expression through this receptor (Nagy *et al.*, 1998). These findings link PPAR $\gamma$  expression and activity in myelomonocytic cells to the pathogenesis of coronary artery disease.

Evidence also exists for the association of this PPAR subtype with different types of human cancers. Significant levels of PPAR $\gamma$  have been detected in colonic tissue (Mansén *et al.*, 1996; Fajas *et al.*, 1997; Auboeuf *et al.*, 1997), and a recent study reports elevated expression of this receptor in colon cancer (DuBois *et al.*, 1998). PPAR $\gamma$  expression has also been observed in normal human breast tissue as well as in most human metastatic breast tumors (Mueller *et al.*, 1998). Upon ligand administration, control of breast epithelial gene expression by PPAR $\gamma$  was shown to result in the acquisition by breast cancer cells of a less malignant, terminally differentiated state (Mueller *et al.*, 1998). Similar levels of PPAR $\gamma$  expression and antineoplastic effects following its activation have been shown in human liposarcoma cells (Tontonoz *et al.*, 1997).

Clearly, the PPAR $\gamma$  isoforms are involved in transcriptional processes governing various biological phenomena in both the normal state and in the development of diseases for which drugs that target tissue-selective PPAR $\gamma$  activity would offer potential therapeutic benefits.

## 1.6 PEROXISOME PROLIFERATOR RESPONSE ELEMENTS

Nuclear hormone receptor transcription factors function by interacting with specific *cis*-acting DNA elements located upstream of hormone-responsive genes, ultimately leading to the transactivation of these genes (reviewed in Tsai and O'Malley, 1994). The *cis*-acting regulatory elements for a number of peroxisome proliferator-responsive genes have been identified and are termed peroxisome proliferator response elements (PPREs). Target genes include those encoding peroxisomal fatty acid  $\beta$ -oxidation enzymes such as acyl-CoA synthetase (Schoonjans *et al.*, 1995), AOx (Osumi *et al.*, 1991; Tugwood *et al.*, 1992; Varanasi *et al.*, 1996), and HD (Zhang *et al.*, 1992; Bardot *et al.*, 1993; Chu *et al.*, 1995a), the microsomal  $\omega$ -oxidation enzymes CYP4A1 (Aldridge *et al.*, 1995) and CYP4A6 (Muerhoff *et al.*, 1992) of the cytochrome P450IV family, fatty acid binding proteins aP2 (Tontonoz *et al.*, 1994a,b) and FABP (Isseemann *et al.*, 1992), lipoprotein lipase (Schoonjans *et al.*, 1996), phosphoenolpyruvate carboxykinase (Tontonoz *et al.*, 1995), as well as other genes involved in energy metabolism and homeostasis. Similar to hormone response elements (HREs), they exhibit enhancer-like properties in that they function independent of orientation or position, they can confer peroxisome proliferator responsiveness onto normally



unresponsive promoters, and multimerization leads to additive transcriptional induction effects.

The subgroup of nuclear hormone receptors that heterodimerize with RXRs, of which PPARs are members, typically bind to DNA elements containing multiple copies of the nuclear hormone receptor consensus binding half-site, AGGTCA, or degenerate sequences thereof, arranged in a direct repeat array and separated by variable nucleotide spacing (reviewed in Glass, 1994). DRn notation is used to specify the arrangement (DR, direct repeats) and spacing (n nucleotides) of half-sites that comprise responsive elements. Spacing, arrangement, orientation, and core sequence of the half-site recognition motifs afford specificity of nuclear hormone receptor binding to response elements. PPAR/RXR heterodimers bind preferentially to DR1 elements (Kliwer *et al.*, 1992), while other receptors within the subgroup recognize binding sites with DR3 (VDR), DR4 (TR), and DR5 (RAR) configurations (Umesono *et al.*, 1991). Recent studies have also demonstrated that 5' flanking sequences of consensus elements are important for maintaining the conformation of the receptor/DNA complex (Palmer *et al.*, 1995), distinguishing between different RXR heterodimers (Ijpenberg *et al.*, 1997), and for determining the specificity of PPAR subtype binding to various natural PPREs (Juge-Aubry *et al.*, 1997). A preference for A-T as the spacer nucleotide in the DR1 elements comprising PPREs has also been demonstrated (Ijpenberg *et al.*, 1997), extending the consensus sequence of these response elements to 5'-AACT AGGTCA A AGGTCA-3'. The particular promoter context of the response element also determines the transcriptional response observed owing to the presence of binding sites for additional stimulatory or repressive factors (Nakshatri and Bhat-Nakshatri, 1998).

## 1.7 CONVERGENCE OF SIGNALLING PATHWAYS

The conservation of domain structure and function among the various nuclear hormone receptors suggests the existence of overlapping substrate specificities. This in turn would facilitate interactions to occur between various hormone signalling pathways. Indeed, the highly homologous DNA-binding domains and dimerization interfaces of members of this transcription factor superfamily enable the convergence of signals at several levels involving protein-protein and protein-DNA interactions.

The identification of the 9-*cis* retinoic acid receptor, RXR, as an obligatory heterodimerization partner for several nuclear hormone receptors to produce effective and maximal hormonal responses establishes this receptor as a master regulator of

multiple hormone signalling pathways (reviewed in Mangelsdorf and Evans, 1995). The absolute dependence of PPARs on heterodimerization with RXR subfamily members ( $\alpha$ ,  $\beta$ ,  $\gamma$ ) for binding to and transactivation through PPREs indicates that the peroxisome proliferator and retinoid signalling pathways converge through the direct interaction of their respective nuclear receptors (Kliwer *et al.*, 1992; Gearing *et al.*, 1993; Miyata *et al.*, 1994).

A number of other nuclear hormone receptors have also been shown to impinge on transcriptional activation mediated by PPARs, suggesting that the pleiotropic effects induced by peroxisome proliferators and natural PPAR activators are the result of the integrated action of several regulatory proteins.

Cross-talk between the thyroid hormone and peroxisome proliferator signalling pathways has been demonstrated by a number of studies assessing the effects of PPAR on thyroid hormone receptor (TR)-mediated transactivation and conversely the role of TR in regulating PPAR activity. Functional interaction between these two nuclear receptors is expected, since peroxisome proliferators and thyroid hormones have overlapping metabolic effects and regulate a similar subset of genes involved in lipid metabolism, cell growth, and differentiation (Hertz *et al.*, 1993; Gharbi-Chihi *et al.*, 1993; Oda *et al.*, 1997). PPAR has been shown to behave as a dominant negative regulator of thyroid hormone action due to the combined effects of direct binding to and therefore sequestration of TR into inactive heterodimers (Bogazzi *et al.*, 1994), competition for the common heterodimeric partner RXR (Meier-Heusler *et al.*, 1995; Juge-Aubry *et al.*, 1995; Chu *et al.*, 1995b) and likely other TR-auxiliary proteins (Juge-Aubry *et al.*, 1995), and inhibitory binding to certain thyroid hormone response elements (Chu *et al.*, 1995b). Through similar mechanisms of inhibition, TR has been observed to interfere with peroxisome proliferator-induced transcriptional activation (Chu *et al.*, 1995b; Hunter *et al.*, 1996; Miyamoto *et al.*, 1997).

LXR, a constitutively active nuclear hormone receptor regulated by products of mevalonate metabolism (Lehmann *et al.*, 1997b; Forman *et al.*, 1997b) inhibits signalling through PPAR in a manner similar to that displayed by TR. Mutual antagonism between PPAR and LXR occurs as a consequence of direct binding of the two receptors, thereby forming transcriptionally inactive heterodimers, and also likely through sequestration of the common activating dimerization partner, RXR (Miyata *et al.*, 1996). These findings indicate a convergence in the control of both lipid and cholesterol homeostasis.

Evidence for signalling cross-talk between PPARs and the steroid hormone receptor for glucocorticoids (GR) as well as that for estrogen (ER) has also been reported (Lemberger *et al.*, 1994; Keller *et al.*, 1995).

Modulation of PPAR activity has also been demonstrated for orphan members of the nuclear hormone receptor superfamily, for which ligands have not as yet been identified. The chicken ovalbumin upstream promoter-transcription factors (COUP-TFs) have been shown to antagonize peroxisome proliferator-mediated signalling and thus negatively regulate target genes (Miyata *et al.*, 1993; Marcus *et al.*, 1996). Hepatocyte nuclear factor-4 (HNF-4) has differential effects on transcription of peroxisome proliferator-responsive genes under the control of PPREs, for example having a repressive effect on the AOx PPRE and an inductive effect on the HD PPRE (Winrow *et al.*, 1994). The retinoid Z receptor (RZR, also known as ROR $\alpha$ ) is another orphan receptor that is able to differentially regulate PPRE-containing promoters, potentiating transcription of the HD gene while having no effect on the AOx PPRE (Winrow *et al.*, 1998). In a recent study, the nuclear orphan receptor TAK1 (also known as TR4) was shown to repress PPAR-mediated transactivation through the PPREs for both AOx and HD by mechanisms involving competition for DNA- and transcriptional co-activator-binding (Yan *et al.*, 1998).

Furthermore, numerous transcriptional co-activator and co-repressor proteins have been identified that promiscuously interact with nuclear hormone receptors (reviewed in Horwitz *et al.*, 1996, and Torchia *et al.*, 1998). These intermediary co-regulatory proteins play essential roles in mediating the transcriptional effects of nuclear receptors by functioning as chromatin remodelling factors and/or by making contacts with components of the basal transcriptional machinery. Co-activators and co-repressors are themselves likely subject to regulation by diverse signal transduction pathways.

Thus it appears that gene regulation by PPARs is the result of an overall transcriptional response achieved through a dynamic balance among several positive and negative regulators of PPAR activity. Co-expression of several different nuclear receptors along with PPARs provides the basis for establishing a complex hormone-signalling network within cells to control both normal lipid homeostasis and the phenomenon of peroxisome proliferation.

## 1.8 FOCUS OF THE THESIS

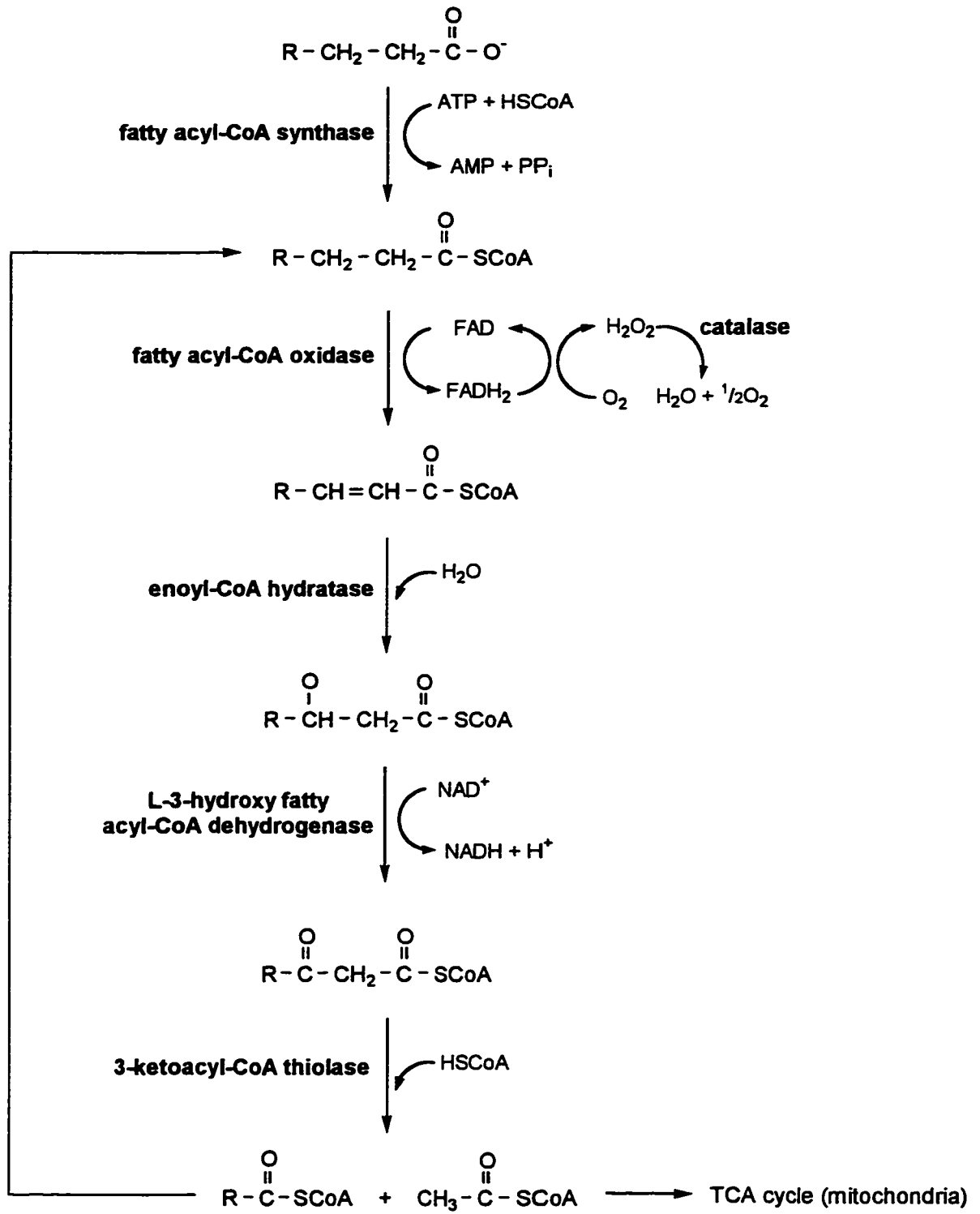
The multiple actions of PPARs within various cell types are currently the focus of intense study. The diverse biological processes in which these proteins function and their association with the pathogenesis of several human diseases has provided the basis for the heightened interest in elucidating their detailed mechanisms of action. Such research holds the promise of leading to the development of therapeutic agents that target PPAR activity to either enhance or repress specific transcriptional events implicated in distinct signalling pathways.

Peroxisome proliferation, the analysis of which yielded the initial discovery of PPARs, remains an important physiological phenomenon to investigate. The precise manner by which peroxisome proliferators are able to induce their pleiotropic effects observed in a number of species, including humans, is largely unknown. Chapter 3 of this thesis describes studies that were performed to attempt to further characterize the molecular basis of the coordinate transcriptional induction of the peroxisomal  $\beta$ -oxidation enzymes, a hallmark of peroxisome proliferation.

The multi-faceted role of the PPAR $\gamma$  subtype in development and in adaptive responses to a variety of signals continues to be illustrated through active research into its wide range of functions. The establishment of its central involvement in the process of adipogenesis was the impetus for the work summarized in chapter 4. Determination of the significance of PPAR $\gamma$  function in congenital generalized lipodystrophy, a human genetic disorder characterized by a severe absence of adipose tissue, was the objective of the research undertaken.

The overall goal of performing studies such as those described here is to gain an increased understanding of the actions of the PPAR family of transcription factors in the metabolic processes underlying normal health and disease.

**Figure 1.1 The peroxisomal straight-chain fatty acid  $\beta$ -oxidation pathway.**  
Enzymatic activities are labelled in boldface.



## **Chapter 2**

### **Materials and Methods**

## 2.1 MATERIALS

The following sections list the suppliers of some key materials. All reagents were of the highest quality available.

### 2.1.1 Reagents and chemicals

absolute ethanol	Commercial Alcohols Inc.
acetic acid	BDH Chemicals
acetone	BDH Chemicals
acetonitrile	EM Science
acrylamide	Gibco/BRL
adenosine 5'-triphosphate (ATP)	Boehringer Mannheim
agar	Difco Laboratories
agarose, electrophoresis grade	Gibco/BRL
agarose, SeaKem® genetic technology grade (GTG)	FMC BioProducts
agarose, NuSieve® GTG	FMC BioProducts
ampicillin	Sigma Chemical Company
aprotinin	Sigma Chemical Company
aqueous counting scintillant (ACS)	Amersham Life Sciences
bacto-tryptone	Difco Laboratories
Bio-Rad protein assay dye reagent	Bio-Rad Laboratories
bovine serum albumin (BSA)	Boehringer Mannheim
5-bromo-4-chloro-3-indolyl- $\beta$ -D-galactoside (X-gal)	Sigma Chemical Company
bromophenol blue	Sigma Chemical Company
cellophane (Saran Wrap™)	Dow Chemical Company
charcoal	BDH Chemicals
chloroform	BDH Chemicals
Coomassie Brilliant Blue (R-250)	ICN Biomedicals
15-deoxy- $\Delta^{12,14}$ -prostaglandin J <sub>2</sub> (15-d-PGJ <sub>2</sub> )	BIOMOL Research Labs
deoxyribonucleotide triphosphates (dNTPs)	Boehringer Mannheim
dexamethasone	Sigma Chemical Company
trans-1,2-diaminocyclohexane-N,N,N',N'-tetraacetic acid (CDTA)	Sigma Chemical Company
diethylpyrocarbonate (DEPC)	Sigma Chemical Company
N,N-dimethylformamide (DMF)	BDH Chemicals
dithiothreitol (DTT)	Boehringer Mannheim
dimethyl sulfoxide (DMSO)	Sigma Chemical Company
Dulbecco's Modified Eagles Medium (DMEM)	Gibco/BRL
ethidium bromide	Sigma Chemical Company
ethylenediaminetetraacetic acid (EDTA)	BDH Chemicals
Expresshyb™ solution	CLONTECH Laboratories
fetal bovine serum	Gibco/BRL
Ficoll	Pharmacia Biotech
film (X-ray)	Kodak/Fuji
Freund's adjuvant (complete & incomplete)	Sigma Chemical Company
formaldehyde	BDH Chemicals
formamide	BDH Chemicals
gelatin	ICN Biomedicals



glucose	BDH Chemicals
L-glutamine	Gibco/BRL
glycerol	BDH Chemicals
glycine	BDH Chemicals
glycylglycine	Sigma Chemical Company
N-2-hydroxyethylpiperazine-N'-2-ethane sulfonic acid (HEPES)	BDH Chemicals
3-hydroxy-4-[2-sulfo-4-(4-sulfo-phenylazo)phenylazo] -2,7-naphthalenedisulfonic acid (Ponceau S)	Sigma Chemical Company
insulin	Sigma Chemical Company
Iscoe's Modified Dulbecco's Medium (IMDM)	Gibco/BRL
isopropanol	Fisher Scientific
N-laurylsarcosine	Sigma Chemical Company
luciferin	Sigma Chemical Company
maltose	BDH Chemicals
$\beta$ -mercaptoethanol	BDH Chemicals
methanol	BDH Chemicals
methylene blue	Sigma Chemical Company
mineral oil	Sigma Chemical Company
Minimum Essential Medium (MEM)	Gibco/BRL
morpholino propane sulfonic acid (MOPS)	BDH Chemicals
nitrocellulose disks	Schleicher & Schuell Inc.
nitrocellulose membrane	Amersham Life Sciences
Nonidet P-40 (NP-40)	BDH Chemicals
nylon membrane	Amersham Life Sciences
nystatin	Gibco/BRL
penicillin/streptomycin	Gibco/BRL
phenol, buffer saturated	Gibco/BRL
phenylmethylsulfonyl fluoride (PMSF)	Boehringer Mannheim
phosphoramidites	Beckman Instruments Inc.
pirinixic acid (wy-14,643)	Wyeth-Ayerst
polyethylene glycol (PEG) 3350, 8000	Sigma Chemical Company
polyvinylpyrrolidone	Sigma Chemical Company
pyruvic acid	Sigma Chemical Company
salmon sperm DNA	Sigma Chemical Company
Sephadex G-50	Pharmacia Biotech
skim milk powder	Lucerne Foods Ltd.
sodium azide	J. T. Baker Inc.
sodium dodecyl sulfate (SDS)	Sigma Chemical Company
tetracycline	Sigma Chemical Company
N,N,N',N'-tetramethyl-ethylenediamine (TEMED)	Gibco/BRL
trichloroacetic acid	Sigma Chemical Company
TRI-Reagent <sup>®</sup>	Molecular Research Center
tris(hydroxymethyl)aminomethane (Tris)	Boehringer Mannheim
Triton X-100	BDH Chemicals
trypsin/EDTA	Gibco/BRL
Tween 20	Sigma Chemical Company
urea	ICN Biomedicals
xylene cyanol	Sigma Chemical Company
yeast extract	Difco Laboratories

### 2.1.2 Enzymes

calf intestinal alkaline phosphatase (CIP)  
 DNA ligase, T4  
 DNA polymerase I, Klenow fragment  
 DNA polymerase, T4  
 DNA polymerase, T7 Sequenase™ (version 1.0)  
 DNA polymerase, *Taq*  
 polynucleotide kinase, T4  
 proteinase K  
 restriction endonucleases  
  
 reverse transcriptase, SuperScript™ RNase H<sup>-</sup>  
 ribonuclease A (RNase A)  
 ribonuclease H (RNase H)  
 ribonuclease inhibitor (RNasin)  
 RNA polymerase, T3  
 terminal transferase

New England Biolabs  
 Gibco/BRL  
 New England Biolabs  
 New England Biolabs  
 United States Biochemicals  
 Boehringer Mannheim  
 New England Biolabs  
 Boehringer Mannheim  
 New England Biolabs;  
 Boehringer Mannheim  
 Gibco/BRL  
 Sigma Chemical Company  
 Boehringer Mannheim  
 Boehringer Mannheim  
 Boehringer Mannheim  
 Promega Corporation

### 2.1.3 Molecular size standards

High molecular weight DNA markers  
 1 kb DNA ladder  
 1 kb-Plus DNA ladder  
 Prestained protein molecular weight markers  
 (broad-range)

Gibco/BRL  
 Gibco/BRL  
 Gibco/BRL  
  
 New England Biolabs

### 2.1.4 Radiochemicals

$\alpha$ [<sup>32</sup>P]-dATP (3000 Ci/mmol, 10  $\mu$ Ci/ $\mu$ L)  
 $\gamma$ [<sup>32</sup>P]-dATP (3000 Ci/mmol, 10  $\mu$ Ci/ $\mu$ L)

ICN Biomedicals;  
 Amersham Life Sciences  
 Amersham Life Sciences

### 2.1.5 Reagent kits

Enhanced Chemiluminescence (ECL) Western Blotting  
 Detection kit  
 Luciferase Assay kit  
 QIAGEN® Plasmid Maxi kit  
 QIAquick™ Gel Extraction kit  
 QIAquick™ PCR Purification kit  
 Random Primed DNA Labelling kit  
 Ready-To-Go® PCR Beads  
 RNeasy™ Total RNA kit  
 Sequenase™ version 2.0 DNA Sequencing kit  
 TNT™ Coupled Reticulocyte Lysate  
*in vitro* transcription/translation kit

Amersham Life Sciences  
 Promega Corporation  
 QIAGEN Inc.  
 QIAGEN Inc.  
 QIAGEN Inc.  
 Boehringer Mannheim  
 Pharmacia Biotech  
 QIAGEN Inc.  
 United States Biochemicals  
  
 Promega Corporation

## UltraFAST Oligonucleotide Cleavage and Deprotection kit

Beckman Instruments, Inc.

### 2.1.6 Plasmids

#### i) *E. coli* vectors

pGEM5Zf(+)  
pGEM7Zf(+)  
pSP73

Promega Corporation  
Promega Corporation  
Promega Corporation

#### ii) Mammalian vectors

pCPS/*luc*  
pRc/CMV  
pSG5  
pSVOALΔ5'

Dr. G. Shore (McGill University, Montreal, PQ)  
Invitrogen, San Diego, CA  
Dr. S. Green (ZENECA, Cheshire, Great Britain)  
Dr. J. K. Reddy (Northwestern University Medical School, Chicago, IL)

### 2.1.7 Antibodies

Table 2.1 lists the primary and secondary antibodies used in this study, the antibody source, immunogen, specificity, and the dilution used for immunoblot analysis.

## 2.2 MAMMALIAN CELL CULTURE STUDIES

### 2.2.1 Propagation of Primary Cultures and Cell Lines

All mammalian cell cultures were grown in monolayer in 10-cm dishes at 37°C in 10% CO<sub>2</sub>. Media was replaced every 2-3 days. Cell growth was monitored by phase contrast microscopy using an Olympus Inverted Research Microscope Model IMT-2 (Olympus Optical Co., Ltd., Tokyo, Japan).

#### 2.2.1.1 *Primary cultures*

95-607 primary human skin fibroblasts were derived from a tissue biopsy obtained from a 16-year-old Caucasian female patient with congenital generalized lipodystrophy (Dr. Howard Parsons and Stephen Hodges, Alberta Children's Hospital, University of Calgary). 95-607 cells were maintained in MEM + 2 mM sodium pyruvate, supplemented with 10% fetal bovine serum, 1% antibiotic solution (5,000 U/mL penicillin G sodium, 5,000 µg/mL streptomycin sulfate in 0.85% saline), and 4 mM L-glutamine in 0.85% NaCl. Cells were split 1:2 every 2-3 weeks.

HSFB primary human skin fibroblasts were explanted from a skin graft obtained from a normal 28-year-old Caucasian female burn patient (Dr. Aziz Ghahari, Department of Experimental Surgery, University of Alberta). HSFB cells were cultured in DMEM supplemented with 10% fetal bovine serum, 1% antibiotic solution, 4 mM L-glutamine, and 20 mM HEPES buffer (pH 7.4). Cells were split 1:5 to 1:6 every 5-6 days.

#### **2.2.1.2 Cell lines**

All cell lines were purchased from the American Type Culture Collection (Rockville, MD). Green monkey kidney cells, BSC40, were cultured in DMEM supplemented with 10% fetal calf serum, 1% antibiotic solution, and 2 mM L-glutamine. Cells were split 1:10 to 1:20 every week.

Human skin fibroblast cell lines 986, 1056, and 1059 were chosen based on sex and age of tissue donor and matched as closely as possible to that of the lipodystrophy patient. Cultures were maintained in IMDM supplemented with 10% fetal bovine serum, 1% antibiotic solution, and 4 mM L-glutamine. Cells were split 1:3 every 5-6 days.

#### **2.2.1.3 Passaging cells**

At or near confluence, cells were washed twice with 5 mL of a phosphate-buffered saline solution (PBS; 137 mM NaCl, 2.7 mM KCl, 4.3 mM Na<sub>2</sub>HPO<sub>4</sub>·7H<sub>2</sub>O, 1.4 mM KH<sub>2</sub>PO<sub>4</sub>, pH 7.4) pre-warmed to 37°C. Subcultivation of cells was performed by treatment with a solution of 0.05% trypsin and 0.53 mM EDTA·4Na for 1-2 minutes at 37°C, followed by aspiration of the trypsin/EDTA solution. Trypsinized cells were mixed with fresh culture medium at an appropriate dilution and replated.

#### **2.2.1.4 Freezing cell stocks**

Frozen cell stocks were prepared by washing confluent plates of cells with PBS followed by trypsinization. Trypsinized cells were mixed with freeze medium (90% culture medium, 10% DMSO), transferred to Nalgene® Cryoware cryovials (Nalge Company/Sybron Corporation, Rochester, NY), and allowed to freeze at a rate of -1°C/minute in a Nalgene® Cryo 1°C Freezing Container placed in a -80°C freezer overnight. Frozen cells were stored in liquid nitrogen.

## 2.2.2 Transient Transfections of BSC40 Cells

### 2.2.2.1 Plasmids

All plasmids used for BSC40 cell transfections were prepared by large-scale isolation and purification of plasmid DNA from bacterial cell cultures (section 2.3.2).

pCPS $luc$  is a luciferase expression vector containing the minimal promoter for the gene encoding rat liver carbamoyl phosphate synthetase (CPS; Howell *et al.*, 1989). pSVOAL $\Delta 5'$  is an SV40-derived mammalian expression vector containing a promoterless luciferase reporter gene (De Wet *et al.*, 1987). Both luciferase expression vectors were used for the construction of reporter plasmids containing sequences located upstream of genes encoding peroxisomal  $\beta$ -oxidation enzymes.

The positive control luciferase reporter construct containing three copies of the HD-PPRE (pHD(x3) $luc$ ), as well as the expression plasmids and parent vectors (pRc/CMV, pSG5) for rPPAR $\alpha$  and RXR $\alpha$  have been previously described (Marcus *et al.*, 1993; Miyata *et al.*, 1993).

The reporter plasmids containing peroxisomal 3-ketoacyl-CoA thiolase (thiolase B) upstream sequences were constructed by Baowei Zhang (McMaster University, Hamilton, ON). pThB(1kb) $\Delta 5'$  was constructed by inserting approximately 1.1 kb of the sequence found immediately upstream of the transcription start site of the thiolase B gene into the pSVOAL $\Delta 5'$  luciferase expression vector. pThB(2kb) $luc$  was constructed by excising the CPS proximal promoter from the pCPS $luc$  luciferase expression vector and inserting in its place approximately 2.1 kb of the thiolase B upstream sequence.

### 2.2.2.2 Transfections and luciferase assays

Transient transfection of BSC40 cells was performed by a modification of the calcium phosphate precipitation procedure (Ausubel *et al.*, 1996). BSC40 cells were grown to 60-80% confluence in 10-cm dishes. Cells were washed twice with PBS and then incubated in transfection medium (DMEM without phenol red indicator, supplemented with 10% dextran-coated charcoal (DCC)-treated fetal bovine serum, 1% antibiotic solution, and 8 mM L-glutamine) for 5 hours at 37°C in 10% CO<sub>2</sub>. A calcium phosphate/DNA co-precipitate suspension (4 mL) was made by combining 80  $\mu$ g total DNA (20  $\mu$ g reporter plasmid, 8  $\mu$ g each RXR $\alpha$  and rPPAR $\alpha$  expression plasmids or empty parent vectors where indicated, and 44  $\mu$ g of 10 mg/mL sonicated salmon sperm

DNA) with 2 M  $\text{CaCl}_2$  and mixing with an equal volume (2 mL) of a 2X HEPES-buffered saline solution (0.28 M NaCl, 50 mM HEPES, 1.5 mM  $\text{Na}_2\text{HPO}_4$ , pH 7.12). The suspension was divided into 1 mL aliquots and added dropwise to the BSC40 cells incubated in the presence of freshly added transfection medium containing either 0.1 mM wy-14,643 (20 mM stock solution in DMSO) or 0.5% DMSO alone. After incubation of transfected cells for 16 hours at 37°C in 3%  $\text{CO}_2$ , cells were washed once with PBS and medium was replaced with fresh medium supplemented with either wy-14,643 or DMSO. Incubation was continued for an additional 24 hours at 37°C in 10%  $\text{CO}_2$ . Transfected cells were then washed twice with PBS, followed by harvesting into 1 mL of cold PBS using a cell lifter (Costar Corporation, Cambridge, MA). Harvested cells were pelleted at  $\sim 13,000 \times g$  for 10 seconds at 4°C in an Eppendorf microcentrifuge (Brinkman Instruments Ltd., Mississauga, ON). Extracts were prepared by suspension of the cell pellets in 100  $\mu\text{L}$  of lysis solution (25 mM Tris-phosphate (pH 7.8), 2 mM DTT, 2 mM CDTA, 10% (w/v) glycerol, 1% (w/v) Triton X-100). Cell debris was removed by centrifugation at  $\sim 13,000 \times g$  for 10 minutes at 4°C in a microcentrifuge. Supernatants were assayed for reporter gene (luciferase) activity with a Luciferase Assay kit (Promega Corporation, Madison, WI) and a luminometer (Model 1253, Bio-Orbit Oy, Turku, Finland) following the manufacturers' protocols. All transfections were performed in duplicate and average luminometer readings taken for transfections performed in the presence and absence of wy-14,643 were used to calculate relative induction of luciferase activity. Comparison of transfections performed using luciferase expression vectors with and without heterologous promoter sequences enabled calculation of fold-induction values.

## 2.2.3 Treatment of Human Fibroblasts with PPAR $\gamma$ Activators

### 2.2.3.1 Preadipocyte differentiation protocol

Stimulation of adipocyte conversion of 95-607 and HSFB fibroblasts was attempted following a modified protocol for adipogenesis of preadipocytic mouse fibroblasts (Chawla *et al.*, 1994). Duplicate plates of 95-607 and HSFB primary cultures were grown to confluence in regular culture media. At confluence, media was replaced with fresh media containing either 450  $\mu\text{M}$  wy-14,643 in DMSO, 10  $\mu\text{M}$  15-deoxy- $\Delta^{12,14}$ -prostaglandin  $\text{J}_2$  (15-d-PGJ $_2$ ) in DMSO, or DMSO alone. Cells were incubated at 37°C in 10%  $\text{CO}_2$  for an additional 10 days accompanied by refeeding every 2 days with

media freshly supplemented with wy-14,643, 15-d-PGJ<sub>2</sub>, or DMSO. Appearance of cell morphology, as visualized by phase contrast microscopy, was monitored daily for evidence of adipogenic conversion (acquisition of rounded shape and accumulation of lipid droplets). Following 10 days of culture maintenance, cells were lysed using the TRI-Reagent<sup>®</sup> lysis reagent (Molecular Research Center Inc., Cincinnati, OH). Lysates were stored at -80°C until further processed for total RNA and protein extraction.

#### **2.2.3.2 *Adipogenesis in non-determined fibroblasts protocol***

An alternate method for stimulation of adipogenesis of 95-607 and HSFB cells was attempted following a protocol similar to that used by Tontonoz *et al.* (1994c). By this method, non-determined NIH 3T3 mouse fibroblasts expressing PPAR $\gamma$  were observed to undergo conversion to adipocytes upon treatment with PPAR $\gamma$  activators. Duplicate plates of 95-607 and HSFB cultures were grown to confluence in differentiation medium (DMEM supplemented with 10% fetal bovine serum and 5  $\mu$ g/mL insulin). At confluence, a fresh change of differentiation medium containing 1  $\mu$ M dexamethasone and either 450  $\mu$ M wy-14,643 in DMSO, 10  $\mu$ M 15-d-PGJ<sub>2</sub> in DMSO, or DMSO alone was added to the cultures. After 48 hours and every 2 days thereafter, media was replaced with differentiation medium freshly supplemented with PPAR $\gamma$  activator or DMSO. Cell morphology was monitored daily by phase contrast microscopy for evidence of adipogenic conversion. Following 10 days of post-confluence culture and assessment of adipogenesis, cells were lysed using the TRI-Reagent<sup>®</sup>. Lysates were stored at -80°C until further processed for total RNA and protein extraction.

### **2.3 DNA MANIPULATION**

#### **2.3.1 Transformation and Growth of Bacterial Cell Cultures**

For propagation of plasmid DNA, *Escherichia coli* (*E. coli*) subcloning efficiency DH5 $\alpha$  competent cells (Gibco/BRL, Bethesda, MD) were transformed either by heat shock or electroporation.

##### **2.3.1.1 *Transformation by heat shock***

1  $\mu$ L of plasmid DNA resuspended in TE (10 mM Tris-HCl (pH 8.0), 1 mM EDTA (pH 8.0)) or a 1  $\mu$ L aliquot of a completed ligation reaction was added to a 25  $\mu$ L

aliquot of thawed DH5 $\alpha$  cells and mixed. Cells were then incubated on ice for 30 minutes, followed by a 20-second heat-shock at 37°C. 975  $\mu$ L of Luria-Bertani (LB) medium (1% (w/v) bacto-tryptone, 0.5% (w/v) yeast extract, 1% (w/v) NaCl, pH 7.5) was added to the transformed cells and cultures were grown at 37°C for 35–45 minutes with shaking. Positive transformants were allowed to grow at 37°C overnight on LB-agar (1.5% (w/v)) plates containing 100  $\mu$ g/mL ampicillin (amp) and 2% X-gal in DMF.

#### 2.3.1.2 Transformation by electroporation

Electrocompetent *E.coli* DH5 $\alpha$  cells were prepared by the following procedure. 50 mL of SOB medium (2% (w/v) bacto-tryptone, 0.5% (w/v) yeast extract, 10 mM NaCl, 2.5 mM KCl) with 20 mM glucose was inoculated with a 25  $\mu$ L aliquot of subcloning efficiency DH5 $\alpha$  cells. An overnight culture was grown at 37°C with shaking. 0.5 mL of the overnight culture was diluted into 500 mL of SOB medium + 20 mM glucose and grown at 37°C with vigorous shaking for ~5 hours to an OD<sub>550</sub> of 0.5 - 0.6, as measured using a Beckman DU 640 Spectrophotometer (Beckman Instruments, Inc., Fullerton, CA). Cells were then harvested by centrifugation at 2,600 x g in a Beckman JA-10 fixed-angle rotor for 10 minutes at 4°C in a Beckman Model J2-HC centrifuge. Cell pellets were washed twice by resuspension in 500 mL of sterile ice-cold 10% (v/v) glycerol and recentrifuging. Washed cell pellets were resuspended in ice-cold 10% (v/v) glycerol to a final volume of ~2 mL (~ 1 x 10<sup>11</sup> cells/mL), flash-frozen in a dry ice-ethanol bath, and stored in 110  $\mu$ L aliquots at -80°C.

For transformation of electrocompetent cells, 1  $\mu$ L of a completed ligation reaction was added to a thawed 20  $\mu$ L aliquot of cells, followed by incubation on ice for 5 minutes. The cell suspension was then placed between the bosses of a chilled microelectroporation chamber (Gibco/BRL) and subjected to a voltage pulse of 395 V boosted to 2.4 kV using a Gibco/BRL Cell-Porator™ in combination with a Voltage Booster (Gibco/BRL). The voltage booster was adjusted to the 330  $\mu$ F capacitance and 4 k $\Omega$  resistance settings. Electroporated cells were immediately transferred to 1 mL of SOC medium (SOB medium with 20 mM glucose, 10 mM MgCl<sub>2</sub>, 10 mM MgSO<sub>4</sub>) and allowed to grow at 37°C for one hour with shaking. Growth of positive transformants was enabled by plating electroporated cells onto LB-agar plates supplemented with 100  $\mu$ M ampicillin and 2% X-gal in DMF, followed by incubation overnight at 37°C.



### **2.3.1.3 Selection and growth of positive transformants**

Bacterial cells containing the plasmid of interest form a white colony on LBamp + X-gal plates by virtue of the presence of an ampicillin-resistance selectable marker and disruption of the  $\beta$ -galactosidase gene contained in the vector upon incorporation of an insert. Cells that do not contain the desired plasmid either do not grow or form a blue colony as a result of the presence of an intact  $\beta$ -galactosidase gene, which functions to metabolize the X-gal to yield a blue-coloured product.

For preparation of liquid cultures to be used for plasmid isolation, 3 mL of LB medium containing 100  $\mu$ g/mL ampicillin was inoculated with a positive transformant (white) colony and allowed to grow overnight at 37°C with shaking.

## **2.3.2 Plasmid DNA Isolation**

### **2.3.2.1 Small-scale isolation**

Plasmid DNA was isolated from small-scale bacterial cultures (3 mL) by a modification of the alkaline lysis method described in Maniatis *et al.* (1989). Bacterial cells were harvested from the overnight culture by centrifugation at  $\sim 13,000 \times g$  for 1 minute at room temperature in a microcentrifuge. Cells were osmotically lysed by resuspension of the pellets in 100  $\mu$ L of lysis solution (50 mM glucose, 10 mM EDTA (pH 8.0), 25 mM Tris-HCl (pH 8.0)) with vigorous vortexing using a Fisher Vortex Genie 2 (Fisher Scientific, Pittsburgh, PA). Following incubation of the lysates at room temperature for 5 minutes, 200  $\mu$ L of denaturing solution (0.2 N NaOH, 1% SDS) was added, mixed with the lysates by inversion, and incubated at room temperature for an additional 5 minutes. Denatured proteins were precipitated by the addition of 150  $\mu$ L of cold 3 M potassium, 5 M acetate solution and mixing by inversion. Incubation on ice for 5 minutes followed by centrifugation at  $\sim 13,000 \times g$  for 5 minutes at 4°C in a microcentrifuge enabled pelleting of the precipitated proteins. Purification of DNA from any remaining contaminating proteins was achieved by extraction of the supernatant with an equal volume of buffer-saturated phenol/chloroform/isoamyl alcohol (25:24:1), followed by extraction with chloroform/isoamyl alcohol (24:1). The DNA was then precipitated from the remaining aqueous layer by the addition of 800  $\mu$ L of absolute ethanol. Plasmid DNA was pelleted by centrifuging at  $\sim 13,000 \times g$  for 5 minutes at room temperature in a microcentrifuge. DNA pellets were washed with 70% ethanol, recentrifuged, and dried for 10 minutes in a CentriVap Centrifugal Concentrator using a

Cold Trap and High Vacuum Pump (speed vac; Labconco Corporation, Kansas City, MO). Dried pellets were resuspended in 40  $\mu$ L of TE (pH 8.0) + 20  $\mu$ g/mL ribonuclease A and stored at 4°C.

#### **2.3.2.2 Large-scale isolation**

For large-scale isolation of plasmid DNA, 500 mL of LB medium containing 100  $\mu$ g/mL ampicillin was inoculated with a small-scale 3 mL overnight culture of transformed bacterial cells. Large-scale cultures were grown for 16-20 hours at 37°C with shaking to an OD<sub>600</sub> of 1.0 - 1.5, corresponding to a cell density of  $\sim 1 \times 10^9$  cells/mL. Cells were then harvested by centrifuging cultures in a Beckman JA-10 fixed-angle rotor at 6,000 x g for 10 minutes at 4°C in a Beckman Model J2-HC centrifuge. Plasmid DNA was subsequently isolated from the cell pellets using a QIAGEN® Plasmid Maxi kit (QIAGEN Inc., Chatsworth, CA) following the manufacturer's protocol. Washed and dried plasmid DNA pellets were resuspended in 500  $\mu$ L of TE (pH 8.0) and stored at 4°C.

### **2.3.3 Genomic DNA Isolation**

#### **2.3.3.1 DNA isolation from cultured mammalian cells**

Cells were grown in monolayer in appropriate media in 10-cm dishes to confluence. At confluence, cells were washed with 10 mL of PBS pre-warmed to 37°C, followed by trypsinization for 1-2 minutes at 37°C. After aspiration of the trypsin/EDTA solution, the trypsinized cells were collected into 1 mL of PBS and transferred to a microfuge tube. Remaining cells in the plate were harvested using a cell lifter and added to the microfuge tube. Cells were then centrifuged at 500 x g for 5 minutes at 4°C in a microcentrifuge. The cell pellet was washed twice by resuspension in 1 mL of cold PBS, recentrifuging after each wash. Genomic DNA was subsequently isolated from the cell pellet using the method described in Ausubel *et al.* (1996). Cell pellets were resuspended in 0.3 mL of digestion buffer (100 mM NaCl, 10 mM Tris-HCl (pH 8.0), 25 mM EDTA (pH 8.0), 0.5% SDS, 0.1 mg/mL proteinase K) and incubated at 50°C for 12-18 hours with shaking. Proteins were removed from the lysates by extraction with an equal volume of phenol/chloroform/isoamyl alcohol (25:24:1) and centrifuging at 1,700 x g for 10 minutes at room temperature to resolve aqueous and organic phases. DNA was precipitated from the aqueous phase upon the addition of a one-half volume of 7.5 M ammonium acetate and 2 (original) volumes of absolute ethanol. The DNA was then

pelleted by centrifugation at 1,700 x g for 2 minutes at room temperature in a microcentrifuge. Pellets were subsequently washed with 70% ethanol, recentrifuged, and air-dried. DNA pellets were resuspended in 50 µL of TE (pH 8.0), allowed to solubilize at room temperature overnight, and stored at -20°C.

#### **2.3.3.2 DNA isolation from blood samples**

Frozen blood samples collected into 10-mL vacutainer tubes were thawed at room temperature. Thawed blood was poured into a sterile 50-mL Falcon tube containing 30 mL of sterile distilled water and the resulting suspension was mixed by inversion. Red blood cells were pelleted by centrifugation in a Beckman JS 4.3 swinging bucket rotor at 1,500 x g for 10 minutes at room temperature in a Beckman Model J2-HC centrifuge. The supernatant was discarded and the pellet was resuspended in 25 mL of 0.1% NP-40 with vortexing. Cells were again pelleted by centrifugation at 1,700 x g for 10 minutes at room temperature. The pellet was subsequently resuspended with vortexing in 10 mL of rapid lysis buffer (1% N-laurylsarcosine, 10 mM CDTA, 0.1 M Tris-HCl (pH 8.0), 0.2 N NaCl, 0.4 M urea) pre-warmed to 55°C. Proteinase K was then mixed with the resuspended blood cells to a final concentration of 12 µg/mL, and the resulting mixtures were incubated at 55°C for 2-4 hours. Proteins were removed from the lysate by adding 10 mL of phenol, mixing by inversion for 20 minutes at 4°C, and then separating the aqueous and organic phases by centrifugation in a Beckman JS 13.1 swinging bucket rotor at 15,000 x g for 15 minutes at 4°C in a Beckman Model J2-HC centrifuge. The extraction was repeated twice with the resulting aqueous layer, first using 10 mL of phenol/chloroform/isoamyl alcohol (25:24:1), and then with 10 mL of chloroform/isoamyl alcohol (24:1). DNA was precipitated from the final aqueous layer by the addition of 10 mL of 5 M ammonium acetate and 40 mL of absolute ethanol pre-cooled to -20°C, followed by incubation at -20°C overnight. The precipitated DNA was pelleted by centrifugation in a Beckman JS 13.1 swinging bucket rotor at 15,000 x g for 15 minutes at 4°C. DNA pellets were washed with 2 mL of ice-cold 70% ethanol, recentrifuged, and allowed to air dry. The dried DNA pellets were resuspended in 400 µL of TE (pH 8.0) and stored at -20°C.

#### **2.3.4 Quantitation of DNA Samples**

Purified plasmid DNA, genomic DNA, and oligonucleotides were quantitated using a Beckman DU 640 Spectrophotometer. OD<sub>260</sub> measurements of DNA samples diluted in 1 mL of sterile distilled water were used to calculate DNA concentrations according to the conversions:

$$1 \text{ OD}_{260} \text{ unit} = 50 \text{ } \mu\text{g/mL of double-stranded DNA}$$

$$\text{nmol of oligonucleotide} = (\text{OD}_{260} \text{ units} \times 90) / \text{the length of the oligonucleotide}$$

OD<sub>260</sub>/OD<sub>280</sub> ratios were used as a measure of the purity of the DNA preparations. Ratios of 1.8 or greater indicate samples are of high purity, while ratios below 1.5 indicate significant protein contamination.

DNA fragments generated by restriction endonuclease digestion (section 2.3.6) or by PCR (section 2.3.14) were roughly quantitated by running the samples through an agarose gel (section 2.3.5) and comparing the intensity of ethidium bromide staining of the DNA fragments with that of comparable-sized DNA fragments of known concentration.

### **2.3.5 Agarose Gel Electrophoresis**

Agarose (electrophoresis grade, SeaKem® GTG agarose for concentrations ≤1.5%, or NuSieve® GTG agarose for concentrations >1.5%) was dissolved in 1X TBE buffer (89 mM Tris-HCl (pH 8.0), 89 mM boric acid, 20 mM EDTA (pH 8.0)) to the desired concentration, followed by the addition of ethidium bromide to a final concentration of 2 µg/mL prior to casting the gel. Before loading, samples were mixed with a one-sixth volume of gel dye (0.36% (w/v) bromophenol blue, 0.36% (w/v) xylene cyanol, 30% (v/v) glycerol). Gels were run in 1X TBE buffer containing 0.5 µg/mL of ethidium bromide at ~10 V/cm using a horizontal submarine electrophoresis apparatus (Hoefer Scientific Instruments, San Francisco, CA). Separation of DNA fragments was monitored by observing the migration of the bromophenol blue and xylene cyanol dye fronts. Ethidium bromide-stained nucleic acid was visualized using a shortwave Foto UV 300 DNA Transilluminator (Fotodyne Incorporated, New Berlin, WI), and gels were photographed with the FCR-10 Camera System and DNA Photographic Filter Kit (Fotodyne Inc.) using Polaroid ISO 3000 black and white film.

### **2.3.6 Restriction Endonuclease Digestion**

Restriction endonuclease digestions were performed using the manufacturer's (New England Biolabs, Ltd., Mississauga, ON; Boehringer Mannheim Biochemicals, Indianapolis, IN) supplied buffer systems at the recommended temperatures for >2 hours in a Multi-Blok Heater (Lab-Line Instruments, Inc., Melrose Park, IL). The volume of total enzyme used did not exceed one-tenth of the digest reaction volume. For some double digests involving two enzymes of incompatible commercial buffer systems, an appropriate dilution of a potassium glutamate-based buffer (5X stock contains 500 mM potassium glutamate, 125 mM Tris-acetate (pH 7.6), 50 mM magnesium acetate, 250 µg/mL BSA, 2.5 mM β-mercaptoethanol) was used according to Hanish and McClelland (1988). For double digests involving two enzymes with no compatible buffer systems or with two different optimal temperatures, the digest was performed in two stages. Digestion with the enzyme requiring the lower salt concentration or temperature was performed first, followed by addition of the second enzyme and concomitant optimization of buffer composition and temperature for the remainder of the incubation.

### **2.3.7 Generation of Blunt-Ended DNA for Subcloning**

#### **2.3.7.1 *Blunt-ending restriction endonuclease-digested DNA fragments***

Following the identification of positive clones through library screening (section 2.4.1), rat genomic library inserts were excised by digestion of positive λ phage DNA with *Sfi*I, generating nonspecific 3' overhangs of the DNA fragments. In order to subclone the inserts, filling-in of the overhangs was performed by incubation of digests with 3 U of T4 DNA polymerase in the presence of 100 µM dNTPs at 11°C for 30 minutes. The reaction was stopped by heat-killing the polymerase at 75°C for 10 minutes. The blunt-ended inserts were isolated by extraction from gel fragments following agarose gel electrophoresis of the reactions (sections 2.3.5 and 2.3.8).

#### **2.3.7.2 *Blunt-ending PCR and RACE products***

DNA fragments amplified by *Taq* DNA polymerase in PCR-based techniques contain a single non-templated nucleotide (nearly always A) at the 3' end of all duplex DNA strands. Such overhangs are repaired by the 3'→5' exonuclease activity of the Klenow fragment of DNA polymerase I. To generate blunt-ended DNA fragments, an aliquot of the amplification reaction was incubated with 10 U of Klenow, 10 U of T4 polynucleotide kinase to ensure phosphorylation of all 5' ends, 1 mM dATP, and

Klenow/PNK buffer (50 mM Tris-HCl (pH 7.5), 10 mM MgCl<sub>2</sub>, 1 mM DTT, 50 µg/mL BSA, 20 µM dNTPs) at 37°C for one hour. The reaction was stopped by the addition of 100 µg/mL proteinase K and 0.1% SDS with incubation at 42°C for one hour. DNA fragments were subsequently purified by phenol/chloroform/isoamyl alcohol (25:24:1) extraction and ethanol precipitation, or by extraction from gel fragments following agarose gel electrophoresis of the blunt-ending reaction products (sections 2.3.5 and 2.3.8).

### **2.3.8 Purification of DNA Fragments**

Following agarose gel electrophoresis of DNA fragments to be purified, gel slices containing the fragments of interest were excised with a razor blade. DNA was subsequently eluted from the gel slices by electroelution for 15–45 minutes in 0.5X TBE using a Model UEA Unidirectional Electroelutor (International Biotechnology Instruments, New Haven, CT) following the manufacturer's protocol. Two 175-µL aliquots were removed from the salt trap and DNA was precipitated with 1 mL of pre-cooled absolute ethanol at -20°C for 30 minutes in the presence of 69.4 ng/mL of linear polyacrylamide as carrier. Alternatively, DNA was extracted from gel slices using a QIAquick™ Gel Extraction kit (QIAGEN Inc.) following the manufacturer's protocol.

### **2.3.9 Concentration of DNA Samples**

Dilute DNA samples were concentrated by the addition of a one-tenth volume of 3 M sodium acetate (pH 5.2) and 2–2.5 volumes of absolute ethanol pre-cooled to -20°C, followed by mixing and precipitation of DNA at -80°C for ~15 minutes or at -20°C for >30 minutes. Precipitated DNA was pelleted by centrifugation at ~13,000 x g for 5 minutes at room temperature in a microcentrifuge. DNA pellets were washed with 1 mL of 70% ethanol, recentrifuged, and dried in a speed vac evaporator for 10 minutes. Dried DNA pellets were subsequently dissolved in an appropriate volume of sterile distilled water or TE (pH 8.0) to achieve the desired concentration.

### **2.3.10 Subcloning DNA Fragments**

#### **2.3.10.1 Vectors**

The vectors pGEM5Zf(+), pGEM7Zf(+), and pSP73 (Promega Corporation) were used for subcloning DNA fragments. pGEM7Zf(+) and pSP73 were more commonly used for ligation of cohesive-ended DNA fragments, while *EcoRV*-restricted pGEM5Zf(+) was preferentially used for the subcloning of blunt-ended DNA fragments. To minimize recircularization of linearized vectors with complementary termini in the ligation reaction, digested vectors were treated with 1 U of calf intestinal alkaline phosphatase (CIP) per  $\mu\text{g}$  of DNA and incubated at 37°C for 45 minutes. The reaction was stopped by heat-killing the enzyme at 75°C for 10 minutes, followed by phenol/chloroform/isoamyl alcohol (25:24:1) extraction and ethanol precipitation of the DNA. If digestion of the vectors resulted in excision of portions of the multiple cloning site, vector DNA was gel purified as previously described (section 2.3.8). Purified vector DNA was dissolved in sterile distilled water or TE (pH 8.0), and concentration was estimated by visual comparison of band intensity with known DNA fragments in an ethidium bromide-stained agarose gel.

#### 2.3.10.2 *Ligation of complementary cohesive termini*

25-50 ng of purified vector DNA was combined with a 3-fold molar excess of purified insert DNA in a 10-20  $\mu\text{L}$  ligation reaction containing no more than 20 ng/ $\mu\text{L}$  total DNA. The reaction was carried out using 0.1 U of T4 DNA ligase in the presence of DNA ligase reaction buffer (50 mM Tris-HCl (pH 7.6), 10 mM  $\text{MgCl}_2$ , 1 mM ATP, 1 mM DTT, 5% (w/v) polyethylene glycol 8000), and incubated at 25°C for 3 hours. Control reactions were simultaneously performed, consisting of the reaction components as described but lacking insert DNA.

#### 2.3.10.3 *Ligation of blunt-ended DNA*

50 ng of purified, CIP-treated vector DNA was combined with a 5-fold molar excess of purified insert DNA in a 20  $\mu\text{L}$  ligation reaction containing no more than 1  $\mu\text{g}$  total DNA. The reaction was performed using 1 U of T4 DNA ligase in the presence of DNA ligase buffer, and incubated at 16°C for 16-20 hours. Control ligations contained all reaction components except insert DNA.

### 2.3.11 Labelling of DNA Probes

#### 2.3.11.1 *End-labelling oligonucleotide probes*

25 pmol of the oligonucleotide to be used as a probe for Southern blot analysis (section 2.3.12) or library screening by hybridization (section 2.4.1) was radioactively end-labelled with 150  $\mu\text{Ci}$  of  $\gamma[^{32}\text{P}]\text{-dATP}$  and 20 U of T4 polynucleotide kinase in a reaction containing 50 mM Tris-HCl (pH 7.5), 10 mM  $\text{MgCl}_2$ , 5 mM DTT, and 50  $\mu\text{g/mL}$  BSA. Reactions were incubated at 37°C for one hour and stopped by the addition of 2  $\mu\text{L}$  of 0.5 M EDTA (pH 8.0). The completed reaction volume was brought up to 100  $\mu\text{L}$  with TE (pH 8.0) prior to purification of the labelled probe.

#### 2.3.11.2 *Random primer labelling of DNA probes*

25 ng of the DNA fragment to be used as a probe for Southern or Northern blot analysis (sections 2.3.12 and 2.5.5) or library screening by hybridization (section 2.4.1) was denatured by boiling for 5 minutes, followed by rapid cooling on wet ice. The denatured fragments were radioactively labelled with 50  $\mu\text{Ci}$   $\alpha[^{32}\text{P}]\text{-dATP}$  and 2 U of DNA polymerase I Klenow fragment using a random primer labelling kit (Boehringer Mannheim Biochemicals) according to the manufacturer's protocol. After incubation at 37°C for 30 minutes, the completed reaction volume was brought up to 50  $\mu\text{L}$  with TE (pH 8.0) prior to purification of the labelled DNA fragment.

#### 2.3.11.3 *Purification and quantitation of labelled probes*

Unincorporated radioactive label was removed from probe preparations by separation on a homemade Sephadex G-50 spin column (Maniatis *et al.*, 1989) equilibrated with TE (pH 8.0), or using a TE Midi Select™-D G-50 Microcentrifuge Spin Column (5 Prime → 3 Prime, Inc., Boulder, CO). The specific activity of purified radiolabelled probes was determined by liquid scintillation counting in a Model 1209 RackBeta Liquid Scintillation Counter (Pharmacia-Wallac Oy, Turku, Finland).

### 2.3.12 Southern Blot Analysis

Southern blotting of genomic DNA samples, excised library inserts, digested plasmid DNA fragments, and PCR products was performed essentially as described by Southern (1977) and modified by Ausubel *et al.* (1996). Rat and human genomic DNA samples were digested with appropriate restriction enzymes for >6 hours prior to Southern analysis. DNA fragments were separated by agarose gel electrophoresis (section 2.3.5) followed by nicking on a shortwave uv DNA transilluminator (Fotodyne



Inc.) for 5-10 minutes. The DNA fragments were then denatured by immersing the gel in denaturing solution (0.5 M NaOH, 1.5 M NaCl) with shaking for 15 minutes. The denaturation step was repeated with a fresh change of solution, followed by two 15-minute washes of the gel in neutralizing solution (0.5 M Tris-HCl (pH 8.0), 1.5 M NaCl). DNA fragments were transferred from the gel to a nitrocellulose membrane (Hybond™-C, Amersham Life Sciences, Oakville, ON) by capillary action using a transfer pyramid and 5X SSC transfer buffer (75 mM tri-sodium citrate (pH 7.0), 750 mM NaCl). Transfer was carried out at room temperature for 12-16 hours. Following transfer, DNA was covalently fixed to the nitrocellulose by ultraviolet cross-linking at 0.12 J/cm<sup>2</sup> using a 254-nm wavelength UV Stratalinker™ 1800 (Stratagene, La Jolla, CA). Agarose gels were removed from the transfer pyramid and stained in 1X TBE containing 0.5 µg/mL of ethidium bromide to assess the efficiency of transfer.

#### 2.3.12.1 *Hybridization with oligonucleotide probes*

For hybridization with oligonucleotide probes, blots were first prehybridized for 5 hours in pre-warmed oligo probe prehybridization solution (1X SSPE [150 mM NaCl, 10 mM NaH<sub>2</sub>PO<sub>4</sub>·H<sub>2</sub>O, 1 mM EDTA (pH 8.0)], 5X Denhardt's solution [0.1% (w/v) Ficoll, 0.1% (w/v) polyvinylpyrrolidone, 0.1% (w/v) BSA], 0.25% SDS, 100 µg/mL denatured salmon sperm DNA) contained in either heat-sealable plastic pouches placed in a heated water bath or in hybridization tubes inside a hybridization incubator (Lab-Line Instruments, Inc.). Prehybridization was carried out at a temperature 20°C below the oligonucleotide probe's estimated dissociation temperature ( $T_d$ ), given by the equation:

$$T_d = 81.5^{\circ}\text{C} + 16.6 \log_{10}[\text{Na}^+] + 0.41(\% \text{ G/C content}) - 500/n$$

where  $[\text{Na}^+] = 0.2 \text{ M}$  for 1X SSPE in the oligo probe prehybridization solution, and  $n$  = the number of nucleotides comprising the oligonucleotide probe. Hybridization was performed by adding heat-denatured probe ( $5 - 6 \times 10^5 \text{ cpm/mL}$ ) to the prehybridization solution in the plastic pouch or hybridization tube containing the blot, and incubating for 16-20 hours at a temperature of  $T_d - 20^{\circ}\text{C}$ . Blots were then washed, first under low stringency conditions in 2X SSC, 0.05% SDS at  $T_d - 30^{\circ}\text{C}$  for one hour with a fresh change of wash solution after 30 minutes. A high stringency wash was subsequently performed in a fresh change of the same wash solution at  $T_d - 20^{\circ}\text{C}$  for 15 minutes. After washing, blots were air-dried, wrapped in cellophane, and exposed to X-ray film.

#### 2.3.12.2 *Hybridization with DNA fragments as probes*

For hybridization with DNA fragments >100 nucleotides in length, blots were first prehybridized for 3 hours in pre-warmed hybridization solution (1.25X SSC, 0.16X Denhardt's solution, 0.001% SDS, 20 mM sodium phosphate, 4 µg/mL denatured salmon sperm DNA) at 65°C. Hybridization was then carried out at 37-50°C for 16-20 hours in a fresh change of the pre-warmed hybridization solution containing 30% (v/v) deionized formamide (Maniatis *et al.*, 1989) and heat-denatured probe (5 - 6 x 10<sup>5</sup> cpm/mL). Blots were subsequently washed in pre-warmed 1X SSC, 0.1% SDS at 55°C for one hour with fresh changes of wash solution every 15 minutes. After washing, blots were air-dried, wrapped in cellophane, and exposed to X-ray film.

#### 2.3.12.3 Hybridization with a $\beta$ -actin control probe

Southern blots of human genomic DNA were additionally probed with a 1.75 kb full-length cDNA for human cytoplasmic  $\beta$ -actin (Genbank accession no. X00351) obtained from CLONTECH Laboratories (Palo Alto, CA). This was a positive control probe used to verify consistency in the amount of DNA samples loaded into agarose gels run for subsequent Southern blotting, as well as in the amount of DNA transferred from each lane of the gel to the nitrocellulose membrane. The appearance of hybridization signals on the resulting film also confirmed the presence of this ubiquitous gene among all human genomic DNA samples probed.

#### 2.3.13 Oligonucleotide Synthesis

Most oligonucleotides used in the studies performed were synthesized on 30 nmol synthesis columns using cyanoethyl-phosphoramidite chemistry on a Beckman Oligo 1000M DNA Synthesizer following the manufacturer's protocol. Following synthesis, oligonucleotides were cleaved from the columns and deprotected using an UltraFAST Cleavage and Deprotection kit (Beckman Instruments, Inc.) following the manufacturer's protocol. Cleaved and deprotected oligonucleotides were dried at 55°C in an evaporation chamber under vacuum set at ~0 in Hg for 15 minutes (slight vacuum) and then at 2 in Hg vacuum for 45 minutes. Dried oligonucleotides were dissolved in 100 µL of sterile distilled water and subsequently quantitated (section 2.3.4).

Some of the oligonucleotides used were synthesized on a Perkin-Elmer/Applied Biosystems Model 394 DNA Synthesizer using cyanoethyl chemistry in the DNA Core Facility in the Department of Biochemistry, University of Alberta.

Table 2.2 gives a list of all synthetic oligonucleotides used as primers for PCR, RACE, and DNA sequencing. The numbering of nucleotide positions spanned by primers corresponding to known cDNA or genomic DNA sequences is based on the following Genbank database entries: rat peroxisomal 3-ketoacyl-CoA thiolase B gene accession no. D90059 (Hijikata *et al.*, 1990); mPPAR $\gamma$ 2 cDNA, accession no. U09138 (Tontonoz *et al.*, 1994a); hPPAR $\gamma$  cDNA, accession no. L40904 (Greene *et al.*, 1995); mouse cytoskeletal  $\beta$ -actin cDNA, accession no. X03672 (Tokunaga *et al.*, 1986); human cytoplasmic  $\beta$ -actin gene, accession no. M10277 (Nakajima-Iijima *et al.*, 1985); human  $\beta$ -actin cDNA, accession no. X00351 (Ponte *et al.*, 1984). The human PPAR $\gamma$  gene intron sequences used to create the hPPAR $\gamma$  exon amplimers are given in Genbank entries with accession numbers AB005520-AB005526 (Okazawa *et al.*, 1997).

### 2.3.14 Polymerase Chain Reactions

DNA fragments were amplified from libraries, genomic DNA, cDNAs, and plasmid DNA using the polymerase chain reaction (PCR), a procedure first described by Saiki *et al.* (1985) and Mullis and Faloona (1987). The protocols followed were modified from Ausubel *et al.* (1996) and Innis *et al.* (1990).

#### 2.3.14.1 Reaction composition and cycling parameters

Reactions consisted of an aliquot of template DNA (as little as 10 ng or less for plasmid DNA, up to 1  $\mu$ g for genomic DNA, or 1-5  $\mu$ L of a library phage stock), 25 pmol of each oligonucleotide primer solution, PCR buffer (customized or commercial) containing magnesium, dNTPs, 2.5 U of commercially prepared *Taq* DNA polymerase, and sterile distilled water to a final volume of 50  $\mu$ L or 100  $\mu$ L. Reactions were overlaid with 3 drops of mineral oil to prevent evaporation during cycling. Optimal reaction composition varied depending on the template and primer sets used, with modifications commonly made to the amount of primers added, PCR buffer composition, and magnesium concentration.

Alternatively, Ready-To-Go<sup>®</sup> PCR Beads (Pharmacia Biotech, Baie D'Urfé, PQ) were utilized according to the manufacturer's protocol for performing PCRs, necessitating the addition of only template DNA, primers, and sterile distilled water to a final volume of 25  $\mu$ L. Upon complete solubilization of the beads, reactions contained

1.5 U of *Taq* DNA polymerase, 10 mM Tris-HCl (pH 9.0), 50 mM KCl, 1.5 mM MgCl<sub>2</sub>, 200 μM dNTPs, and stabilizers including BSA.

All PCRs were performed in a RoboCycler 40 Temperature Cycler (Stratagene). Typical reactions were initiated with one cycle of template denaturation for 5 minutes at 95°C. This was followed by 25–40 cycles of denaturation for 1 minute at 95°C, annealing of the oligonucleotide primers to denatured template DNA for 1 minute at 5°C below the lowest primer melting temperature ( $T_m$ ), determined by the equation:

$$T_m = 2(A + T) + 4(G + C)$$

and extension of annealed primers by *Taq* DNA polymerase at 72°C for 1 minute per length in kilobases of the desired product. A final extension cycle at 72°C for 7 minutes completed the reactions. As for reaction composition, optimal cycle parameters also varied depending on the particular reaction performed. A greater number of cycles was used for the amplification of lower abundance species. Variable annealing temperatures were used for varying the stringency conditions for the hybridization of primers to template DNA. As well, changes in the duration of the extension step in the amplification were made based on the length of the desired products.

#### 2.3.14.2 *Analysis of PCR products*

Following completion of PCRs, one-tenth of the reaction volume was loaded into an agarose gel of appropriate concentration and reaction products were analyzed and quantitated by agarose gel electrophoresis (sections 2.3.4 and 2.3.5). For subsequent subcloning and/or sequencing of PCR products, products of interest were first digested with appropriate restriction endonucleases (section 2.3.6) or blunt-ended (section 2.3.7.2) where necessary, and then purified either by electroelution (section 2.3.8) or through the use of a QIAquick™ PCR Purification or QIAquick™ Gel Extraction kit (QIAGEN Inc.) according to the manufacturer's protocol. For direct sequencing of purified PCR products, dilute preparations were concentrated to ~1 ng/base in 5 μL of sterile distilled water (section 2.3.9). PCR products subjected to DNA sequencing were reamplified and resequenced to account for the occasional occurrence of nucleotide incorporation errors made by *Taq* DNA polymerase.

### 2.3.15 DNA Sequencing

#### 2.3.15.1 *Manual sequencing*

Double-stranded plasmid DNA prepared by the alkaline lysis method (section 2.3.2.1) was used as a template for dideoxynucleotide sequencing of both strands (Sanger *et al.*, 1977; Zhang *et al.*, 1988) using the Sequenase™ version 2.0 DNA Sequencing kit and T7 Sequenase™ DNA polymerase version 1.0 (United States Biochemicals, Cleveland, OH) according to the manufacturer's protocol. Reaction products were resolved on 5% Long Ranger™ acrylamide gels (J. T. Baker Inc., Toronto, ON) containing 8 M urea and 1.2X TBE. Gels were run on a Model S2 Sequencing Gel Electrophoresis Apparatus (Gibco/BRL) in 0.6X TBE running buffer at 60 watts per gel, dried on a Bio-Rad Model 583 Gel Dryer (Bio-Rad Laboratories, Hercules, CA), and exposed to X-ray film.

#### 2.3.15.2 *Automated sequencing*

Purified PCR products corresponding to amplified human PPAR $\gamma$  exon sequences were subjected to direct sequencing using PRISM™ Dye Terminator chemistry with a Perkin-Elmer/Applied Biosystems Model 373A DNA Sequenator (PE Applied Biosystems, Foster City, CA) in the DNA Core Facility in the Department of Biochemistry, University of Alberta.

#### 2.3.15.3 *DNA sequence analysis*

Computer analysis of DNA sequences was performed using the PC/GENE software (IntelliGenetics, Inc., Mountain View, CA). Homology searches were performed using the Basic Local Alignment Search Tool (BLAST) algorithm (Altschul *et al.*, 1990) of the National Center for Biotechnology Information (NCBI; Bethesda, MD). Analysis of nucleotide and protein databases was performed using the blastn and blastp search programs respectively. Both the Standard BLAST server (<http://www.ncbi.nlm.nih.gov>) and the NCBI BLAST Email server ([blast@ncbi.nlm.nih.gov](mailto:blast@ncbi.nlm.nih.gov)) were used for performing the homology searches.

## 2.4 LIBRARY SCREENING

### 2.4.1 Library Screening by Hybridization

For the isolation of thiolase B promoter sequences, a rat liver genomic library constructed in Lambda GEM™-11 (Promega Corporation) was titred and screened using a protocol modified from Ausubel *et al.* (1996). The host bacterial strain used for plating

the library was *E. coli*. Strain KW251 (Promega Corporation). KW251 cells were maintained on a stock plate of LB agar supplemented with 25 µg/mL of tetracycline in 70% ethanol, from which colonies were picked for growth of overnight host cultures in 3 mL of LB containing 0.2% (w/v) maltose.

#### 2.4.1.1 *Plating phage*

For plating phage, 200 µL of the overnight host culture was mixed with 100 µL of phage dilution buffer (10 mM Tris-HCl (pH 7.5), 10 mM MgCl<sub>2</sub>) and an appropriate dilution of the library containing approximately 10,000 plaque-forming units (pfu). The mixtures were incubated at room temperature for 20 minutes prior to the addition of 3 mL of melted LB soft top agarose (0.7% (w/v) electrophoresis grade agarose in LB) cooled to 47°C, followed by mixing with vortexing. The mixtures were immediately plated onto 84-mm diameter LB plates pre-warmed to 37°C and allowed to solidify at room temperature. Plates were incubated at 39°C for 6-12 hours until bacteriophage plaques approached confluence.

#### 2.4.1.2 *Plaque lifts*

Double lifts of the plates containing subconfluent plaques were performed by overlaying the top agarose with two 82-mm nitrocellulose discs (Schleicher & Schuell, Inc., Keene, NH) in succession. The first disc was placed on the lysed bacterial lawn for one minute, and the second disc remained on the surface of the top agarose for 2-3 minutes. The orientation of each disc was marked by stabbing a 20-G needle through the nitrocellulose into the underlying agar at several asymmetric points around the edge of the plate. After removal of the discs, the phage were lysed and the DNA was denatured by overlaying the discs, phage-side up, onto 1 mL of denaturing solution (0.5 M NaOH, 1.5 M NaCl) for 1 minute. The discs were then immersed in neutralizing solution for 8 minutes, followed by washing in 5X SSC for 5 minutes. The discs were allowed to air dry prior to fixing the phage DNA to the nitrocellulose by exposure to uv light (section 2.3.12).

#### 2.4.1.3 *Detection of positive phage plaques*

Following uv cross-linking, the discs were prehybridized, hybridized with a radioactively labelled probe corresponding to a region of the thiolase B promoter, and washed to remove excess probe according to the protocol used for Southern blotting

(section 2.3.12.2). Dried discs were wrapped in cellophane and exposed to X-ray film for 24 hours at -80°C using a DuPont Cronex® Lightning Plus intensifying screen (DuPont Biotechnology Systems, Boston, MA). Positive phage plaques were identified by aligning the hybridization signals on film to the orientation of the nitrocellulose discs applied to the phage-containing plate.

#### 2.4.1.4 *Phage purification*

Positive phage plaques were picked from the plate using the wide end of a flame-sterile Pasteur pipette to excise a plug of agar containing the plaque of interest. The phage plug was immersed in 1 mL of SM buffer (100 mM NaCl, 8 mM MgSO<sub>4</sub>·7H<sub>2</sub>O, 50 mM Tris-HCl (pH 7.5), 0.01% gelatin) containing one drop of chloroform. Phage were eluted from the plug by incubation at room temperature for 3–4 hours or at 4°C for long-term storage. An aliquot of an appropriate dilution of the phage plug suspension in SM was used for a secondary screen, followed by excision of a single positive phage plaque, phage elution into SM, and a subsequent tertiary screen to ensure homogeneity of the phage within the positive plaque isolated. A 5 µL aliquot of a more concentrated phage plug suspension (a smaller plug excised using the narrow end of a Pasteur pipette and immersed in 25 µL of sterile distilled water) was occasionally used as the source of DNA template in PCR reactions (section 2.3.14) performed for the direct amplification and analysis of library inserts in positive phage plaques.

#### 2.4.1.5 *Harvesting positive phage clones*

Plate lysates were made for positive phage by plating 50 µL of the tertiary phage plug suspension in SM mixed with 100 µL of a host KW251 overnight bacterial culture and 3 mL of melted LB soft top agarose onto LB agar plates. Plates were incubated at 39°C for 6–8 hours until near complete lysis of the bacterial lawn was achieved. The top agarose was then scraped off the agar surface using the edge of a flame-sterilized glass microscope slide and transferred to a sterile 50-mL high-speed centrifuge tube. The plate was rinsed with 5 mL of SM buffer and the rinse was added to the centrifuge tube. The top agarose and SM rinses of up to 4 plates were placed in each centrifuge tube, along with 100 µL of chloroform per plate. The centrifuge tubes were tightly capped and vortexed vigorously followed by incubation at room temperature for 10 minutes. The agarose and bacterial cell debris was pelleted by centrifugation in a Beckman JA-17 fixed-angle rotor at 13,800 x g for 10 minutes at 4°C. The supernatant

was transferred to a sterile centrifuge tube and stored at 4°C with one drop of chloroform added per plate used to create the lysate.

#### **2.4.1.6 *DNA isolation from plate lysates***

Positive phage DNA was isolated from plate lysates using the LambdaSorb® Phage Adsorbant (Promega Corporation) following the manufacturer's protocol. To eliminate any contaminating RNA present in the DNA preparations, isolated DNA samples were subjected to RNase A treatment according to the manufacturer's protocol supplied.

#### **2.4.1.7 *Analysis of positive phage DNA***

RNase A-treated DNA samples were quantitated using OD<sub>260</sub> measurements (section 2.3.4). Southern blotting of DNA samples with the probe used for library screening was performed to confirm hybridization (section 2.3.12). Library inserts were excised from the lambda phage DNA arms by restriction endonuclease digestion with *Sfi*I (section 2.3.6). Inserts were blunt-ended (section 2.3.7) and subcloned (section 2.3.10.3) into *Sma*I-digested pGEM7Zf(+) for subsequent restriction mapping, further subcloning, DNA sequencing, and use in PCR.

### **2.4.2 Library Screening by PCR**

Specific oligonucleotides were synthesized (section 2.3.13) for the isolation and amplification of DNA sequences by PCR from genomic and cDNA libraries constructed in plasmid and/or phage  $\lambda$  vectors.

#### **2.4.2.1 *Screening plasmid libraries***

For screening libraries constructed in a plasmid vector, an appropriate library dilution was made to enable the use of up to 1  $\mu$ g of plasmid DNA as template in a 100  $\mu$ L final PCR reaction volume. Reactions were performed and analyzed as previously described (section 2.3.14).

#### **2.4.2.2 *Screening phage libraries***

For screening libraries constructed in a phage  $\lambda$  vector, a protocol modified from Innis *et al.* (1990) was followed. An aliquot of the library or an appropriate dilution containing ~50,000 pfu was used as the source of template DNA in a 100  $\mu$ L PCR



reaction volume. Prior to the addition of *Taq* DNA polymerase, assembled reaction components were heated at 95°C for 3 minutes to disrupt phage particles. Following cooling of the heated reaction mixtures on wet ice and a brief spin at ~13,000 x g in a microcentrifuge at room temperature to collect condensate, *Taq* DNA polymerase was added and the reactions were overlaid with three drops of mineral oil. PCR was then performed and reaction products were analyzed as previously described (section 2.3.14).

#### **2.4.2.3 Screening with single-sided specificity PCR**

To isolate and amplify previously unidentified sequences, such as promoter regions or the 5' and 3' termini of novel coding sequences, a PCR procedure was employed using one gene-specific oligonucleotide primer and one non-specific primer. The gene-specific primer was designed from the known sequence of DNA immediately adjacent to the region to be isolated. Two non-specific primers were designed for each library screened in this manner, corresponding to specific sequences found in the multiple cloning site regions of the library vector flanking the insert. Two PCRs were performed in attempts to amplify each unknown sequence, utilizing each of the non-specific primers in conjunction with the gene-specific primer to account for the bi-directional cloning of inserts within the libraries screened.

## **2.5 RNA MANIPULATION**

To inhibit RNase activity, all solutions used for procedures involving RNA manipulation were treated with diethylpyrocarbonate (DEPC) as described in Ausubel *et al.* (1996). In addition, all glassware used in such procedures was baked at 300°C in a Fisher Isotemp® Oven (Fisher Scientific, Pittsburgh, PA) for 3 hours. Where possible, RNase-free plasticware was also used.

### **2.5.1 Isolation and Quantitation of Total RNA**

Total RNA was extracted from cultured mammalian cells by a phenol/guanidine thiocyanate-based method using the TRI Reagent® RNA/DNA/Protein Isolation Reagent (Molecular Research Center, Inc., Cincinnati, OH) following the manufacturer's protocol. Alternatively, an RNeasy™ Total RNA kit (QIAGEN Inc.) was occasionally used following

the manufacturer's protocol. Isolated total RNA samples were dissolved in DEPC-treated sterile distilled water. Assessment of yield and purity of total RNA preparations was performed as described for purified DNA samples (section 2.3.4). RNA concentration was calculated according to the conversion:

$$1 \text{ OD}_{260} \text{ unit} = 40 \text{ } \mu\text{g/mL of RNA}$$

Pure RNA samples prepared by the above methods were free of contaminating DNA and proteins as determined by an  $\text{OD}_{260}/\text{OD}_{280}$  ratio of 1.6-2.0.

### 2.5.2 Isolation of Poly(A)<sup>+</sup> RNA

Poly(A)<sup>+</sup> RNA was isolated from total RNA preparations by biomagnetic separation using Dynabeads<sup>®</sup> Oligo (dT)<sub>25</sub> (DynaL Inc., Lake Success, NY) following the manufacturer's protocol. By this method, the binding of RNA species containing poly(A) tails to oligo(dT)<sub>25</sub> sequences covalently coupled to magnetic beads enabled the elimination of all unbound ribosomal and transfer RNA molecules found in the total RNA sample. The predicted yield of poly(A)<sup>+</sup> RNA isolated using this procedure was 1  $\mu\text{g}$  per 37.5  $\mu\text{g}$  total RNA starting material, or roughly 2.7%. Following separation, the poly(A)<sup>+</sup> RNA was either eluted from the beads into RNA loading buffer for subsequent Northern blotting (section 2.5.5), or remained bound to the beads for use in downstream enzymatic amplifications such as RT-PCR (section 2.5.3) or RACE (section 2.5.4).

### 2.5.3 Reverse Transcription – Polymerase Chain Reaction (RT-PCR)

Enzymatic amplification of RNA by PCR was performed using a modified protocol from Ausubel *et al.* (1996). Total RNA or poly(A)<sup>+</sup> RNA (either bound to or eluted from oligo(dT)<sub>25</sub>-conjugated magnetic beads (section 2.5.2)) was used as the starting template for reverse transcription using either an oligo(dT)-based, gene-specific, or random hexamer cDNA synthesis primer.

#### 2.5.3.1 Preparation of primed templates

For RNA template molecules free in solution, 3 pmol of cDNA primer was annealed with 2  $\mu\text{g}$  of the RNA sample first by co-precipitation with 0.3 M sodium acetate (pH 5.2) and 2 volumes of absolute ethanol incubated overnight at -20°C. Co-precipitated primers and templates were pelleted by centrifugation at ~13,000 x g for 15 minutes at 4°C in a microcentrifuge. Pellets were washed with 70% ethanol,

recentrifuged, and dried for 10 minutes in a speed vac evaporator. The pellets were dissolved in 80 mM Tris-HCl (pH 8.3), 80 mM KCl, heated to 90°C in a heating block, and cooled slowly to 67°C to initiate annealing. The mixtures were then microcentrifuged for 1 second to collect condensation, followed by incubation at 52°C for 3 hours to proceed with the annealing. The mixtures were again centrifuged to collect condensation prior to reverse transcription.

For poly(A)<sup>+</sup> RNA templates bound to oligo(dT)<sub>25</sub>-conjugated magnetic beads, the primer used for cDNA synthesis was the oligo(dT)<sub>25</sub> sequence already annealed to the poly(A)<sup>+</sup> RNA molecules. Thus, in effect a solid-phase first-strand cDNA library was synthesized by reverse transcription. The poly(A)<sup>+</sup> RNA-beads preparation was washed three times with cold reverse transcriptase wash buffer (10 mM Tris-HCl (pH 8.3), 75 mM KCl) prior to reverse transcription.

#### 2.5.3.2 *Reverse transcription*

Preparations of annealed RNA templates and cDNA primers were subjected to reverse transcription in a 50 µL reaction volume containing reverse transcriptase reaction buffer (50 mM Tris-HCl (pH 8.3), 75 mM KCl, 10 mM DTT, 3 mM MgCl<sub>2</sub>, 0.5 mM dNTPs), 20 U of RNasin RNase inhibitor and 200 U of SuperScript™ RNase H<sup>-</sup> Reverse Transcriptase (Gibco/BRL). The reactions were carried out for 1 hour at 37-55°C depending on primer composition.

#### 2.5.3.3 *cDNA purification*

Following cDNA synthesis, reverse transcription reactions not involving the use of magnetic beads were mixed with 150 µL of 10 mM Tris-HCl (pH 7.5), 10 mM EDTA (pH 7.5), and proteins were extracted with the addition of 200 µL of buffered phenol. DNA was precipitated from the final aqueous phase with 0.3 M sodium acetate (pH 5.2) and absolute ethanol following an additional organic extraction with an equal volume of chloroform/isoamyl alcohol (24:1). DNA allowed to precipitate for 15 minutes at -80°C or overnight at -20°C was subsequently pelleted by centrifugation at ~13,000 x g for 15 minutes at 4°C in a microcentrifuge. The purified cDNA pellets were dried for 10 minutes in a speed vac evaporator, resuspended in 40 µL of sterile distilled water, and stored at -20°C prior to PCR amplification.

For reverse transcription reactions performed using the oligo(dT)<sub>25</sub>-conjugated magnetic beads, the beads on which the cDNA was synthesized were isolated from the reactions using a Magnetic Particle Concentrator (MPC; Dynal, Inc.) following the manufacturer's protocol. The cDNA attached to the beads was then purified away from the poly(A)<sup>+</sup> RNA strands by heating at 95°C for 1 minute, removal of the denatured free RNA molecules using the MPC, and treatment with 2 U of RNase H for 10 minutes at 55°C to remove any residual RNA bound to the cDNA. The resulting preparation of purified cDNA molecules conjugated to the beads was stored in 1<sup>st</sup> strand cDNA storage buffer (20 mM Tris-HCl (pH 8.3), 50 mM KCl, 1.5 mM MgCl<sub>2</sub>, 0.1 mg/mL BSA) at 4°C prior to PCR amplification.

#### **2.5.3.4 *PCR amplification of cDNA***

For purified cDNA samples without attached magnetic beads, a 5 µL aliquot was used as the template in a PCR reaction to amplify cDNA sequences using nested gene-specific primers, i.e. primers internal to those used for cDNA synthesis. PCR was performed and the products were analyzed as previously described (section 2.3.14).

For purified cDNA samples coupled to magnetic beads, a 2<sup>nd</sup> strand cDNA synthesis reaction was performed in a PCR 'pre-cycle'. The beads were first washed with cold PCR reaction buffer. The 2<sup>nd</sup> strand cDNA synthesis reaction mix was assembled using standard PCR reaction components (section 2.3.14) and a single primer designed from the sequence at the 5' end of the transcript in order to prime synthesis of the 2<sup>nd</sup> strand. The reaction was incubated at 60°C for 2 minutes to enable annealing of the primer with the 1<sup>st</sup> strand cDNA, followed by extension of the primer by *Taq* DNA polymerase for 40 minutes at 72°C. The resulting double-stranded cDNA molecules attached to the beads via the oligo(dT)<sub>25</sub> sequence at the 5' end of the 1<sup>st</sup> strand were purified using the MPC, washed with PCR reaction buffer, and subsequently used as templates for PCR. Amplification of the cDNA was performed with nested gene-specific primers and the products were analyzed as previously described (section 2.3.14).

#### **2.5.4 Rapid Amplification of cDNA Ends (RACE)**

For the isolation and identification of novel sequences at the 5' and 3' termini of partial cDNA molecules to generate full-length cDNA copies of mRNA transcripts, a

modification of the RT-PCR procedure (section 2.5.3) termed rapid amplification of cDNA ends (RACE) was performed (Frohman *et al.*, 1988). The protocols followed were adapted from Innis *et al.* (1990). Poly(A)<sup>+</sup> RNA was isolated from total RNA preparations as described (section 2.5.2), followed by reverse transcription and purification of synthesized 1<sup>st</sup> strand cDNA molecules attached to magnetic beads (sections 2.5.3.1 - 2.5.3.3). Subsequent steps varied depending on the desired isolation of either 5' or 3' cDNA sequences.

#### 2.5.4.1 5' RACE

To amplify regions upstream of a known sequence, 5' RACE was performed. The purified 1<sup>st</sup> strand cDNA attached to the beads was washed with cold terminal deoxynucleotidyltransferase (TdT) buffer (100 mM cacodylate buffer (pH 6.8), 1 mM CoCl<sub>2</sub>, 0.1 mM DTT, 0.1 mg/mL BSA), followed by heating at 70°C for 5 minutes and quick cooling on wet ice to eliminate secondary structure. A poly(C) tail was then appended onto the 3' end of the 1<sup>st</sup> strand cDNA in a reaction containing 10 U of terminal transferase, 0.2 mM dCTP, TdT buffer, and a final concentration of 2.5 mM CoCl<sub>2</sub>. The tailing reactions were carried out at 37°C for 10 minutes, and the reactions stopped by heat-inactivating the terminal transferase enzyme at 68°C for 15 minutes. The poly(C)-tailed 1<sup>st</sup> strand cDNA attached to the beads was purified using the MPC and then washed with cold PCR reaction buffer. 2<sup>nd</sup> strand cDNA synthesis was subsequently performed as previously described (section 2.5.3.4), using 1 pmol of a 5' RACE Anchor Primer (Gibco/BRL) consisting of the sequence:

5'-(CUA)<sub>4</sub> GGC CAC GCG TCG ACT AGT ACG GGI IGG GII GGG IIG-3'

The 48-nucleotide primer contains deoxyinosine (I) residues strategically positioned to maximize specific priming from the poly(C) tail.

Following 2<sup>nd</sup> strand cDNA synthesis, the double-stranded cDNA molecules were purified using the MPC and subsequently served as the template for PCR amplification reactions (section 2.3.14). Single-sided specificity PCR was performed (section 2.4.2.3) using a gene-specific primer designed from the known sequence of the cDNA as the reverse primer, and a non-specific primer consisting of 21 nucleotides at the 5' end of the anchor primer, or the anchor primer itself, as the forward primer. Positive control PCRs were also performed to amplify fragments of known cDNA sequences synthesized from transcripts known to be present in the initial RNA sample (e.g.  $\beta$ -actin). The resulting PCR products were first analyzed by agarose gel

electrophoresis (section 2.3.14), followed by Southern blotting (section 2.3.12) with a specific probe corresponding to the known region at the 3' end of the cDNAs amplified to confirm the specificity of the generated products. Specific products were subsequently blunt-ended (section 2.3.7.2), purified (section 2.3.8), subcloned (section 2.3.10.3), and manually sequenced (section 2.3.15.1) as previously described.

As a result of <100% efficiency of the reverse transcription step, most 5' RACE products analyzed did not contain sequences corresponding to the extreme 5' termini of the cDNAs amplified. Further attempts to amplify full-length cDNA sequences in the PCR reactions were performed using a gene-specific primer positioned in a region further upstream of the originally known cDNA sequence, as identified by sequencing of previous 5' RACE products.

#### **2.5.4.2 3' RACE**

To amplify regions downstream of a known sequence, 3' RACE was performed. The procedure followed was essentially as that described for RT-PCR involving amplification of 1<sup>st</sup> strand cDNA samples coupled to magnetic beads (section 2.5.3.4). As with 5' RACE (section 2.5.4.1), the PCR reactions were performed with single-sided specificity, in this case using one gene-specific primer as the forward primer and a non-specific oligo(dT)-based primer as the reverse primer. Positive control PCRs were also performed, and all PCR products were subsequently analyzed as described for those generated by 5' RACE (section 2.5.4.1).

#### **2.5.5 Northern Blot Analysis**

Northern blotting of total RNA and poly(A)+ RNA preparations was performed by a protocol adapted from Ausubel *et al.* (1996). RNA samples were mixed with 3 volumes of RNA loading buffer (~65.2% (v/v) deionized formamide, ~21.7% (v/v) formaldehyde, ~13.0% (v/v) 20X borate buffer [0.4 M boric acid, 4 mM EDTA (pH 8.3)]) and 1  $\mu$ L of 10 mg/mL ethidium bromide for direct visualization in agarose gels exposed to ultraviolet light. The mixtures were heated at 65°C for 5 minutes and quick-cooled on wet ice to eliminate secondary structure. A one-sixth volume of gel dye (section 2.3.5) was added prior to loading of the samples into a 1% formaldehyde-agarose gel (1% GTG agarose, 1X borate buffer, and 9% (v/v) formaldehyde made up to the appropriate volume with DEPC-treated sterile distilled water). RNA molecules were separated by

electrophoresis in 1X borate buffer at ~5 V/cm in a horizontal submarine electrophoresis apparatus (Hoefer Scientific Instruments). Gels were run until adequate resolution of the 18S and 28S ribosomal RNA internal marker molecules was achieved, as determined by visualization of the corresponding discrete ethidium bromide-stained bands when gels were viewed on a uv transilluminator and photographed. Upon completion of electrophoresis, formaldehyde was removed from gels with three 10-minute washes in DEPC-treated sterile distilled water. Gels were then soaked in 10X SSC for 45 minutes, followed by transfer of the RNA molecules to a nylon membrane (Hybond™-N, Amersham Life Sciences) by capillary action using a transfer pyramid and 20X SSC transfer buffer (0.3 M tri-sodium citrate (pH 7.0), 3 M NaCl). Transfer was carried out at room temperature for 12-16 hours. Following transfer, blots were briefly rinsed in 2X SSC and air-dried. RNA molecules were covalently fixed to the nylon membrane by uv cross-linking as described for Southern blots (section 2.3.12).

#### 2.5.5.1 *Assessment of RNA transfer efficiency*

The efficiency of transfer of the RNA molecules to the nylon membrane was assessed by two methods. Following uv cross-linking, blots were stained for 1 minute in a solution of 0.03% (w/v) methylene blue dissolved in 0.3 M sodium acetate (pH 5.2). Blots were then destained in DEPC-treated sterile distilled water for 2 minutes and photographed. RNA present on the blot was stained a bright blue colour. Continued destaining of the blot in DEPC-treated sterile distilled water removed most of the methylene blue from the RNA samples.

Additionally, agarose gels were stained with ethidium bromide following transfer as described for Southern blotting (section 2.3.12).

#### 2.5.5.2 *Hybridization with radiolabelled DNA probes*

Prehybridization of Northern blots was performed at 68°C for 30 minutes in pre-warmed ExpressHyb™ Hybridization solution (CLONTECH Laboratories Inc.). Hybridization was then carried out in fresh, pre-warmed ExpressHyb™ solution containing  $1-2 \times 10^6$  cpm/mL of heat-denatured radiolabelled probe at 68°C for one hour. Blots were washed four times in low stringency wash buffer (2X SSC, 0.1% SDS) at room temperature for 10 minutes per wash, followed by two 20-minute washes in pre-warmed high stringency wash buffer (0.1X SSC, 0.1% SDS) at 50°C. Moist blots were

then wrapped in cellophane and exposed to X-ray film with an intensifying screen at -80°C for 1-7 days.

#### **2.5.5.3 *Stripping and reprobing blots***

In order to detect the presence of different transcripts in RNA samples using a number of different DNA probes, Northern blots were successively stripped and reprobed. Following exposure to film, moist blots were immersed in boiling stripping solution (0.1X SSC, 10 mM EDTA (pH 8.0), 0.1% SDS, made up to 500 mL with DEPC-treated sterile distilled water) for 5 minutes, then transferred to a fresh volume of boiling stripping solution for an additional 5-minute incubation. Blots were then rinsed briefly in 0.1X SSC, air-dried, and stored at room temperature between sheets of Whatman paper (Whatman Paper Ltd., Clifton, NJ) prior to reprobing. Before subsequent prehybridization, dry blots were rewet by immersion in 0.1X SSC.

Reprobing of Northern blots with a human  $\beta$ -actin cDNA probe was performed to verify that equal amounts of RNA were present in each lane on the blot, as done for DNA samples in Southern blots (section 2.3.12.3), and that RNA transcripts remained intact throughout the Northern blotting procedure. In addition,  $\beta$ -actin hybridization signals were used to normalize densitometry measurements.

#### **2.5.5.4 *Quantitative analysis of hybridization signals by densitometry***

Quantitation of hybridization signals appearing on autoradiographs of Northern blots was performed by densitometry using a LKB 2222-010 UltroScan XL Laser Densitometer (LKB-Produkter AB, Bromma, Sweden) following the manufacturer's protocol. Measurements of signal intensity were taken for the darkest region of each band appearing on the X-ray films analyzed.

#### **2.5.5.5 *Multiple tissue Northern blot***

A human multiple tissue Northern blot containing approximately 2  $\mu$ g of poly(A)<sup>+</sup> RNA from each of 8 different human tissues (heart, brain, placenta, lung, liver, skeletal muscle, kidney, pancreas) was purchased from CLONTECH Laboratories and stored at 4°C. This blot was probed with a human PPAR $\gamma$  cDNA fragment corresponding to sequences found in exons 3 and 4 of the PPAR $\gamma$  gene. Hybridization and stripping of the blot were performed as previously described (sections 2.5.5.2 and 2.5.5.3).



## **2.6 PROTEIN ANALYSIS**

### **2.6.1 Preparation of Protein Samples**

#### **2.6.1.1 *Protein extracts of cultured cells***

Proteins were isolated from cultured mammalian cells (after total RNA extraction and removal of the DNA-containing phase from the remaining total cell lysate) using the TRI-Reagent® (Molecular Research Center, Inc.) according to the manufacturer's protocol. Protein pellets were dissolved in 40 µL of 1% SDS with incubation at 50°C for a few hours. Insoluble material was removed by centrifuging at 10,000 x g for 10 minutes at 4°C in a microcentrifuge, and transferring the supernatant containing soluble proteins to a new tube. Protein samples were then quantitated (section 2.6.2) prior to storage at -80°C.

Alternatively, cultured cells grown to confluence were first washed twice with 5 mL of PBS pre-warmed to 37°C, then harvested into 1 mL of cold PBS using a cell lifter and transferred to a microcentrifuge tube. Harvested cells were pelleted by centrifugation at ~13,000 x g for 10 seconds at 4°C and the supernatant was discarded. Cell pellets were resuspended in 150 µL of lysis buffer (50 mM Tris-HCl (pH 8.0), 0.1% NP-40, 0.2 U/mL aprotinin, 1 mM PMSF in ethanol), followed by incubation on ice for 30 minutes with intermittent vortexing. Cell debris was pelleted by centrifugation at ~13,000 x g for 10 minutes at 4°C in a microcentrifuge. The supernatants were then transferred to a fresh microfuge tube and assayed for protein concentration (section 2.6.2) prior to storage at -80°C.

#### **2.6.1.2 *In vitro transcribed/translated protein samples***

For use as a positive control protein sample in Western blots, *in vitro* transcribed and translated PPAR $\gamma$  protein was prepared from a plasmid obtained from Dr. Bruce Spiegelman (Dana-Farber Cancer Institute, Boston, MA) encoding the mPPAR $\gamma$ 2 cDNA cloned into the pSV-SPORT vector (Gibco/BRL). Protein was synthesized using the TNT™ Coupled Reticulocyte Lysate System (Promega Corporation) in a non-radioactive reaction according to the manufacturer's protocol.

### **2.6.2 Quantitation of Protein Samples**

Total protein was measured using a Bio-Rad protein assay based on the method of Bradford (1976). Duplicate aliquots of the protein sample to be quantitated were diluted in 100  $\mu$ L of sterile distilled water and mixed with Bio-Rad protein assay dye by vortexing. Following incubation for 10 minutes at room temperature, OD<sub>595</sub> measurements were taken using a Beckman DU 640 Spectrophotometer. Five dilutions of a 1 mg/mL BSA solution were used to generate a standard curve from which the concentrations of the unknown protein samples were determined.

### **2.6.3 Concentration of Protein Samples**

To concentrate dilute protein samples in a smaller volume, proteins were precipitated upon the addition of 10% (v/v) trichloroacetic acid and incubation on ice for 15 minutes. Proteins were then pelleted by centrifugation at  $\sim 13,000 \times g$  for 30 minutes at 4°C in a microcentrifuge. Protein pellets were washed twice with 1 mL of 80% acetone pre-cooled to -20°C, with a 5-minute centrifugation at 4°C after each wash. The washed pellets were dried in a speed vac evaporator for 10 minutes and resuspended in an appropriate volume of SDS-PAGE sample buffer (section 2.6.4). Protein samples were then boiled for 5 minutes prior to storage at -20°C or immediate use in SDS-PAGE (section 2.6.4).

### **2.6.4 Sodium Dodecyl Sulfate - Polyacrylamide Gel Electrophoresis (SDS-PAGE)**

Protein samples to be analyzed by SDS-PAGE were first mixed with SDS-PAGE sample buffer (83 mM Tris-HCl (pH 6.8), 1% SDS, 1% DTT, 10% glycerol, 0.0025% bromophenol blue) followed by boiling for 5 minutes. Heat-denatured protein samples were separated by SDS-PAGE according to the basic protocol of Laemmli (1970). 7.5% or 10% discontinuous polyacrylamide gels were cast and run using a Mini-Protean II Dual Slab Cell apparatus (Bio-Rad). Resolving gels consisted of 368 mM Tris-HCl (pH 8.8), 0.1% SDS, 0.1% (v/v) TEMED, 0.43% ammonium persulfate, and an appropriate volume of a 30% acrylamide/0.8% bis-acrylamide solution to achieve the required acrylamide concentration. Resolving gels were overlaid with isopropanol and allowed to polymerize for 30 minutes prior to pouring of the stacking gel, which contained 60 mM Tris-HCl (pH 6.8), 0.1% SDS, 0.1% (v/v) TEMED, 0.43% ammonium persulfate, 3% acrylamide and 0.08% bis-acrylamide. Stacking gels, into which 10-well, 0.75-mm

thickness combs were inserted, were allowed to polymerize for 30 minutes. After loading protein samples, mini-gels were electrophoresed at 50-200 V in running buffer (50 mM Tris-HCl (pH 8.8), 0.4 M glycine, 0.1% SDS). Prestained broad-range protein molecular weight markers (New England Biolabs, Ltd.) were used to monitor the extent of electrophoresis. Gels were run until the desired marker distribution was achieved.

### **2.6.5 Western Blot Analysis**

Analysis of proteins by Western blotting was performed according to a protocol adapted from Coligan *et al.* (1995).

#### **2.6.5.1 *Transfer of proteins to nitrocellulose***

Following separation by SDS-PAGE, proteins in resolving gels were electrophoretically transferred to a nitrocellulose membrane (Hybond™-C, Amersham Life Sciences) using either a Bio-Rad Trans-Blot Transfer Cell with plate electrodes or a TE Series Transphor Electrophoresis Unit (Hoefer Scientific Instruments). Transfer was carried out at 100 mA for 12-16 hours in transfer buffer (20 mM Tris-HCl (pH 7.5), 150 mM glycine, 20% (v/v) methanol) with continuous stirring.

The efficiency of transfer was assessed by staining the resolving gel in Coomassie blue stain (0.1% Coomassie Brilliant Blue (R-250), 10% (v/v) acetic acid, 35% (v/v) methanol) to enable direct visualization of proteins remaining in the gel following transfer. Additionally, the nitrocellulose blots were immersed in a solution of 0.1% Ponceau S (w/v) in 1% acetic acid for 2-3 minutes, followed by destaining for 2 minutes in sterile distilled water. Proteins transferred to the nitrocellulose were visualized by the appearance of red-stained bands. Continued destaining of the blots in fresh changes of sterile distilled water enabled near complete removal of the Ponceau S stain from the protein samples.

#### **2.6.5.2 *Immunoblotting***

Following assessment of protein transfer (section 2.6.5.1), nitrocellulose blots were blocked in TBST (20 mM Tris-HCl (pH 7.5), 150 mM NaCl, 0.05% (w/v) Tween 20) containing 5% skim milk powder for 30 minutes at room temperature or overnight at 4°C. Blocking solution was replaced by primary detection antibodies diluted in TBST-5% skim milk (Table 2.1) and incubated for 1.5 hours at room temperature or for 12-16 hours at 4°C. Blots were then washed three times in TBST at room temperature for 15 minutes

per wash prior to incubation with horseradish peroxidase (HRP)-conjugated secondary detection antibodies diluted in TBST-5% skim milk (Table 2.1) for 30 minutes at room temperature. Blots were again washed three times in TBST at room temperature for 15 minutes per wash. HRP-conjugated secondary antibodies bound to the blots were detected using the Enhanced Chemiluminescence Western Blotting Detection kit (Amersham Life Sciences) according to the manufacturer's protocol, followed by exposure of the treated blots to Fuji RX X-ray film. Where necessary, moist blots were subsequently wrapped in cellophane and stored at 4°C prior to stripping and reprobing (section 2.6.5.3).

#### **2.6.5.3 *Stripping and reprobing blots***

Occasionally, complete removal of primary and secondary antibodies from nitrocellulose membranes was performed to enable reprobing of Western blots with different antibodies. Blots were immersed in stripping buffer (100 mM  $\beta$ -mercaptoethanol, 2% SDS, 62.5 mM Tris-HCl (pH 6.8)) and incubated at 50°C for 30 minutes with occasional agitation. Blots were then washed twice in TBST at room temperature for 10 minutes per wash, followed by blocking of the nitrocellulose membranes in TBST-5% skim milk overnight at 4°C. Immunodetection was then performed as described (section 2.6.5.2).

### **2.6.6 Antibody Production**

Protocols followed for the production of rabbit polyclonal antibodies raised against a human PPAR $\gamma$ -specific synthetic peptide were modified from Harlow and Lane (1988). Immunization of rabbits and collection of serum was performed by the Health Sciences Laboratory and Animal Services Facility in the Faculty of Medicine, University of Alberta.

#### **2.6.6.1 *Antigen preparation***

A synthetic peptide consisting of the sequence NH<sub>2</sub>-Y-K-Y-D-L-K-L-Q-E-Y-CO<sub>2</sub>H, encompassing amino acids 63-72 of human PPAR $\gamma$ 1 (identical to amino acids 93-102 of hPPAR $\gamma$ 2), was selected as the immunogen for antibody production based on its species and isoform specificity for hPPAR $\gamma$  proteins. The peptide was synthesized as a keyhole limpet hemocyanin (KLH) conjugate used for injection of rabbits, and also as a

BSA conjugate used as a positive control peptide for analysis of antibody specificity in subsequent Western blots (section 2.6.6.3). Peptide synthesis was performed using a Perkin-Elmer/Applied Biosystems Model 430A Peptide Synthesizer with t-Boc and/or Fmoc Na-protection, benzyl/Boc side-chain protection, and HBTU chemistry (PE Applied Biosystems) by the Alberta Peptide Institute, University of Alberta. A 1 mg/mL solution of the KLH-peptide conjugate was prepared by dissolving an appropriate quantity of the lyophilized peptide-conjugate in PBS (pH 8.0) with incubation at 60°C overnight followed by brief sonication to facilitate solubilization. A 0.5 mg/mL BSA-peptide conjugate solution in PBS was similarly prepared for use as an antigen in analytical Western blots (section 2.6.6.3).

#### 2.6.6.2 *Immunization of rabbits*

A 1:1 mixture of an appropriate volume of the KLH-peptide conjugate solution and Freund's complete adjuvant was prepared using a double luer lok syringe assembly. 0.5 mL aliquots of the resulting mixture, containing approximately 250 µg of the KLH-peptide conjugate, were injected subcutaneously into each of two female New Zealand White rabbits. Subsequent to the primary injection, rabbits were injected subcutaneously at six-week intervals with a mixture of 250 µg of the peptide immunogen in 50% Freund's incomplete adjuvant. A total of three injections of each rabbit was performed.

#### 2.6.6.3 *Serum sampling and analysis*

Pre-immune bleeds were obtained from each rabbit prior to injection, and sample bleeds were taken 12 days after each injection. Rabbits were euthanized and terminal bleeds were taken two weeks after the final injections were administered. Serum was cleared of cells by clotting at room temperature for 2-3 hours and at 4°C for 12-16 hours. Clots were removed by centrifugation at approximately 2,000 x g for 15 minutes at room temperature in a clinical centrifuge (International Equipment Co., Needham Heights, MA). Serum was decanted into a sterile 15-mL Falcon tube, followed by recentrifugation to pellet any remaining red blood cells. 0.02% sodium azide was added to the cleared serum and 1-mL aliquots were stored at -80°C.

Serum samples were tested for the presence of antibodies specific for the hPPAR $\gamma$  synthetic peptide immunogen by probing Western blots of the BSA-peptide conjugate subjected to SDS-PAGE followed by transfer to nitrocellulose (sections 2.6.4

and 2.6.5). Multiple blots containing 10 µg of the BSA-peptide conjugate run alongside 10 µg of pure BSA were probed with a series of dilutions of the cleared rabbit serum in TBST-5% skim milk as the primary antibody solution. Immunodetection using HRP-conjugated donkey anti-rabbit IgG as the secondary antibody followed by ECL enabled visualization of protein samples recognized by the antiserum as well as determination of an appropriate dilution of the serum to be used as the primary antibody in subsequent Western blot analyses.

Table 2.1 Properties of antibodies used for immunoblot analyses

antibody/ source	animal <sup>a</sup>	immunogen	specificity <sup>b</sup>	dilution
<i>Primary:</i>				
anti-PPAR $\gamma$ 1,2 BIOMOL Research Laboratories, Inc.	rb	mPPAR $\gamma$ 2 peptide (amino acids 284-298)	h, m, r PPAR $\gamma$ 1,2	1:2,000
anti-PPARs BIOMOL Research Laboratories, Inc.	rb	mPPAR $\gamma$ 2 C-terminal peptide (amino acids 484-498)	h, m, r PPAR $\alpha$ , $\beta$ , $\gamma$ 1, $\gamma$ 2	1:2,000
anti-PPAR $\gamma$ Santa Cruz Biotechnology, Inc.	gt	hPPAR $\gamma$ 1 N-terminal peptide (amino acids 2-20)	h, m, r PPAR $\gamma$ 1,2	1:2,000
anti-PPAR $\alpha$ Santa Cruz Biotechnology, Inc.	gt	hPPAR $\alpha$ N-terminal peptide (amino acids 2-21)	h, m, r PPAR $\alpha$	1:2,000
anti-PPAR $\gamma$ Dr. Joel Berger, Merck Research Labs	rb	hPPAR $\gamma$ 1 peptide (amino acids 87-101)	h, m, r PPAR $\gamma$ 1,2	1:1,000
anti-PPAR $\gamma$ P. Lagali, University of Alberta	rb	hPPAR $\gamma$ 1 peptide (amino acids 63-72)	hPPAR $\gamma$ 1,2	1:500
anti-PPAR $\alpha$ S. Marcus, McMaster University	gp	rPPAR $\alpha$ -MBP fusion protein	rPPAR $\alpha$	1:500
<i>Secondary:</i>				
anti-rabbit IgG:HRP Amersham Life Sciences	dk		rabbit IgG	1:30,000
anti-guinea pig IgG:HRP Sigma Chemical Company	rb		guinea pig IgG	1:50,000
anti-goat IgG:HRP Santa Cruz Biotechnology, Inc.	dk		goat IgG	1:10,000

<sup>a</sup> rb, rabbit; gt, goat; gp, guinea pig; dk, donkey

<sup>b</sup> h, human; m, mouse; r, rat

Table 2.2 Synthetic oligonucleotides used for PCR, RACE, and DNA sequencing

name	sequence	description	T <sub>m</sub>
TPP	5'-AGGCGGTATCTCTAAAC-3'	thiolase B promoter primer (-1173 to -1156)	50°C
TUP	5'-CTGCACCTGTGATGGTGCAAGTCGTT-3'	thiolase B upstream primer (-204 to -229)	61°C
SP6	5'-GATTTAGGTGACACTATAG-3'	SP6 promoter (cloning vector multiple cloning site) primer	52°C
T7	5'-TAATACGACTCACTATAGGG-3'	T7 promoter (cloning vector multiple cloning site) primer	56°C
λgt11-FOR	5'-GACGACTCCTGGAGCCCGTCAGTATC-3'	λgt11 library left phage arm cloning vector primer	84°C
λgt11-REV	5'-CAGACCAACTGGTAATGGTAGCGACC-3'	λgt11 library right phage arm cloning vector primer	80°C
mPPAR <sub>γ</sub> 2-for	5'-ATTCTCGAGGCTGTATGGGTGAAAC-3'	5' mPPAR <sub>γ</sub> 2 cDNA primer with XhoI site (+34 to +50)	50°C
mPPAR <sub>γ</sub> 2-back	5'-ATTCTCGAGCTGCTAATAACAAGTCC-3'	3' mPPAR <sub>γ</sub> 2 cDNA primer with XhoI site (+1560 to +1545)	48°C
mPPAR <sub>γ</sub> 2-for2	5'-TTATGCTGTTATGGGTGAAACTCTGG-3'	5' mPPAR <sub>γ</sub> 2 cDNA primer (+30 to +55)	74°C
mPPAR <sub>γ</sub> 2-rev2	5'-CAATAGAGGAACACAGTTGTCAGCGG-3'	3' mPPAR <sub>γ</sub> 2 mouse-specific cDNA primer (+1597 to +1572)	78°C
uMPPARG2-f	5'-GCATCAGGCTTCCACTATGGAGTTCA-3'	mPPAR <sub>γ</sub> 2 mouse-specific cDNA primer (+475 to +500)	78°C
MPPARG2-rev3	5'-TTAAGGAATTCATGTCGTAGATGACA-3'	mPPAR <sub>γ</sub> 2 cDNA primer (+889 to +864)	70°C
uHPPARG-f (GSP1)	5'-TTCACTATGGAGTTTCATGCTTGTGAA-3'	hPPAR <sub>γ</sub> human-specific cDNA primer (+534 to +559)	72°C
uHPPARG-r	5'-TTCCCTCAGAATAGTGCAACTGGAAG-3'	3' hPPAR <sub>γ</sub> human-specific cDNA primer (+1669 to +1644)	76°C
HPPARG-rev2	5'-GTCTGTTGCTTTCTTGTCAGATCG-3'	hPPAR <sub>γ</sub> cDNA primer (+904 to +879)	78°C
HPPARG f-1 FOR	5'-CAGGAGACAGCACCATTGGTGGTTCT-3'	5' hPPAR <sub>γ</sub> full-length cDNA primer (+41 to +66)	82°C
HPPARG f-1 REV	5'-GAAATGTTGCAGTGGCTCAGGACTC-3'	3' hPPAR <sub>γ</sub> full-length cDNA primer (+1639 to +1614)	80°C
HPPARG-f3 (GSP2)	5'-TCATGCTGTGAAGGATGCAAGGGTT-3'	hPPAR <sub>γ</sub> cDNA/gene-specific primer (+547 to +572)	76°C
HPPARG-r4 (GSP2)	5'-GGAAGGACTTTATGTATGAGTCATAC-3'	hPPAR <sub>γ</sub> cDNA/gene-specific primer (+854 to +829)	72°C
HPPARG ex2-for	5'-CTCATGGCAATTGAATGTCGTGCTCTG-3'	hPPAR <sub>γ</sub> exon 2-specific cDNA primer (+488 to +513)	76°C
hPPAR <sub>γ</sub> ex2mRNA-for	5'-GTGGAGCCTGCATCTCCACCT-3'	hPPAR <sub>γ</sub> exon 2-specific cDNA primer (+410 to +430)	63°C
hPPAR <sub>γ</sub> ex2mRNA-rev	5'-CTTGCACTCCTTCACAAGCATG-3'	hPPAR <sub>γ</sub> exon 2-specific cDNA primer (+568 to +548)	57°C
HPPARG ex3-for	5'-GAGAACAAATCAGATTGAAGCTTATCT-3'	hPPAR <sub>γ</sub> exon 3-specific cDNA primer (+580 to +605)	70°C
HPPARG ex3-rev	5'-CATTATGAGACATCCCCACTGCAAGG-3'	hPPAR <sub>γ</sub> exon 3-specific cDNA primer (+707 to +682)	78°C
hPPAR <sub>γ</sub> Ex2-for	5'-AACTGATGTCTTGACTCATGG-3'	hPPAR <sub>γ</sub> exon γ2 amplicon (5' UTR sequence)	60°C
hPPAR <sub>γ</sub> Ex2-rev	5'-CTGGAAGACAACTACAAGAG-3'	hPPAR <sub>γ</sub> exon γ2 amplicon (intron 1 sequence)	60°C
hPPAR <sub>γ</sub> Ex1-for	5'-CTGAAACTCTGTGAGATTGC-3'	hPPAR <sub>γ</sub> exon 1 amplicon (intron 1 sequence)	58°C
hPPAR <sub>γ</sub> Ex1-rev	5'-AGGTCCAATTCTAGTCCTAG-3'	hPPAR <sub>γ</sub> exon 1 amplicon (intron 2 sequence)	58°C
hPPAR <sub>γ</sub> Ex2-for	5'-CTGTTTTTCATGGGATAATTATCC-3'	hPPAR <sub>γ</sub> exon 2 amplicon (intron 2 sequence)	62°C
hPPAR <sub>γ</sub> Ex2-rev	5'-AGCAAGATACTCTTCCATGAAG-3'	hPPAR <sub>γ</sub> exon 2 amplicon (intron 3 sequence)	62°C
hPPAR <sub>γ</sub> Ex3-for	5'-GCTGCTTCCATGTGTCATAAAG-3'	hPPAR <sub>γ</sub> exon 3 amplicon (intron 3 sequence)	64°C
hPPAR <sub>γ</sub> Ex3-rev	5'-CTGGTCTGGCAGCTATAATGAG-3'	hPPAR <sub>γ</sub> exon 3 amplicon (intron 4 sequence)	66°C



Table 2.2 Synthetic oligonucleotides used for PCR, RACE, and DNA sequencing (continued)

name	sequence	description	T <sub>m</sub>
hPPAR <sub>γ</sub> Ex4-for	5'-GTAGTAATCCAATGATTTCATCC-3'	hPPAR <sub>γ</sub> exon 4 amplicon (intron 4 sequence)	60°C
hPPAR <sub>γ</sub> Ex4-rev	5'-GTAGCGCAGTAAACCAATTTAC-3'	hPPAR <sub>γ</sub> exon 4 amplicon (intron 5 sequence)	60°C
hPPAR <sub>γ</sub> Ex5-for	5'-TTCACCTGTGAGTTAGAAATC-3'	hPPAR <sub>γ</sub> exon 5 amplicon (intron 5 sequence)	54°C
hPPAR <sub>γ</sub> Ex5-rev	5'-CAATGCAGACTAACACTAAGG-3'	hPPAR <sub>γ</sub> exon 5 amplicon (intron 6 sequence)	60°C
hPPAR <sub>γ</sub> Ex6-for	5'-GTTGCTTGGTAGAGCTGCCTAG-3'	hPPAR <sub>γ</sub> exon 6 amplicon (intron 6 sequence)	68°C
hPPAR <sub>γ</sub> Ex6-rev	5'-AAATGTTGGCAGTGGCTCAGG-3'	hPPAR <sub>γ</sub> exon 6 amplicon (3' UTR sequence)	64°C
MBACTIN-f	5'-CTGAGGAGCACCCCTGTGCTGCTCACC-3'	mouse β-actin cDNA primer (+373 to +398)	86°C
MBACTIN-r	5'-GGTGAGGGACTTCTGTAAACCACTTA-3'	3' mouse β-actin cDNA primer (+1575 to +1550)	78°C
MBACTIN-rev2	5'-AGCTAGAGCAACATAGCACAGCTTC-3'	mouse β-actin cDNA primer (+747 to +722)	76°C
HBACTIN-f	5'-GGACGCCCTCCGACCAAGTGTTCCTT-3'	human β-actin gene primer (+914 to +939)	84°C
HBACTIN-r	5'-ACTCGTCATACCTCCTGCTTGCTGATC-3'	3' human β-actin gene primer (+2965 to +2940)	78°C
HBACTIN-rev2	5'-CGGGAGGCTCCTGTGCAGAGAAAGCG-3'	human β-actin gene primer (+1293 to +1268)	88°C
HBACTIN-for3	5'-GCATCTCTGCCCTTACAGATCATGTTT-3'	human β-actin gene primer (+2012 to +2037)	74°C
HBACTIN-rev3	5'-CGCTCATTTGCCAATGGTGATGACCTG-3'	human β-actin gene primer (+2426 to +2401)	80°C
HBACTIN mRNA-f	5'-GTCCACACCCGCCGACGCTCACCAT-3'	5' human β-actin cDNA primer (+18 to +43)	88°C
HBACTIN mRNA-r	5'-ACTGGTCTCAAGTCAGTGACAGGTA-3'	3' human β-actin cDNA primer (+1740 to +1715)	76°C
3' RACE Q <sub>T</sub>	5'-CCAGTGACGAGTGACGAGGACTCGAGCTCAAGC(T) <sub>17</sub> -3'	3' RACE nonspecific anchor primer	69°C
3' RACE Q <sub>0</sub>	5'-CCAGTGACGAGTGACG-3'	3' RACE anchor sub-primer	58°C
3' RACE Q <sub>1</sub>	5'-GAGGACTCGAGCTCAAGC-3'	3' RACE anchor sub-primer	58°C
3' RACE anchor	5'-GAGGACTCGAGCTCAAGC(T) <sub>12</sub> X-3'	3' RACE nonspecific anchor primer	58°C
5' RACE AS	5'-AGGCCACGCGTCGACTAGTAC-3'	5' RACE anchor sub-primer	68°C
5-1,1 rev-1	5'-TGGATCCGACAGTTAAG-3'	5' RACE product sequencing primer	50°C
5-1,1 rev-2	5'-ATGCTGGAGAAAGTCAAC-3'	5' RACE product sequencing primer	50°C
3-2,1 for-1	5'-CGAAGACATTCATTCA-3'	5' RACE product sequencing primer	48°C
9-6c2 for	5'-TAAGTGACTTGCTAAAGTCACCAG-3'	hybrid RACE product unknown sequence primer	70°C
9-6c2 jnc-for	5'-ACCTGCCCTTTCTGTATCCAGGGT-3'	hybrid RACE product junction-specific primer	76°C
9-6c2 jnc-rev	5'-TGTTCTCCGGAAGAAACCCCTGGGAA-3'	hybrid RACE product junction-specific primer	76°C
9-6c2 (?) -for	5'-CTTTATTTTATAGCAGAGAAC-3'	hybrid RACE product unknown sequence primer	54°C
9-6c2 (?) -rev	5'-GGGAATCAGAAAAGGCAGGTT-3'	hybrid RACE product unknown sequence primer	62°C
9-6c2 HPPARG-for	5'-AGGGTTCTTCGGGAGAACAA-3'	hybrid RACE product hPPAR <sub>γ</sub> sequence primer	62°C
9-6c2 for-2	5'-GCAGAGAACATTTAGTTCAGAGAGG-3'	hybrid RACE product unknown sequence primer	76°C
9-6c2 rev	5'-CGGAATCAGCGGACTCTGGATTTCAGC-3'	hybrid RACE product hPPAR <sub>γ</sub> sequence primer	82°C

## **Chapter 3**

### **Promoter Analysis of the Peroxisomal 3-ketoacyl-CoA Thiolase B Gene for the Identification of a PPRE**

### 3.1 INTRODUCTION

A number of studies have demonstrated the coordinate regulation of the three enzymes catalyzing the reactions of the peroxisomal straight-chain fatty acid  $\beta$ -oxidation spiral upon peroxisome proliferation. Both enzyme synthesis and activity increase for the fatty acyl-CoA oxidase (AOx), enoyl-CoA hydratase/3-hydroxyacyl-CoA dehydrogenase bifunctional enzyme (HD), and 3-ketoacyl-CoA thiolase enzymes when responsive cells are treated with peroxisome proliferators or various fatty acids (Lazarow *et al.*, 1982; Hashimoto, 1982; Osumi *et al.*, 1990; Karpichev *et al.*, 1997). Through transient transfection studies using promoter sequences linked to reporter genes, PPREs have been identified in the 5' upstream regions of the genes encoding the first two enzymes of the peroxisomal  $\beta$ -oxidation pathway, AOx (Osumi *et al.*, 1991; Tugwood *et al.*, 1992; Varanasi *et al.*, 1996) and HD (Zhang *et al.*, 1992; Bardot *et al.*, 1993; Chu *et al.*, 1995a). Two copies of the nuclear hormone receptor consensus binding half-site motif in direct tandem repeat and separated by one nucleotide (DR1) appear in the AOx gene promoter. The PPRE of the HD gene consists of four imperfect AGGTCA half-sites arranged as two consecutive DR1 elements overlapping a DR2 element. As of yet, a functional PPRE for the gene encoding the enzyme catalyzing the third and final reaction of the peroxisomal straight-chain fatty acid  $\beta$ -oxidation pathway, 3-ketoacyl-CoA thiolase, has not been identified. Coordinate transcriptional induction of all three enzymes of the pathway led to the hypothesis that thiolase is regulated in a manner similar to both AOx and HD.

Two closely related peroxisomal thiolase genes have been cloned from rat, thiolase A (thiolase 2) and thiolase B (thiolase 1) (Bodnar and Rachubinski, 1990; Hijikata *et al.*, 1990). They are each comprised of 12 exons and 11 introns, exhibiting approximately 97% similarity in their coding regions as well as a high degree of homology in many intron sequences (Bodnar and Rachubinski, 1990; Hijikata *et al.*, 1990). However their expression is differentially regulated, and their respective 5' and 3' flanking sequences are distinct (Bodnar and Rachubinski, 1990; Hijikata *et al.*, 1990). Thiolase A is constitutively expressed and mRNA levels increase approximately two-fold upon treatment of rats with clofibrate, a potent hypolipidemic agent and peroxisome proliferator (Bodnar and Rachubinski, 1990). In contrast, thiolase B is strictly inducible, normally present in very low amounts but induced more than 10-fold upon peroxisome proliferator administration (Bodnar and Rachubinski, 1990; Hijikata *et al.*, 1990).

A single gene for human peroxisomal 3-oxoacyl-CoA thiolase has also been identified (Bout *et al.*, 1991). The structure of the human thiolase gene closely resembles that of the rat genes with respect to the number and positions of exons and introns, the length of introns, and sequence similarity for some of the introns (Bout *et al.*, 1991). As well, there is 87% sequence similarity between the human and rat thiolases at the amino acid level. Interestingly, the human gene, similar to the rat thiolase A gene, cannot be induced by peroxisome proliferators (Hertz *et al.*, 1987). This is consistent with the observation that the human thiolase and rat thiolase A gene promoters share common features, including multiple GC boxes and the absence of a TATA box (Bout *et al.*, 1991). In contrast, the rat thiolase B gene promoter does not contain GC boxes, does contain a TATA element, and also contains a number of sequences commonly found in the 5' flanking regions of the other two inducible peroxisomal  $\beta$ -oxidation genes (Hijikata *et al.*, 1990; Bout *et al.*, 1991).

A DR1 element located at position -681 to -669 of the rat thiolase B gene promoter has been shown to bind rPPAR $\alpha$ /RXR $\alpha$  heterodimers in *in vitro* electrophoretic mobility shift assays (Kliwer *et al.*, 1992), however the function of this element as a PPRE in the context of the natural thiolase promoter or upstream of a heterologous promoter linked to a reporter gene has not been reported. Identification and characterization of the thiolase B gene PPRE will lead to a more complete understanding of the nature of the coordinated transcriptional regulation of the genes encoding the peroxisomal  $\beta$ -oxidation enzymes and their activation in response to peroxisome proliferators. Studies described in this chapter were undertaken to attempt to identify and subsequently characterize the PPRE for thiolase B, as previously performed for both the AOx and HD genes.

## **3.2 RESULTS**

### **3.2.1 Testing promoter regions 1 kb and 2 kb upstream of the rat thiolase B coding sequence for PPRE activity**

Preliminary work performed by Baowei Zhang at McMaster University, Hamilton, ON, involved screening a rat genomic library using the previously sequenced 1kb region upstream of the rat thiolase B gene (Hijikata *et al.*, 1990) to obtain further upstream sequences. A genomic DNA fragment of approximately 2.6 kb was isolated and subcloned into a luciferase expression vector following elimination of the transcription

start site and coding regions located within the genomic clone. Reporter constructs were made in which either the 1-kb or 2-kb 5' flanking sequence of thiolase B (ThB(1kb) or ThB(2kb) respectively, as indicated in Figure 3.1) was linked to the firefly luciferase reporter gene. These constructs were transiently transfected into H4IIEC3 cells, a rat hepatoma cell line responsive to peroxisome proliferators (Osumi *et al.*, 1990), utilizing a modified calcium phosphate procedure (see Materials and Methods section 2.2.2.2). No transcriptional induction was observed with either construct, implying that the thiolase PPRE may lie in a region further upstream.

To account for the possibility of the presence of endogenous inhibitors or repressors of the peroxisome proliferative response within the H4IIEC3 cells, I performed transient transfections with BSC40 cells, a monkey kidney cell line which is not responsive to peroxisome proliferators in the absence of added PPAR $\alpha$  and RXR $\alpha$  (Miyata *et al.*, 1992). Again, no induction of the luciferase gene was observed when cells were transfected with expression vectors for rPPAR $\alpha$  and RXR $\alpha$  and treated with the potent peroxisome proliferator wy-14,643, while strong induction was observed for the positive control reporter construct containing three copies of the HD PPRE (Figures 3.2 and 3.3). These results suggest the absence of a functional responsive element within the 2-kb upstream region of thiolase B that is sufficient for eliciting transcriptional activation induced by peroxisome proliferators.

### **3.2.2 Attempts to isolate further upstream sequences within the rat thiolase B gene promoter**

A DNA probe was generated consisting of the 1-kb sequence located between approximately -1 kb and -2 kb upstream of the rat thiolase B gene coding region (Probe 1 in Figure 3.1). Rat genomic DNA was digested with different restriction enzymes and Southern analysis was performed in an attempt to localize further upstream sequences. A representative Southern blot is shown in Figure 3.4, showing diffuse smears without the appearance of discrete bands on the autoradiograph. Repeated analyses yielded no distinct autoradiographic signal, and thus no specific genomic fragments binding to the probe were detected.

Utilizing the same 1-kb probe as that employed in the Southern analysis of digested rat genomic DNA, a rat genomic library was screened by hybridization. Screening of approximately 320,000 plaques yielded eight potentially positive clones. Southern blotting of the DNA extracted from each of the putative positive clones verified

binding of the probe used for the screening (Figure 3.5A). However restriction endonuclease mapping of the excised inserts yielded results inconsistent with the published map for the thiolase B upstream sequence (Hijikata *et al.*, 1990). Additionally, sequencing of the ends of the genomic inserts and insert fragments for the independent library clones analyzed did not show homology to any known thiolase sequences. Southern analysis of the genomic insert-containing lambda DNA extracted from the eight phage clones, using the approximately 1-kb region located immediately upstream of the thiolase B coding region (Probe 2 in Figure 3.1) as a probe, was subsequently performed to detect any homology to known thiolase B promoter sequences. No autoradiographic signals were generated (Figure 3.5B), suggesting that the -1 kb to -2 kb region initially used as the probe for library screening and Southern blotting of rat genomic DNA (Probe 1) was binding nonspecifically to a variety of genomic DNA sequences.

Oligonucleotides specific for the thiolase B promoter region were synthesized, corresponding to the TPP and TUP sequences shown in Figure 3.1, and were used as primers for both PCR and sequencing of the eight individual clones obtained from the screening of the rat genomic library. Results of the PCR reactions performed are shown in Figure 3.6. No sequences or PCR products were generated using these primers, providing further evidence that the eight clones did not contain sequences specific for the upstream region of thiolase B.

Further attempts to isolate additional thiolase B promoter sequences were made using the thiolase B-specific oligonucleotide TPP and lambda phage arm cloning vector-specific primers in single-sided specificity PCR of the rat genomic library, however no distinct products were obtained.

These studies illustrate the need for alternate, more specific techniques to isolate further upstream sequences for the rat thiolase B gene.

### 3.3 DISCUSSION

In this chapter, studies aimed at identifying the PPRE for the inducible rat peroxisomal 3-ketacyl-CoA thiolase B gene were performed. The transfection experiments indicate that a functional PPRE sufficient to confer peroxisome proliferator responsiveness is not present in up to 2 kb of sequence immediately upstream of the thiolase B coding region (Figures 3.2 and 3.3). This is an unexpected finding given that a DR1 element that is able to bind rPPAR $\alpha$ /RXR $\alpha$  heterodimers has been identified at

position -681 to -669 of the thiolase B promoter region (Kliwer *et al.*, 1992). The observation that transcriptional induction does not occur in either cells responsive to peroxisome proliferators (B. Zhang, unpublished results) or in the non-responsive BSC40 cells provides evidence that the H4IEC3 responsive cell line does not selectively contain endogenous inhibitors that may be interfering with the transmission of proliferative signals through this element via these receptors. However there may exist inhibitors common to both cell types that are able to act specifically on the thiolase B promoter sequences analyzed. Such inhibitory molecules may recognize specific repressive elements present in the thiolase B proximal promoter region and in turn prohibit activation mediated by the DR1 element. There are several individual AGGTCA-like half-site motifs and also a DR0 element (located at -249 to -238) present in the 1-kb region immediately upstream of the thiolase B coding sequence (Hijikata *et al.*, 1990). These sites may be targets for other members of the nuclear hormone receptor family of transcription factors which bind to DNA as monomers, homodimers, or heterodimers (reviewed in Glass, 1994), and may contribute to repression of thiolase B gene transcription in the cell lines tested. Two *cis*-acting regulatory elements have been identified in the 5' upstream region of the rat peroxisomal acyl-CoA oxidase gene: one mediates transcriptional induction by peroxisome proliferators, while the other exhibits a repressive effect on activation of the AOx promoter in both the presence and absence of the positive regulatory element (Osumi *et al.*, 1991; Dreyer *et al.*, 1992). Nuclear factors were shown to bind both of these sites (Osumi *et al.*, 1991), indicating that the response to peroxisome proliferators is controlled at multiple sequence elements for the AOx gene promoter. This may also be a possible mechanism for regulation of thiolase B gene transcription. Experiments assessing the function of the DR1 element alone linked to a heterologous promoter controlling expression of a reporter gene would address the question of whether this element is sufficient for the observed induction by peroxisome proliferators, and if the presence of other sequences located in the 1-kb and 2-kb upstream regions have an effect on inhibiting transcriptional activation of the thiolase B gene. Analysis of internal deletions of the 1-kb and 2-kb sequences could also be performed to localize the positions of minimal responsive elements and repressive elements if present within these promoter regions.

An alternative explanation for the lack of transcriptional activation observed is that the regulatory sequences mediating peroxisome proliferator responsiveness of the rat thiolase B gene may not conform to a conventional PPRE. There may exist a PPRE

binding unit for the thiolase B gene, similar to that found for the rat HD gene, consisting of multiple DR1 elements binding to PPAR $\alpha$ /RXR $\alpha$  heterodimers and functioning in combination to elicit maximal transcriptional induction (Chu *et al.*, 1995a). Alternatively, there may be a more complex enhancer architecture that confers the maximal response, such as that described for the glucocorticoid response unit (Imai *et al.*, 1990; Imai *et al.*, 1993; Scott *et al.*, 1996) and the phenobarbital response unit (Stoltz *et al.*, 1998). Such multicomponent enhancers consist of several regulatory elements that bind different transcription factors, which functionally interact with one another to bring about complete induction of target genes in response to hormones and xenobiotics. It would be important to establish an appropriate experimental system to test these possibilities. Cell lines which contain the regulatory proteins and accessory factors required for both basal and activated transcription from the thiolase B promoter, for example those known to express endogenous thiolase B, may be more suitable for such analyses.

Additional studies point to a different mechanism of regulation between the thiolase B gene and the other peroxisomal  $\beta$ -oxidation enzymes. Targeted disruption of the  $\alpha$  isoform of PPAR in mice results in a lack of induction of the AOX and HD genes in response to peroxisome proliferator treatment, however an increase in thiolase mRNA levels was surprisingly observed (Lee *et al.*, 1995). Incomplete abolishment of the transcriptional activation of the thiolase gene in these mice suggests that additional factors are involved in its regulation in response to peroxisome proliferators. It has recently been shown that different PPREs have varying binding specificities for the different PPAR isoforms, dictated by the 5' flanking nucleotides adjacent to the consensus DR1 response element (Juge-Aubry *et al.*, 1997). Most PPREs identified to date are able to bind all three of the PPAR subtypes to varying extents, and it has been observed that PPAR $\gamma$  binds to natural PPREs more strongly than the other PPAR subtypes (Juge-Aubry *et al.*, 1997). In addition, the PPREs of the first two enzymes of the peroxisomal  $\beta$ -oxidation spiral exhibit differential transcriptional responsiveness upon binding to different PPAR subtypes (Marcus *et al.*, 1993). Of particular significance was the observation that PPAR $\gamma$  could stimulate expression of a reporter gene linked to the AOX PPRE but not to the HD PPRE (Marcus *et al.*, 1993). PPAR $\alpha$  may also be selective in mediating transcriptional induction through certain response elements but not others. Thus it may not in fact be the PPAR $\alpha$  isoform that serves as the regulatory transcription factor which functionally interacts with the DR1 element located at -681 to -669 of the



thiolase B gene, but rather the PPAR $\gamma$  subtype that mediates transcriptional activation through this element upon exposure to peroxisome proliferators. Though incomplete, a significant reduction in thiolase gene expression was observed in the PPAR $\alpha$  knockout mouse compared to wild-type mice (Lee *et al.*, 1995), indicating that the  $\alpha$  isoform does indeed play a role in the peroxisome proliferator responsiveness of the inducible thiolase promoter. Therefore, it may be the case that multiple DR1 (or other sequence) elements found upstream of the thiolase B gene, recognizing different PPAR isoforms (or other regulatory proteins), act additively or synergistically to produce maximal transcriptional induction. Transient transfection experiments utilizing an expression construct for PPAR $\gamma$  instead of PPAR $\alpha$  in BSC40 cells would address the question of subtype specificity of the PPAR/RXR $\alpha$ -binding DR1 element found upstream of the rat thiolase B gene. Co-transfection of both PPAR $\alpha$  and PPAR $\gamma$  could be performed to observe cooperativity or antagonism in the actions of these two subtypes on transcription from the thiolase promoter. PPAR $\delta$  could also be tested in this manner to determine if this receptor contributes to the activation or repression of the thiolase gene.

Another possibility is that the DR1 element at position -681 to -669 of the rat thiolase B gene may not in fact be a true responsive element that imparts peroxisome proliferator-sensitivity to the thiolase B promoter. It has previously been demonstrated that peroxisome proliferator-induced transcriptional activation is not an obligatory response of the interaction of PPARs with PPRE sequences. (Marcus *et al.*, 1993). Binding of specifically PPAR $\alpha$ /RXR $\alpha$  heterodimers to DR1 elements alone is also not necessarily sufficient for transcriptional induction, as observed for the individual half-site direct repeats of the rat HD gene response element (Chu *et al.*, 1995a). The actual DR1 element responsible for peroxisome proliferator-inducible expression of thiolase B may lie in a region further than 2 kb upstream of the transcription start site. Indeed, the PPRES of some peroxisome proliferator-responsive genes lie at more distal sites, including that for the rat HD gene at position -2954 to -2927 (Chu *et al.*, 1995a) and the PPRES located at ~4300 nucleotides upstream of the rat CYP4A1 gene (Aldridge *et al.*, 1995).

In order to isolate promoter regions further than 2 kb upstream of the thiolase B coding sequence, a variety of approaches could be employed. Screening of the rat genomic library could be repeated using a more specific probe, such as one containing exon 1 sequences of the thiolase B gene, to minimize the number of nonspecific clones

identified as a result of binding of the non-coding promoter regions to various genomic DNA fragments, as was observed. As well, greater stringency conditions would assist in ensuring a greater degree of specificity of the sequences hybridizing to the probe. Enriched or selective libraries could be created to further reduce the occurrence of probe hybridization to sequences other than those of interest, for example a library specific for DNA comprising the chromosome on which the thiolase B gene resides. As another alternative, commercial screening services can be employed to obtain YAC, P1-based, or other artificial clones containing species-specific large DNA fragments spanning the entire gene of interest as well as flanking sequences.

A number of single-sided specificity PCR-based techniques could also be used for screening. Some of these methods include inverse PCR (Triglia *et al.*, 1988; Ochman *et al.*, 1988), oligo-cassette mediated PCR (Rosenthal and Jones, 1990), vectorette PCR (Riley *et al.*, 1990; Arnold and Hodgson, 1991), splinkerette PCR (Devon *et al.*, 1995), panhandle PCR (Jones and Winistorfer, 1992; Jones and Winistorfer, 1997), and boomerang DNA amplification (Hengen, 1995).

It remains important to identify the sequences responsible for peroxisome proliferator-induced transcription of the rat thiolase B gene in order to fully understand the mechanism of action of these agents in regulating the peroxisomal  $\beta$ -oxidation enzymes and other proteins involved in lipid metabolism. Furthermore, as additional genes are identified as targets of peroxisome proliferator signalling, it will continue to be of interest to study the mechanisms of regulation of other gene products whose expression is altered upon exposure to these potentially carcinogenic compounds.

**Figure 3.1 Partial map of the rat peroxisomal 3-ketoacyl-CoA thiolase B gene promoter region.** Shown is a schematic diagram of the 5' flanking region of the rat peroxisomal 3-ketoacyl-CoA thiolase B gene indicating the positions of DNA fragments used in transient transfections, library screening, Southern blotting, PCR, and DNA sequencing, and (see text for details). Nucleotide positions are numbered relative to the transcription start site at position +1.

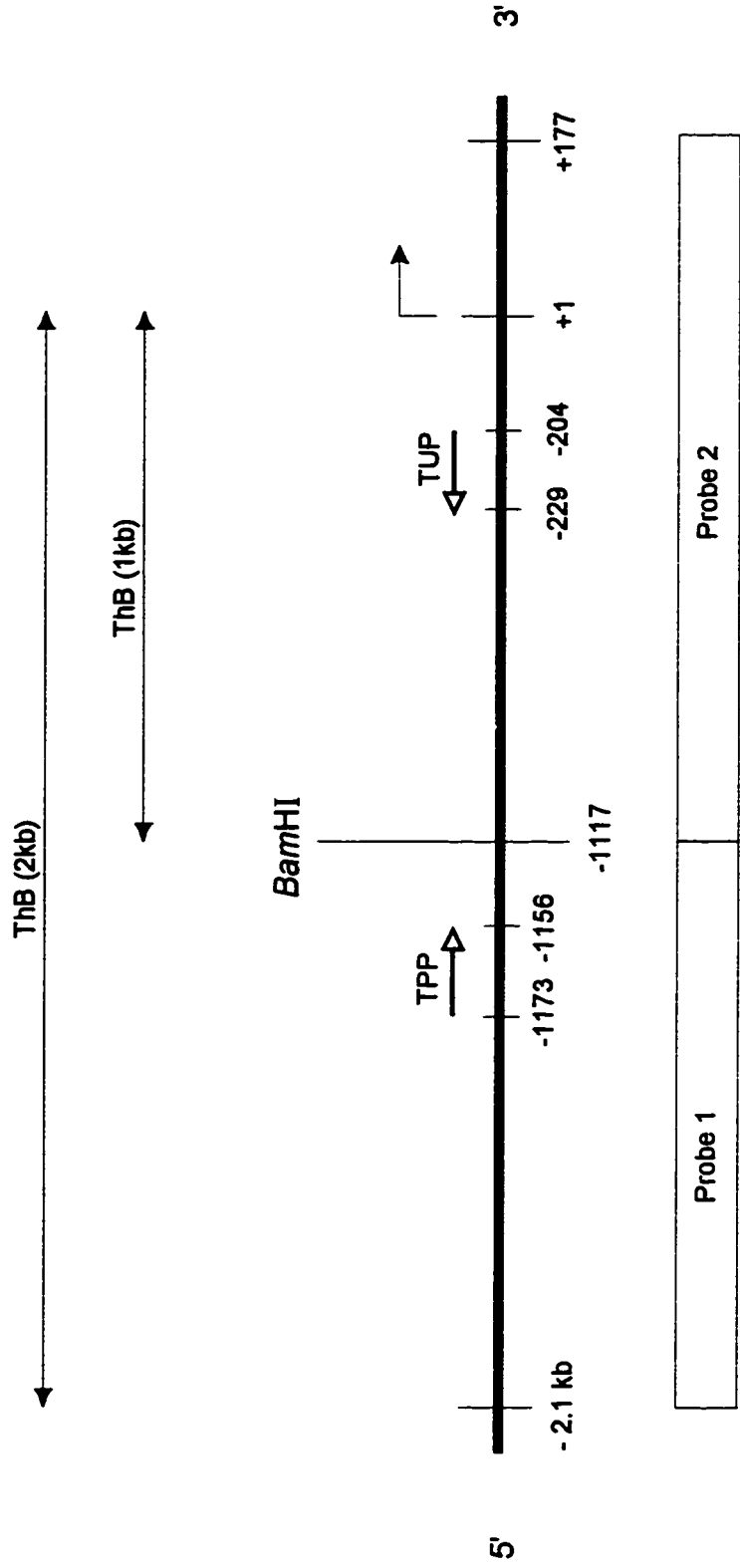


**Figure 3.2 Promoter sequences within the 1-kb region found upstream of the rat peroxisomal 3-ketoacyl-CoA thiolase B gene do not confer wy-14,643-responsiveness.** BSC40 cells were co-transfected with the indicated reporter plasmid and expression plasmid constructs in the presence or absence of 0.1 mM wy-14,643, and luciferase assays were performed on the transfected cell lysates. *pSVOALΔ5'*, luciferase reporter plasmid lacking the 5' region (including the basal promoter) of an intronless luciferase gene; *pThB(1kb)Δ5'*, ~1.1 kb of the rat peroxisomal 3-ketoacyl-CoA thiolase B gene promoter region inserted upstream of the luciferase gene; *pHD(x3)luc*, three copies of the rat peroxisomal enoyl-CoA hydratase/3-hydroxyacyl-CoA dehydrogenase (HD) gene PPRE inserted upstream of the luciferase reporter gene in the pCPS*luc* reporter plasmid containing the minimal carbamoyl-phosphate synthetase promoter. The values represent the relative induction ratios of luciferase activity measured in the presence and absence of wy-14,643 normalized to the ratio obtained with the *pSVOALΔ5'* control plasmid (given the nominal value of 1)  $\pm$  standard error of the mean. Values reported are from transfections carried out in duplicate.

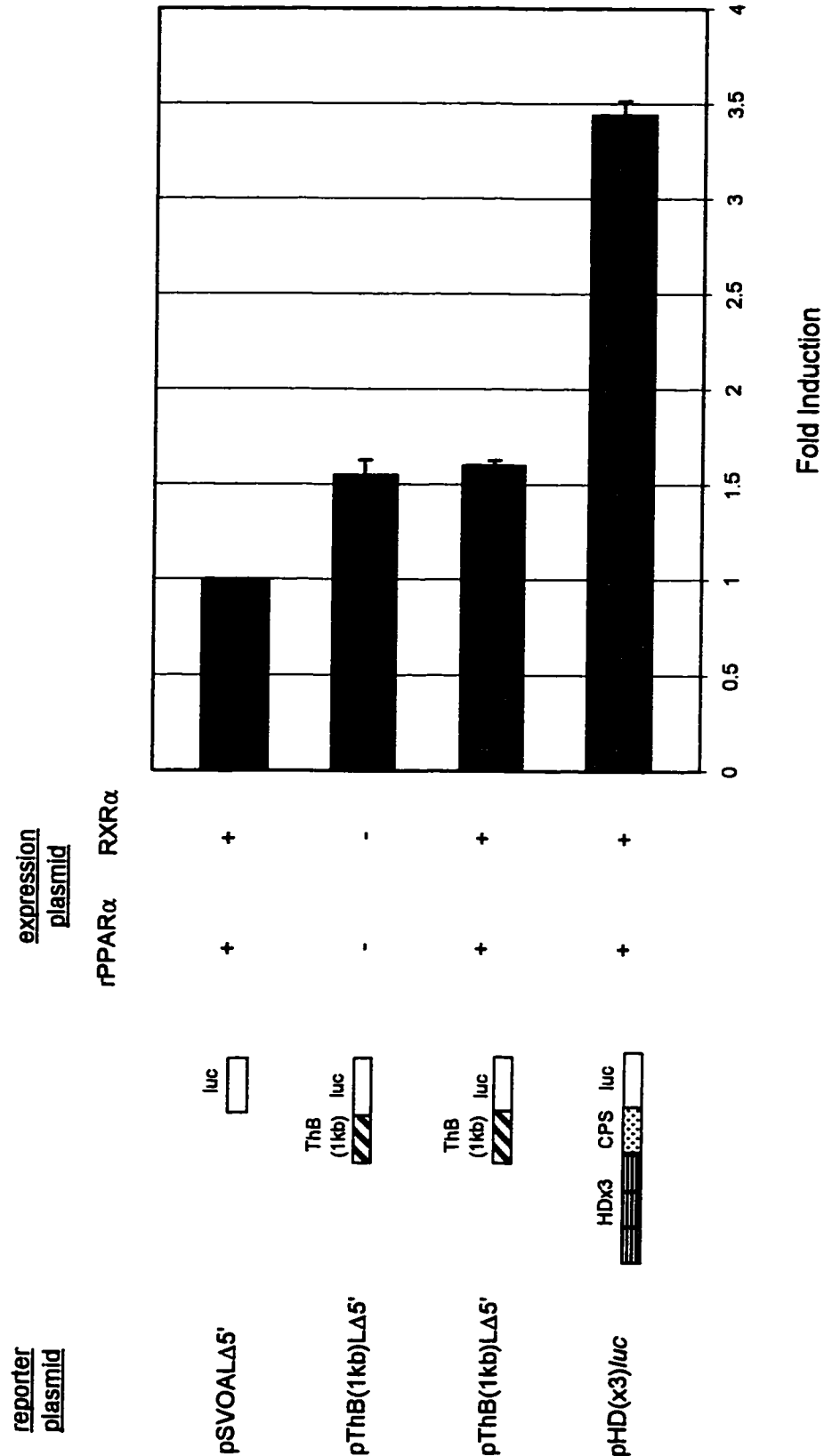


**Figure 3.3 Promoter sequences within the 2-kb region found upstream of the rat peroxisomal 3-ketoacyl-CoA thiolase B gene do not confer wy-14,643-responsiveness.** BSC40 cells were co-transfected with the indicated reporter plasmid and expression plasmid constructs in the presence or absence of 0.1 mM wy-14,643, and luciferase assays were performed on the transfected cell lysates. *pCPSluc*, luciferase reporter plasmid containing the minimal carbamoyl-phosphate synthetase (CPS) promoter; *pThB(2kb)luc*, ~2.1 kb of the rat peroxisomal 3-ketoacyl-CoA thiolase B gene promoter region inserted upstream of the luciferase gene in place of the minimal CPS promoter; *pHD(x3)luc*, three copies of the rat peroxisomal HD gene PPRE inserted upstream of the luciferase reporter gene in *pCPSluc*. The values represent the relative induction ratios of luciferase activity measured in the presence and absence of wy-14,643 normalized to the ratio obtained with the *pCPSluc* control plasmid (given the nominal value of 1)  $\pm$  standard error of the mean. Values reported are from transfections carried out in duplicate.

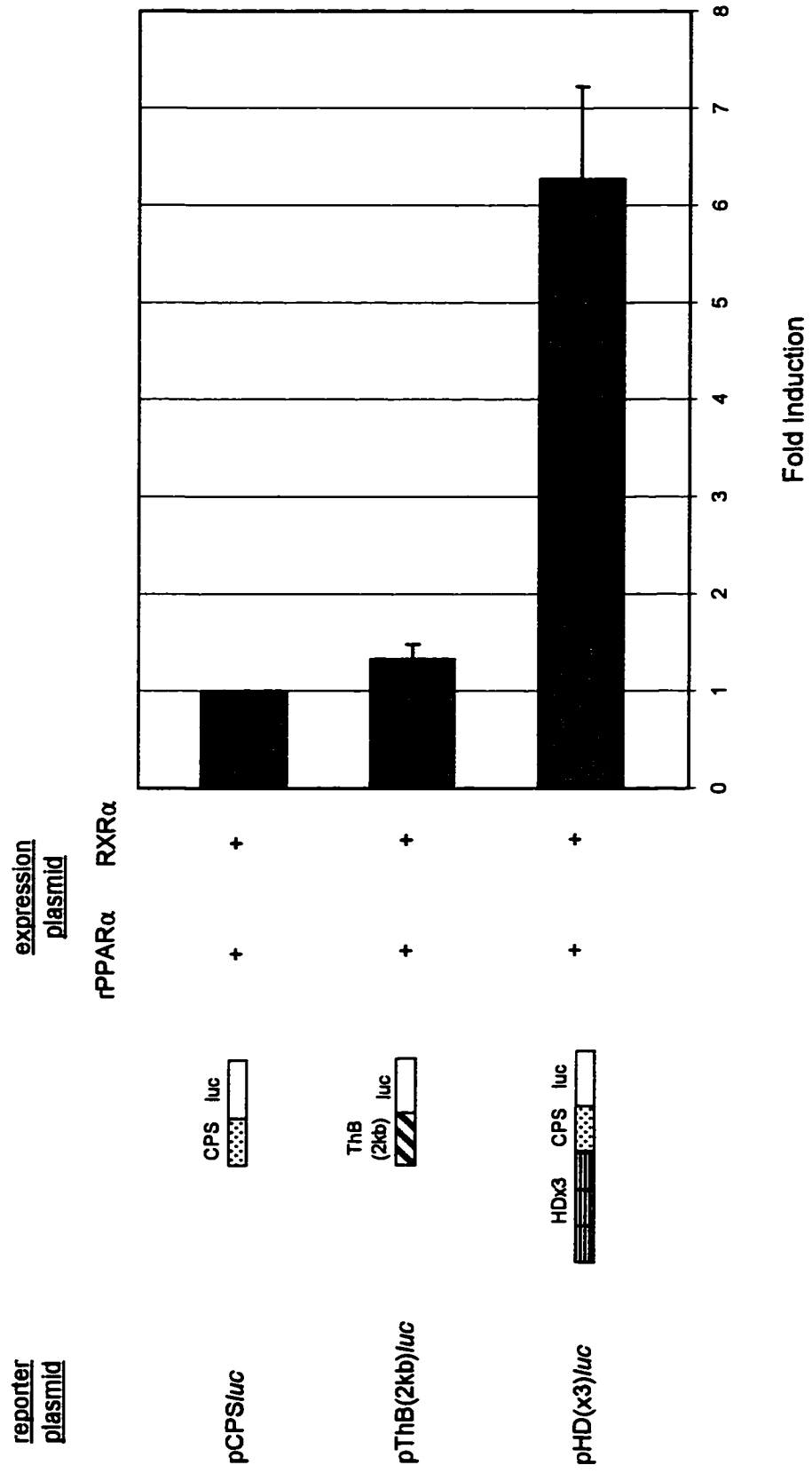




**Figure 3.4** No distinct rat peroxisomal 3-ketoacyl-CoA thiolase B gene upstream regions are isolated from rat genomic DNA by Southern blotting. 5 µg of rat genomic DNA digested with *EcoRI/KpnI* (lane 1) and *EcoRI/HindIII* (lane 2) were run alongside 0.1 µg of undigested DNA (lane 3) in a 1% agarose gel. Shown is an autoradiograph (2-hour exposure) of a Southern blot of the gel probed with a radiolabelled DNA fragment corresponding to a portion of the rat peroxisomal 3-ketoacyl-CoA thiolase B gene upstream region (Probe 1 in Figure 3.1). Approximate positions of DNA size markers are indicated.

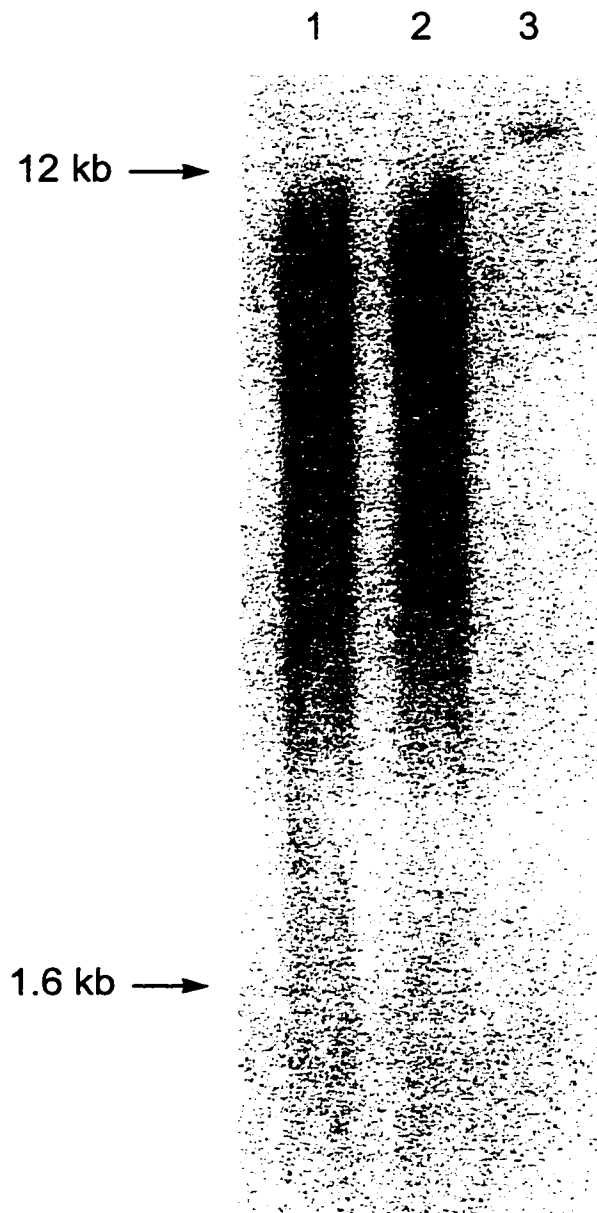
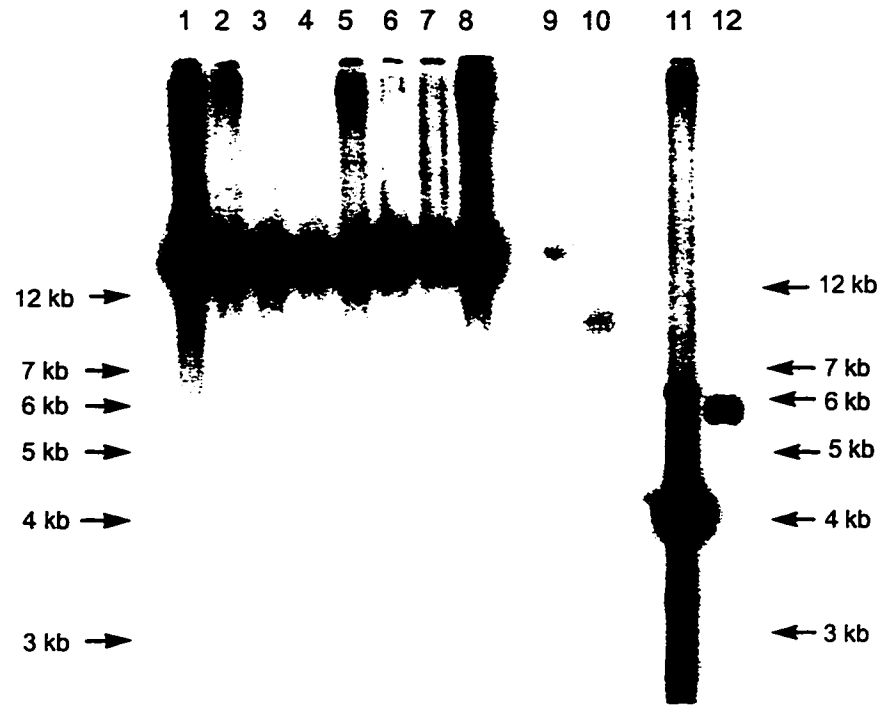


**Figure 3.5 DNA from isolated rat liver genomic library phage clones hybridizes with Probe 1 but not with Probe 2.** DNA was isolated from library phage clones selected on the basis of positive hybridization of plaques with Probe 1. Duplicate samples of approximately 300 ng of lambda phage DNA purified from each of eight library clones (Panels A and B, lanes 1-8) were electrophoresed in 1% agarose gels. Similar amounts of negative control samples, corresponding to DNA isolated from a negative library phage clone (lane 9) and linearized unrelated plasmid DNA (lane 10), were also run on the gel. Linearized plasmid DNA containing either one copy of Probe 1 (lane 11) or two copies of Probe 2 (lane 12) cloned into pGEM7Zf were used as positive controls. Shown are autoradiographs of Southern blots of the gels probed with either radiolabelled Probe 1 (Panel A) or Probe 2 (Panel B) DNA fragments corresponding to rat peroxisomal 3-ketoacyl-CoA thiolase B gene promoter regions (see Figure 3.1). Approximate positions of DNA size markers are indicated.

A



B

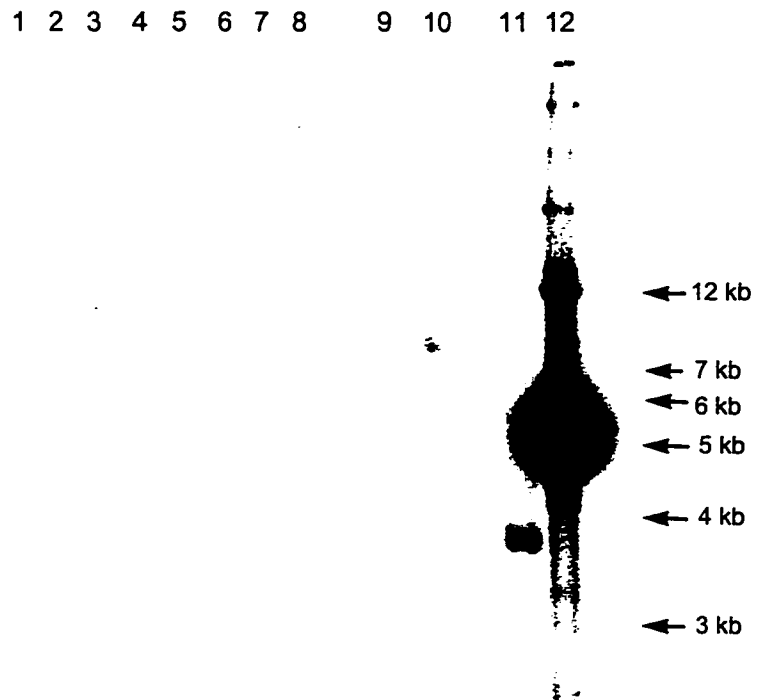
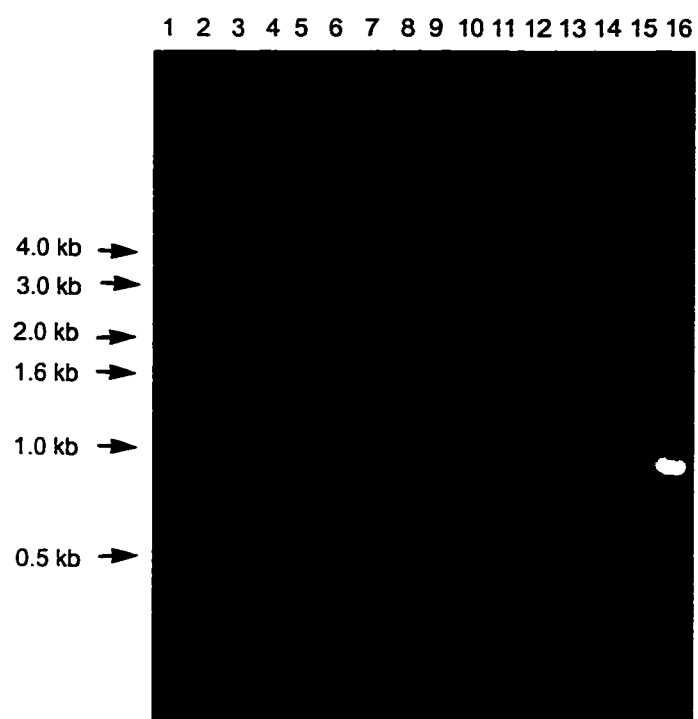


**Figure 3.6 No amplification products are obtained in PCRs of DNA from isolated rat liver genomic library phage clones using rat peroxisomal 3-ketoacyl-CoA thiolase B gene upstream region-specific primers.** PCR reactions were performed to amplify rat peroxisomal 3-ketoacyl-CoA thiolase B gene promoter sequences using 50 pmol of each of the TUP and TPP oligonucleotide primers (see Figure 3.1). Reactions were carried out as described (section 2.3.14) using an annealing temperature of 45°C and 30 amplification cycles. A 970-bp product is expected for templates containing both primer binding sites encompassing nucleotides -1173 to -204 upstream of the thiolase B gene transcription start site. Approximately 50 ng of each DNA sample was used as the template in each 100 µL reaction. Shown is a photograph of the PCR products obtained and electrophoresed on a 1% agarose gel containing ethidium bromide. DNA templates used were as follows: *lanes 2-4*, isolated lambda phage clone 1 DNA; *lane 5*, clone 2 DNA; *lanes 6 and 7*, clone 3 DNA; *lanes 8-12*, clones 4-8 DNA, respectively; *lane 13*, negative lambda phage clone DNA; *lane 14*, unrelated plasmid DNA; *lane 15*, pThB(1kb)Δ5' reporter plasmid; *lane 16*, pThB(2kb)/*luc* reporter plasmid. Lane 1 contains a 1kb DNA ladder consisting of DNA size markers as indicated.



## **Chapter 4**

### **Investigating the Involvement of PPAR $\gamma$ in Congenital Generalized Lipodystrophy**

## 4.1 INTRODUCTION

### 4.1.1 Adipogenesis

The process of adipogenesis occurs throughout the lifespan of vertebrate organisms, beginning late in embryonic development and continuing well into adulthood in response to nutritional demand and intake. The development of several cell culture models for adipocyte differentiation has facilitated characterization of the cellular and molecular events of the adipogenic program (reviewed in Smas and Sul, 1995, and Hwang *et al.*, 1997). The adipose lineage arises from multipotential stem cells of mesodermal origin which also give rise to the muscle and cartilage lineages. The first step in the adipocyte differentiation program is commitment of the multipotent stem cell to the adipose cell lineage. The resulting "preadipocytes" are susceptible to a variety of exogenous inducers, such as insulin, glucocorticoids, cyclic AMP, and fatty acids, which function synergistically to trigger subsequent differentiation events. Several rounds of mitotic clonal expansion are initiated upon induction, followed by a period of quiescence during which coordinate transcriptional activation of adipocyte genes occurs. Specific gene expression is accompanied by dramatic biochemical and morphological changes that lead to the establishment of the differentiated adipocyte phenotype.

Adipose tissue mass reflects both adipocyte size and number (reviewed in Prins and O'Rahilly, 1997). The continuous processes of lipogenesis and lipolysis in all adipocytes contribute to the flux observed in average fat cell volume, while a balance of adipose cell acquisition and cell loss determines the size of the adipocyte population. The variability in adipose cell number within and between individuals, owing to the opposing processes of preadipocyte and adipocyte replication and apoptosis, as well as preadipocyte differentiation and adipocyte de-differentiation, illustrates the dynamic nature of this tissue.

Studies of the regulation of adipocyte-specific genes have led to the identification of several transcription factors that play important roles in the adipogenic program (Figure 4.1; reviewed in Brun *et al.*, 1996b, Hwang *et al.*, 1997, and Fajas *et al.*, 1998).

The involvement of PPAR $\gamma$  in promoting adipocyte development was first evidenced by its discovery as a component (partnered with RXR $\alpha$ ) of the differentiation-dependent regulatory factor ARF6, which activates transcription of the adipocyte-specific aP2 gene encoding the adipocyte fatty acid binding protein (Tontonoz *et al.*, 1994a,b). Subsequently, a number of fat-related genes have been shown to be under the control of



PPAR $\gamma$ , including those encoding phosphoenolpyruvate carboxykinase (Tontonoz *et al.*, 1995), brown adipocyte uncoupling protein (Sears *et al.*, 1996), lipoprotein lipase (Schoonjans *et al.*, 1996), and the insulin-dependent glucose transporter, GLUT4 (Wu *et al.*, 1998). PPAR $\gamma$  expression occurs early and specifically during the differentiation of cultured adipocyte cell lines (Tontonoz *et al.*, 1994a), and its induction results in the cell cycle arrest required for differentiation to proceed (Altioek *et al.*, 1997). In the presence of activating ligands, ectopic expression of PPAR $\gamma$  is able to stimulate adipose differentiation of non-determined mouse fibroblasts (Tontonoz *et al.*, 1994c). Transdifferentiation of determined myoblasts into mature adipocytes is also dependent on PPAR $\gamma$  expression (Hu *et al.*, 1995), and treatment of myogenic cells with PPAR $\gamma$  ligands has been shown to be sufficient for commitment to the adipocyte lineage (Teboul *et al.*, 1995). Furthermore, activation of endogenous PPAR $\gamma$  in human liposarcoma and breast cancer cells promotes their terminal differentiation, resulting in conversion to cells that accumulate lipid and display a less malignant phenotype (Tontonoz *et al.*, 1997; Mueller *et al.*, 1998). Together these observations suggest that this transcription factor plays a key role as "master regulator" of the adipogenic program.

Members of the CAATT/enhancer binding protein (C/EBP) family of transcription factors also act as positive regulators of adipocyte differentiation. These proteins possess carboxy-terminal basic region/leucine zipper (bZIP) domains, conferring upon them the ability to bind sequence-specific DNA elements and to homo- or heterodimerize with other family members. Three members of this multi-gene family have been implicated in the induction of adipogenesis: C/EBP $\alpha$ , C/EBP $\beta$ , and C/EBP $\delta$ . Expression of C/EBPs is not tissue-restricted, however all three subtypes are upregulated at various stages during the adipocyte developmental program (Cao *et al.*, 1991).

C/EBP $\alpha$  is believed to play multiple roles in adipose cell differentiation, including termination of preadipocyte mitotic cell growth, coordinate transcriptional activation of adipocyte-specific genes, and transcriptional autoactivation of the C/EBP $\alpha$  gene for the maintenance of the terminally differentiated state (reviewed in MacDougald and Lane, 1995, and Hwang *et al.*, 1997). Retroviral expression of C/EBP $\alpha$  has been shown to promote adipocyte differentiation in a variety of fibroblast and preadipocyte cell lines (Freytag *et al.*, 1994; Lin and Lane, 1994). Furthermore, expression of antisense C/EBP $\alpha$  RNA in preadipocytes prevents differentiation (Lin and Lane, 1992), and mice deficient in C/EBP $\alpha$  completely lack mature white or brown adipose tissue (Wang *et al.*,

1995), definitively demonstrating the importance of this particular regulatory protein in the adipogenic process.

Several lines of evidence indicate that C/EBP $\alpha$  and PPAR $\gamma$  act synergistically to promote adipogenesis. Together with mitotic arrest, C/EBP $\alpha$  and PPAR $\gamma$  co-expression is sufficient for irreversible commitment to adipocyte differentiation (Shao and Lazar, 1997). High levels of adipocytic conversion of fibroblasts are observed when both transcription factors are co-expressed in the absence of exogenous activators (Tontonoz *et al.*, 1994c). Efficient transdifferentiation of myoblasts to adipocytes also requires the presence of both C/EBP $\alpha$  and PPAR $\gamma$  proteins (Hu *et al.*, 1995). Moreover, the promoters of many fat cell-specific genes contain binding sites for both of these regulatory factors, indicating another level of cooperative interplay between them during adipocyte development. Additionally, reciprocal gene activation is demonstrated by the observation that forced expression of either C/EBP $\alpha$  or PPAR $\gamma$  alone induces expression of the other (Tontonoz *et al.*, 1994c). These findings clearly illustrate the requirement of both transcription factors for effective adipose tissue development, however the precise mechanism of their interaction remains unknown.

C/EBP $\beta$  and C/EBP $\delta$  are thought to function early in the sequence of events leading to adipocyte differentiation. Expression of these two transcription factors is induced rapidly and transiently following the induction of preadipocyte differentiation in response to hormonal stimulation (Yeh *et al.*, 1995). The appearance of C/EBP $\beta$  and C/EBP $\delta$  precedes expression of both PPAR $\gamma$  and C/EBP $\alpha$  (Cao *et al.*, 1991; Tontonoz *et al.*, 1994c). Similar to PPAR $\gamma$  and C/EBP $\alpha$ , C/EBP $\beta$  and C/EBP $\delta$  have been shown to promote adipogenesis when ectopically expressed in fibroblasts (Yeh *et al.*, 1995). PPAR $\gamma$  levels are increased in these cells, and co-expression of both C/EBP $\beta$  and C/EBP $\delta$  is required for maximal PPAR $\gamma$  induction to the levels seen in differentiated adipocytes (Wu *et al.*, 1995; Wu *et al.*, 1996). Direct transcriptional activation of PPAR $\gamma$  by C/EBP $\beta$  and C/EBP $\delta$  is suggested by the presence of C/EBP-binding sites in the PPAR $\gamma$ 1 and PPAR $\gamma$ 2 promoters (Zhu *et al.*, 1995). A similar site in the C/EBP $\alpha$  gene that can mediate transactivation by C/EBP family members also exists (Lin *et al.*, 1993). However, C/EBP $\beta$ -C/EBP $\delta$  double knockout mice exhibit normal expression of C/EBP $\alpha$  and PPAR $\gamma$  despite severely impaired adipogenesis (Tanaka *et al.*, 1997). This observation implies that other transcription factors may contribute to PPAR $\gamma$  and C/EBP $\alpha$  induction, and that alternative pathways leading to their expression may exist *in*

*vivo*. The involvement of C/EBP $\beta$  and C/EBP $\delta$  in the regulation of additional target genes whose function is crucial to fat development is also suggested.

Another regulatory molecule implicated in the process of adipocyte development is adipocyte determination and differentiation factor 1/sterol response element binding protein 1 (ADD1/SREBP1). This transcription factor is a member of the basic helix-loop-helix (bHLH) family of proteins that was independently identified as a potential regulator of adipogenesis and fatty acid metabolism (Tontonoz *et al.*, 1993), and a factor involved in cholesterol homeostasis (Yokoyama *et al.*, 1993). Expression of ADD1/SREBP1 is induced very early in the fat cell developmental program, and ectopic expression in fibroblasts results in increased PPAR $\gamma$  activity as well as transcriptional activation of adipocyte-specific lipid metabolizing enzymes (Kim and Spiegelman, 1996). Recent studies demonstrate that ADD1/SREBP1 activates PPAR $\gamma$  through promoting the production of endogenous ligand for this nuclear hormone receptor (Kim *et al.*, 1998). Direct activation of PPAR $\gamma$  expression through interaction with a response element in the PPAR $\gamma$ 3 promoter has also been suggested as a mechanism for the adipogenic activity of ADD1/SREBP1 (Fajas *et al.*, 1998).

Also critical for adipocyte maturation are additional positive regulatory proteins involved in differentiation-specific activation of certain fat cell genes, as well as the timely repression of a number of inhibitory *trans*-acting factors at various stages of the process (reviewed in MacDougald and Lane, 1995, and Fajas *et al.*, 1998). A variety of endocrine and paracrine signals as well as extracellular matrix components are also important for the control of adipose tissue development (reviewed in Smas and Sul, 1995, and Hwang *et al.*, 1997).

#### **4.1.2 Congenital Generalized Lipodystrophy**

Congenital generalized lipodystrophy (CGL), also known as lipoatrophic diabetes or Seip-Berardinelli syndrome, is a rare genetic disease characterized by an extreme lack of body fat and metabolic abnormalities including insulin resistance, hyperglycemia, and hypertriglyceridemia (Foster, 1998). The occurrence of the disorder among siblings and the high incidence of parental consanguinity in affected families suggest autosomal recessive transmission as the mode of inheritance. Generalized deficiency of adipose tissue is usually obvious at birth. Mechanical fat, serving a supportive or cushioning function, appears to be spared, while metabolically active fat depots are dramatically

absent (Seip and Trygstad, 1996; Foster, 1998). Paucity of fat is observed in subcutaneous and other adipose tissue sites, with a reduction in both the number and volume of adipocytes present compared to normal individuals (Seip and Trygstad, 1996). In atrophic areas, adipose cells can be detected microscopically, however they do not contain triglyceride stores (Foster, 1998).

A major clinical feature of CGL is hyperlipidemia, a predictable manifestation of such a disease defined by near complete absence of fat storage depots. Other common characteristics of patients with CGL include mental retardation, diabetes, hepatomegaly, cardiomegaly, muscular and genital hypertrophy, skeletal sclerosis, and intellectual and psychomotor disabilities (Moller and O'Rahilly, 1993; Seip and Trygstad, 1996; Foster, 1998). Lethality of the disease is dependent upon the severity of the lipodystrophy and accompanying abnormalities. Hepatic failure, hemorrhage from esophageal varices, renal failure, and recurrent pancreatitis are frequent causes of death (Foster, 1998). Dietary fat restriction is generally prescribed for CGL patients, however there is no specific treatment for the disease. Prognosis of the disorder is variable, with most afflicted individuals experiencing limited life expectancy.

The nature of the defect(s) responsible for the lipoatrophy observed in CGL patients is unknown. The lack of adipose tissue may be the consequence of failure of adipocyte development, active destruction of adipocytes, or both. The inability to sequester excess circulating lipids may additionally or alternatively be due to ineffective synthesis and storage of triglycerides or accelerated lipolysis in existing adipocytes. Studies of affected families aimed at identifying the genetic loci contributing to the etiology of CGL have eliminated several candidate genes involved in insulin action and lipid metabolism, the physiological processes in which major alterations are observed. Among the genes that have been excluded are those encoding the insulin receptor and various downstream molecular targets of insulin signalling, several lipases and apolipoproteins, the  $\beta$ -3-adrenergic receptor involved in lipolysis and thermogenesis, and the body fat-regulating hormone leptin (van der Vorm *et al.*, 1993; Desbois-Mouthon *et al.*, 1995; Vigouroux *et al.*, 1997; Silver *et al.*, 1997).

The remarkable observation that PPAR $\gamma$  activity is able to stimulate the adipogenic program in preadipocytes, in non-determined fibroblasts, and in cells committed to the myocyte lineage suggests a potential mechanism whereby similar cell populations within CGL patients may be converted to adipocytes in an effort to restore fat cell mass. If the CGL phenotype is the result of impaired adipocyte differentiation

and gene expression essential for normal lipid metabolism, it is possible that the function of PPAR $\gamma$ , a key regulator of these processes, may be compromised in individuals with this disease. The studies described in this chapter were performed to assess the role played by this nuclear hormone receptor in both the pathogenesis and potential treatment of CGL using fibroblasts derived from a patient diagnosed with the disorder.

## **4.2 RESULTS**

### **4.2.1 Clinical Report**

The patient from whom the CGL fibroblasts under study were derived is a 19-year-old Caucasian female born to nonconsanguineous parents. Both parents are healthy. She was diagnosed with CGL based on the presentation of multiple medical problems that include absence of body fat, hyperglycemia, hypertriglyceridemia, and hepatomegaly. The patient has Type 2 diabetes (NIDDM). Body fat content as measured by deuterium dilution was 5% of total body weight at age 16. This contrasts with normal fat content for age-matched females, which is typically 23% of total body weight. An enlarged fatty liver is observed, as well as multiple xanthomas (depositions of cholesterol in the skin and tendons) covering most of her body.

Serum analysis reveals drastically increased triglyceride levels, measuring as high as 67.03 mmol/L (normal range = 0.26 - 1.56 mmol/L), which have been observed to drop to 15 mmol/L when her diabetes and diet are well controlled. Elevated VLDL levels are also evident, accounting for an abnormally high proportion of the lipoproteins. Lipoprotein electrophoresis shows that her cholesterol floats along with her triglycerides in the VLDL range. The VLDL fraction also appears to migrate faster than the control VLDL. Lower than normal HDL cholesterol levels are detected, while LDL cholesterol levels are not able to be accurately determined due to the proportionately elevated triglyceride levels. Plasma lipoprotein lipase activity is present, however measures at 29% of normal controls.

### **4.2.2 Cloning of mPPAR $\gamma$ 2 cDNA**

As an initial step in studying the function of the PPAR $\gamma$  nuclear hormone receptor in lipodystrophic cells, isolation of the mPPAR $\gamma$ 2 cDNA from a 14-day mouse whole embryo cDNA library (Chevray and Nathans, 1992) was attempted by PCR amplification using primers designed from the published cDNA sequence of mPPAR $\gamma$ 2 (Tontonoz *et*

*al.*, 1994a). The full-length cDNA was successfully cloned from the library (Figure 4.2), as verified by subcloning and sequencing of the PCR product.

#### **4.2.3 Detection of an aberrant hPPAR $\gamma$ mRNA species in CGL human fibroblasts**

To detect hPPAR $\gamma$  expression in normal and CGL primary human fibroblasts, RT-PCR was performed using total RNA preparations and oligonucleotide primers designed from the published hPPAR $\gamma$  cDNA sequence (Greene *et al.*, 1995). Several attempts at amplification of the full-length hPPAR $\gamma$  cDNA were unsuccessful, however an internal fragment was successfully amplified from RNA within these cell types (Figure 4.3). Internal fragments of human cytoplasmic  $\beta$ -actin were also amplified as positive controls. Thus transcripts derived from the hPPAR $\gamma$  gene are found within normal and CGL human skin fibroblasts. The inability to amplify the full-length cDNA may be attributable to incomplete reverse transcription of the hPPAR $\gamma$  transcripts, therefore resulting in shorter than full-length 1<sup>st</sup> strand cDNA templates for PCR. Alternatively, the 5' and 3' untranslated regions of the transcripts found in fibroblasts may be distinct from hPPAR $\gamma$  messages identified in other cell types, potentially suggesting the existence of a novel PPAR $\gamma$  isoform within this tissue. In the CGL cells, there may additionally be aberrations in the 5' and 3' termini of the transcripts which prevent primer recognition and which may possibly affect PPAR $\gamma$  function within these fibroblasts.

5' and 3' RACE were subsequently performed to identify further upstream and downstream sequences of the hPPAR $\gamma$  message. Reactions performed using total RNA isolated from normal human primary fibroblasts yielded products comprised entirely of normal hPPAR $\gamma$  sequence. However, one of the 5' RACE products generated from CGL fibroblast-derived RNA consisted of a sequence of unknown origin ~100 bp in length at the 5' end fused to ~300 bp of normal hPPAR $\gamma$  coding sequence at the 3' end (Figure 4.4). The 5' 103-nucleotide sequence of unknown origin shows no similarity to any previously identified sequences, as determined through homology searches carried out using the BLAST algorithms of the National Center for Biotechnology Information (Bethesda, MD). The remaining 288-bp region positioned downstream is identical to normal hPPAR $\gamma$  exon 3 and exon 4 sequences. Translation of the RACE product 5' sequence in frame with the normal hPPAR $\gamma$  coding region reveals the occurrence of two potential stop codons. The first of these that would be encountered by the translational machinery would result in premature translation termination prior to synthesis of the

DNA-binding C domain of the receptor (Figure 4.4). Thus translation of the full-length mRNA from which this "hybrid" product is derived would yield a truncated PPAR $\gamma$  protein lacking all functional domains beyond the N-terminal A/B domain, followed by several additional amino acids specified by the sequence of unknown origin appended to the normal exon 2 coding region. The extent of this novel stretch of amino acids would depend on the length of the sequence downstream of exon 2 and the presence of additional stop codons encoded by this portion of the mature message. Absence of the crucial DNA-binding, ligand-binding, dimerization, and remaining domains would render this form of the receptor dysfunctional. The point of divergence between the normal hPPAR $\gamma$  sequence and the transcript found within CGL cells is positioned immediately upstream of hPPAR $\gamma$  exon 3 and corresponds to a consensus eukaryotic exon-intron boundary, specifically an intron splice acceptor site (Padgett *et al.*, 1986). This suggests that the hybrid mRNA species amplified by RACE may have arisen from aberrant splicing of the hPPAR $\gamma$  primary transcript within the CGL cells. Alternatively, the fusion of the unknown sequence to the hPPAR $\gamma$  coding sequence may be the result of a chromosomal translocation or insertion event disrupting the hPPAR $\gamma$  gene.

If the existence of the hybrid RACE product reflects the occurrence of aberrant splicing of the PPAR $\gamma$  RNA transcript in the CGL cells, with the 103-bp 5' region representing normal intron sequence found between exons 2 and 3 of the hPPAR $\gamma$  gene, its sequence is expected to be found within the genomic DNA of both CGL and normal cells. If the RACE product is generated from a disrupted hPPAR $\gamma$  gene owing to a chromosomal insertion or translocation event occurring specifically in the CGL cells, this would also be detected in the genomic DNA sequence of the CGL patient, but not within normal cells. In order to determine if the 103-bp sequence of unknown origin is indeed found in genomic DNA, Southern blotting was performed. Blots containing samples of genomic DNA isolated from normal fibroblasts, CGL fibroblasts, and blood samples from the CGL patient and patient's parents were probed with the 103-bp sequence found at the 5' end of the RACE product (Figure 4.5A) or with the cDNA for human cytoplasmic  $\beta$ -actin (Figure 4.5B). No discrete hybridization signals were observed for the blot probed with the RACE product-specific DNA fragment. Faint smears spanning the length of each lane containing the digested DNA samples were instead apparent, suggesting recognition by the probe of highly repetitive human DNA sequences, or alternatively nonspecific hybridization of the probe with a variety of genomic fragments. In contrast,

the  $\beta$ -actin positive control probe generated discrete signals on the autoradiograph for all the DNA samples tested. Notably, no significant differences were observed between the results obtained for the normal fibroblasts and for the CGL-associated cells.

PCR was performed as an additional, more sensitive method to analyze genomic DNA for the presence of the sequence of the hybrid RACE product found fused to the hPPAR $\gamma$  exon 3 coding region. Oligonucleotides specific for the RACE product 5' sequence and normal hPPAR $\gamma$  exon 3 were used as primers, and template DNA consisted of genomic DNA isolated from normal and CGL cells. Similar reactions were performed using genomic DNA derived from both the mother and father of the patient to determine whether either or both of these individuals harbor the same abnormal PPAR $\gamma$  coding sequence if indeed present in the patient, providing clues as to the basis for the inheritance of the disorder. As shown in Figure 4.6, an approximately 300-bp fragment is amplified from all genomic DNA samples tested. This indicates that the sequence of the hybrid RACE product is found in genomic DNA of normal and CGL-associated individuals. Consequently, the RACE product is not derived from gross abnormalities in the PPAR $\gamma$  gene of the CGL patient.

Interestingly, the size of the PCR products generated is significantly larger than the 232-bp product amplified from the hybrid RACE product itself in a control reaction (Figure 4.6, lane 7). In addition, published sequences for intron DNA found immediately upstream of hPPAR $\gamma$  exon 3 (Okazawa *et al.*, 1997) do not correspond to the 5' sequence of the RACE product. These observations suggest that uncharacterized genomic DNA sequences comprise the 103 nucleotides found at the 5' end of the hybrid product, and that a mechanism other than failed splicing at the natural exon-intron boundary is responsible for its presence in RNA transcripts. Sequencing of the PCR products generated from genomic DNA templates revealed that the 103-bp unknown region corresponds to intron DNA located further upstream of exon 3 in the hPPAR $\gamma$  gene than the reported normal flanking intron sequence, and that it is found in both normal and CGL-associated genomic DNA (shown as '98 bp-CCCAG' in Figure 4.7). Thus the hybrid RACE product consists of normal hPPAR $\gamma$  intron DNA fused to hPPAR $\gamma$  cDNA sequences, with 81 nucleotides normally found upstream of exon 3 missing in the RNA transcript. This would suggest that an incorrect splice donor site is recognized in the hPPAR $\gamma$  primary transcript, resulting in only partial excision of the 9.5 kb intron found upstream of exon 3, and consequently producing an incorrectly spliced mRNA species



that could serve as a template for amplification of the hybrid RACE product. This is supported by the identification of specific sequence motifs within the missing 81 nucleotides that may be responsible for its excision (Figure 4.7; see Discussion). To determine if such an event is occurring specifically in the CGL cells, thus possibly contributing to the CGL phenotype, or if it is a natural phenomenon in hPPAR $\gamma$  transcript processing within all cells, RNA samples extracted from both normal and CGL human fibroblasts were analyzed for the presence of the aberrant message. RT-PCR performed using poly(A)<sup>+</sup> RNA extracts showed that the hybrid RACE product sequence is not specific to the CGL cells but in fact is synthesized from mRNA templates found in normal fibroblast cells as well (Figure 4.8). This finding indicates that the hybrid sequence is generated as a result of molecular events occurring in both normal and CGL cell types and is not derived from a transcript that is unique to the messenger RNA pool found within the CGL fibroblasts.

#### **4.2.4 Analysis of hPPAR $\gamma$ message levels in normal and CGL human fibroblasts**

Detection of hPPAR $\gamma$  sequences by RT-PCR of RNA from both normal and CGL cells suggests that this PPAR isoform is indeed expressed within human fibroblast cells, for which no previous reports in the literature exist. The identification of PPAR $\gamma$  expression in a variety of human tissues and its involvement in an ever-increasing number of both normal and pathophysiological processes prompted the hypothesis that differences in the expression and/or function of this transcription factor between normal and CGL fibroblasts may somehow contribute to the development of this particular disease. To determine whether there is a difference in the level of expression of PPAR $\gamma$  within these two cell populations, Northern blotting of RNA extracted from both the normal and CGL cells was performed. The 288-bp normal hPPAR $\gamma$  sequence contained within the hybrid RACE product was used as a probe. Verification that this cDNA fragment specifically recognizes hPPAR $\gamma$  transcripts was made by probing a commercially-obtained multiple tissue Northern blot containing poly(A)<sup>+</sup> RNA isolated from a variety of human tissues (Figure 4.9). The hybridization signals generated match those of published results (Lambe and Tugwood, 1996; Tugwood *et al.*, 1996). Therefore, the 288-bp cDNA fragment is specific for and can recognize PPAR $\gamma$  within human tissues where it is known to be expressed. Subsequent use of this probe in Northern blots of poly(A)<sup>+</sup> RNA extracted from the fibroblast cells under study shows a striking difference in the levels of

hPPAR $\gamma$  message detected within the normal and CGL cells (Figure 4.10, panels A1 and A2). Variability in the amounts of hPPAR $\gamma$  mRNA among the different normal human fibroblast cultures was apparent, however a near absence of corresponding message in the CGL cells was consistently observed. Quantitation of the hybridization signal intensities, normalized to the  $\beta$ -actin signals generated (Figure 4.10, panels B1 and B2), confirms that a dramatically reduced level of hPPAR $\gamma$  mRNA is found in the CGL cells compared to all of the normal cell lines and primary cultures examined (Figure 4.11). These results indicate a clear distinction between the normal and CGL fibroblasts with respect to PPAR $\gamma$  expression.

#### **4.2.5 Analysis of hPPAR $\gamma$ protein in normal and CGL fibroblasts by immunoblotting**

If PPAR $\gamma$  message exists in skin fibroblast cells, it follows that PPAR $\gamma$  protein is produced in these cells. Given the marked difference between the amount of PPAR $\gamma$  mRNA present within normal cells and the CGL cells, the corresponding protein levels are also expected to differ. For hPPAR $\gamma$  protein analysis, total protein was extracted from normal and CGL human fibroblasts and subjected to immunoblotting. Rabbit polyclonal antibodies were raised against a hPPAR $\gamma$ -specific synthetic peptide for use as a probe in the immunoblot analyses. Figure 4.12 shows the specificity of the antibodies for the hPPAR $\gamma$  peptide used as the antigen. Specificity of the polyclonal antibodies for human PPAR $\gamma$  protein *versus* mouse PPAR $\gamma$ 2 protein was also demonstrated (Figure 4.13, lane 3). However, the antibodies were not able to recognize hPPAR $\gamma$  protein within positive control protein extracts of COS cells transfected with an expression plasmid encoding hPPAR $\gamma$  (Figure 4.13). A commercial PPAR $\gamma$ -specific goat polyclonal antibody preparation was additionally used in immunoblots of the human fibroblast total protein extracts. As shown in Figure 4.14, the commercial antibodies recognized proteins of the expected size in positive control samples (lanes 7 and 8). A faint signal at the expected molecular weight (~55 kDa) was observed for the protein sample from only one of the normal cell lines (Figure 4.14, lane 4), and no corresponding signals were apparent for the remaining human cell cultures examined (Figure 4.14, lanes 2-5). Interestingly, a higher molecular weight species, running at approximately 80 kDa, was detected on the immunoblots (Figure 4.14, lanes 1-5). Cross-reactivity with the pre-immune serum or the secondary antibody was not observed. This protein may represent a post-

translationally modified form of PPAR $\gamma$  found specifically within human fibroblasts, as its existence has not been previously reported for other tissues. In any case, this protein appears in all but one of the normal cell cultures under study, and also in the CGL extract, suggesting that its presence or absence likely does not contribute to the CGL phenotype.

#### **4.2.6 Treatment of normal and CGL primary fibroblasts with PPAR $\gamma$ activators**

A number of studies have shown that activators and ligands of PPAR $\gamma$  can effectively promote differentiation of fibroblasts to adipocytes (Chawla and Lazar, 1994; Chawla *et al.*, 1994; Tontonoz *et al.*, 1994c; Kliewer *et al.*, 1995). Furthermore, adipogenesis in other cell types such as bone marrow stromal cells and transdifferentiation of determined myoblasts into mature adipocytes are processes stimulated upon PPAR $\gamma$  expression and activation (Gimble *et al.*, 1996; Hu *et al.*, 1995; Teboul *et al.*, 1995). Recent work demonstrates the ability of PPAR $\gamma$  ligands to induce terminal differentiation of human liposarcoma and breast cancer cells (Tontonoz *et al.*, 1997; Mueller *et al.*, 1998). Together these findings illustrate the central role played by PPAR $\gamma$  in promoting the adipocyte developmental program, and the requirement of specific activators for its effective function.

Stimulation of adipogenesis in patients with CGL may correct the altered phenotype of these individuals resulting from the lack of adipose tissue. To determine if activation of endogenous PPAR $\gamma$  can participate in the conversion of CGL fibroblasts to adipocytes, experiments were performed involving treatment of CGL and primary human skin fibroblast (HSFB) cells with PPAR $\gamma$  activators. Different methods for stimulation of adipogenesis in fibroblast cell cultures have been described (Chawla and Lazar, 1994; Chawla *et al.*, 1994; Tontonoz *et al.*, 1994c; Kliewer *et al.*, 1995). Two such methods were used in the cell culture studies performed.

For the first experiment, a preadipocyte differentiation assay was used (Chawla *et al.*, 1994). CGL and primary HSFB cells were cultured in normal growth medium until confluent and then switched to growth medium supplemented with 0.45 mM wy-14,643 (pirinixic acid, a potent peroxisome proliferator known to activate all PPARs), 10  $\mu$ M 15-deoxy- $\Delta^{12,14}$ -PGJ $_2$  (a natural PPAR $\gamma$  ligand), or DMSO (the solvent used for both compounds) as a control. Cells were refed every two days with fresh media and test compounds. At 10 days post-confluence, cells were lysed for total RNA extraction.

Stimulation of the adipose differentiation process in human adipocyte precursor cells is promoted by the addition of certain hormones including insulin and glucocorticoids to the growth media (Green and Kehinde, 1975; Hauner *et al.*, 1989). Differentiation medium for the conversion of fibroblasts to adipose cells typically contains these adipogenic factors. In the second experiment, CGL and primary HSFB cells were cultured in normal growth medium supplemented with 5  $\mu\text{g/mL}$  insulin according to a procedure developed for adipogenic conversion of non-determined fibroblasts (Tontonoz *et al.*, 1994c). At confluence, 1  $\mu\text{M}$  dexamethasone and 0.45 mM wy-14,643, 10  $\mu\text{M}$  15-deoxy- $\Delta^{12,14}$ -PGJ<sub>2</sub>, or DMSO were added to a fresh change of media. At two days post-confluence and every two days thereafter, cells were refed with fresh media (containing insulin) plus PPAR $\gamma$  activator or DMSO. At 10 days post-confluence, cells were lysed for total RNA extraction.

For both experiments, Northern blotting was performed on the total RNA extracts using the 288-bp hPPAR $\gamma$  cDNA fragment as a probe. Very faint signals, if any, were detectable on the Northern blots containing either 8  $\mu\text{g}$  or 20  $\mu\text{g}$  of total RNA extracted from the CGL and HSFB cells regardless of the presence or absence of insulin or the test compound added to the growth media (Figure 4.15, panels A1 and A2). Probing of the blots with a human  $\beta$ -actin cDNA probe generated equivalent signals for all of the RNA samples tested (Figure 4.15, panels B1 and B2). These results likely reflect the extremely low abundance of hPPAR $\gamma$  message in the fibroblast cells, and indicates that significant induction of PPAR $\gamma$  gene expression does not occur upon treatment of these cells with the compounds wy-14,643 or 15-deoxy- $\Delta^{12,14}$ -PGJ<sub>2</sub> in the amounts used and under the culture conditions employed.

#### **4.2.7 Detection of an aberrant hPPAR $\gamma$ sequence in genomic DNA from the CGL patient and the patient's father**

Characterization of the structural organization of the human PPAR $\gamma$  gene and sequencing of the exon-intron boundaries (Fajas *et al.*, 1997; Okazawa *et al.*, 1997) enabled an analysis of the hPPAR $\gamma$  exon sequences contained within the genomic DNA of the CGL patient. PCR was performed to amplify each of the seven exons of the hPPAR $\gamma$  gene, followed by sequencing of the products to detect any coding errors that may contribute to altered PPAR $\gamma$  function. The primers used for the PCR amplifications and expected product sizes are given in Table 4.1. In addition to DNA isolated from the

CGL cells, genomic DNA samples extracted from normal fibroblast cells and from blood taken from the CGL patient's parents were similarly assessed. All PCR results are shown in Figure 4.16. Analysis of the CGL patient's DNA revealed that six of the seven hPPAR $\gamma$  exons amplified consisted of normal sequences found within the hPPAR $\gamma$  gene, as seen by the appearance of products of the expected size (Figure 4.16A) and confirmed by DNA sequencing. For some of the reactions, PCR was repeated using a higher annealing temperature to eliminate nonspecific products (Figure 4.16B). All PCRs performed to amplify hPPAR $\gamma$  exon 2 from the patient's DNA consistently resulted in the appearance of three distinct bands (Figure 4.16A, lane 4 and Figure 4.16B, lane 2). Similar PCR analysis of genomic DNA from the patient's mother as well as from two different normal cell lines produced only the expected DNA fragments (Figures 4.16C,E,F). However, an identical variation as that seen for the CGL patient was observed in the hPPAR $\gamma$  exon 2 products generated from the patient's father's genomic DNA (Figure 4.16D, lane 4).

The hPPAR $\gamma$  exon 2 products amplified from all the genomic DNA samples tested were subjected to DNA sequencing. As predicted by PCR, DNA fragments generated from the patient's mother's DNA as well as from both normal cell lines consisted of normal hPPAR $\gamma$  sequence. However sequencing of one of the multiple exon 2 products from PCR of the patient's and patient's father's DNA revealed the existence of a 4-nucleotide deletion within the exon 2 coding region (Figure 4.17). This deletion lies in the DNA-binding domain-encoding region of the hPPAR $\gamma$  gene and causes a shift in the reading frame that would yield a prematurely truncated translation product. The other two exon 2 amplification products observed for the CGL patient and patient's father are comprised of normal hPPAR $\gamma$  coding sequence. The identification of multiple exon 2 PCR products as well as an aberrant exon 2 sequence in the genomic DNA of the CGL patient and the patient's father, but not observed for either of the normal cell lines, is suggestive of a possible role played by the hPPAR $\gamma$  gene in the development of CGL.

### 4.3 DISCUSSION

Individuals with CGL suffer from a variety of abnormalities affecting multiple organ systems. This would be expected in view of the considerable importance of adipose tissue, serving vital functions throughout the body. The case of CGL studied as

described in this chapter involves a patient that presents with classical features of the disease, including fat depletion, elevated plasma insulin, glucose, and triglyceride levels, and organomegaly. Given the established role of PPAR $\gamma$  in adipogenesis and its implication in insulin signalling, it was hypothesized that defects in the hPPAR $\gamma$  gene or its expression may contribute to the development of CGL and may serve as a potential target for therapeutic intervention.

The discovery of the hybrid RACE product sequence in the mRNA pool within CGL cells suggested the occurrence of a splicing error in the processing of the hPPAR $\gamma$  primary transcript. Similar products consisting of consensus exon-intron boundary sites fused to exon sequences have been observed by others for PCR amplifications using coding sequence templates (e.g. cDNA libraries) and are also believed to be products of defective splicing (Johansson and Karlsson, 1997). Further characterization of the hybrid species in both normal and CGL cells supports the theory that aberrant splicing leads to its production, however the molecular events responsible for its generation, as well as the cell types in which it is detected, were not as initially postulated.

The ability to amplify the hybrid RACE product DNA segments from both normal and CGL-associated genomic DNA templates (Figure 4.6) indicates the presence of the constituent nucleotide sequences in all human cells. Characterization of these sequences and the observed differences between the RNA-derived and genomic DNA-derived PCR products suggests that incorrect processing of the hPPAR $\gamma$  transcript results in the synthesis of an mRNA molecule that contains both intron and exon DNA found within the gene. Examination of the stretch of 81 nucleotides missing from the RACE product reveals the presence of a putative branch site to which the cleaved 5' intron sequence joins to form the lariat splicing intermediate structure (Figure 4.7). The sequence at this site resembles the consensus motif for eukaryotic branch sequences typically found 20-55 nucleotides from the 3' intron boundary, characterized by the sequence 5'-CURAY-3', in which the C, U, and A nucleotide positions are the most highly conserved in human introns (Keller and Noon, 1984). Also present in the excised DNA region is a potential intron splice donor site at the 5' end (Figure 4.7). However, the requirement of virtually invariant GU nucleotides at the 5' terminus of eukaryotic introns precludes the possibility of this site serving as an exon-intron boundary (Padgett *et al.*, 1986).

Recently, enzymatic activities that alter the nucleotide sequence of mRNAs at specific sites through processes known as RNA editing have been identified in

mammalian cells (reviewed in Maas *et al.*, 1997, and Ashkenas, 1997). Post-transcriptional conversion of a single cytidine to a uridine in a number of mRNAs as a result of cytidine deaminase activity has been observed (Hadjigapiou *et al.*, 1994; Yamanaka *et al.*, 1995; Skuse *et al.*, 1996). The catalytic component and auxiliary proteins comprising the "editosome" are expressed in a variety of cell types, suggesting that this may be a common mechanism for generating different RNA transcripts from the same gene (Driscoll and Zhang, 1994; Yamanaka *et al.*, 1994; Nakamuta *et al.*, 1995). Therefore, it is possible that the GC dinucleotide sequence at the 5' end of the 81 nucleotides missing from the hybrid RACE product could be converted to GU through RNA editing and hence form a novel consensus splice donor site in the hPPAR $\gamma$  intron found upstream of exon 3. Specificity of C $\rightarrow$ U editing at particular sites is imparted by an 11-nucleotide sequence, 5'-TGATCAGTATA-3', called a mooring element, located downstream of the target cytidine (Backus *et al.*, 1991). Reduced efficiency of editing is observed for alterations in the mooring element sequence (Yamanaka *et al.*, 1996). Positioned immediately 3' to the cytidine proposed to undergo deamination to form the novel 5' splice site in the hPPAR $\gamma$  transcript is a stretch of seven nucleotides identical to a portion of the mooring element (Figure 4.7). This sequence may be sufficient to promote a low level of RNA editing at the suggested site, enough to result in production of the defectively spliced species that could be detected by PCR. Efficient editing is not expected, since this would result in significant amounts of abnormal hPPAR $\gamma$  mRNA synthesized in both normal and CGL cells, which was not observed.

For the production of aberrantly spliced mRNAs as a result of mutations or editing events that create a novel splice site, the new site must out-compete the normal site in the reaction. Recognition of and cleavage at a proposed novel 5' splice donor site would not preclude cleavage at the normal splice site found at the boundary of the upstream exon. Instead, the splicing machinery would likely recognize a cryptic 3' splice acceptor site located elsewhere within the intron, upstream of the new 5' splice site, to complete the excision of intron DNA initiated at the normal 5' splice donor site (Padgett *et al.*, 1986). Indeed, such a mechanism has been observed to occur for the human  $\beta$ -globin gene (Treisman *et al.*, 1983), and would explain how mRNA molecules containing the hybrid RACE product sequence may be generated as a result of hPPAR $\gamma$  transcript processing in fibroblast cells. Also lending support to this hypothesis is the observation that most if not all natural mutations of mammalian genes identified that involve the creation of a new splice site occur within introns near the normal 3' splice acceptor sites

(Padgett *et al.*, 1986). Accordingly, the novel 5' splice donor site presumed to be responsible for generating the aberrant hPPAR $\gamma$  mRNA species lies in the ~9.5 kb intron at a mere 81 nucleotides upstream of exon 3.

That the hybrid RACE product is detected in poly(A)<sup>+</sup> RNA fractions is indicative of the occurrence of polyadenylation prior to splicing and possibly editing of hPPAR $\gamma$  pre-mRNAs, as has been demonstrated for the order of processing events *in vitro* (Niwa and Berget, 1991).

Detection of the hybrid RACE product constituent sequences in the genomic DNA and in mRNA pools of both CGL and normal cells suggests that the mechanisms responsible for its production do not contribute to the development of CGL and likely occur in the context of normal biological phenomena. Processes such as nonsense-mediated mRNA decay likely function to eliminate such defective mRNA molecules, thus preventing the deleterious effects that may result from their translation (Maquat, 1996). Additionally, it appears that correct hPPAR $\gamma$  transcript processing does occur within the normal and CGL human skin fibroblasts examined. This is evidenced by the appearance of RT-PCR-generated internal fragments of hPPAR $\gamma$  mRNA spanning exons 2 to 4 (Figure 4.3) and hybridization signals on Northern blots corresponding to the expected size of hPPAR $\gamma$  message (Figure 4.10).

PPAR $\gamma$  expression has been detected in a variety of human tissues, as can be seen in Figure 4.9, and mRNA levels appear to vary greatly among the different tissues examined (Elbrecht *et al.*, 1996; Lambe and Tugwood, 1996; Tugwood *et al.*, 1996; Mukherjee *et al.*, 1997; Fajas *et al.*, 1997). No studies of PPAR $\gamma$  analysis in human fibroblast cells have been reported in the literature to date. The RT-PCR and Northern blot experiments performed in this study clearly show that PPAR $\gamma$  is indeed expressed in human skin fibroblast cells (Figures 4.3 and 4.10). Additionally, it appears that there is dramatically reduced PPAR $\gamma$  expression in fibroblasts derived from the CGL patient (Figures 4.10 and 4.11). The function of PPAR $\gamma$  in human skin fibroblasts is at present unknown, as is the case for several other cell types in which hPPAR $\gamma$  transcripts have been found. However the marked difference between the normal and CGL cells analyzed with respect to the presence of PPAR $\gamma$  message suggests that there may be a functional contribution of this disparity to the development of the CGL phenotype. The near absence of PPAR $\gamma$  detected in the poly(A)<sup>+</sup> RNA pool from the CGL fibroblasts may reflect either decreased hPPAR $\gamma$  gene transcription or enhanced degradation of hPPAR $\gamma$



mRNA transcripts within these cells. Either of these possibilities may lead to altered PPAR $\gamma$  protein levels and resulting function compared to the normal state, perhaps contributing to the development of the disorder. Elucidation of the role played by this nuclear hormone receptor in human skin fibroblast cells will shed some light on the effects of its reduced expression within this tissue.

Fibroblasts are versatile connective tissue cells, displaying a remarkable capacity to differentiate into several cell lineages, including cartilage, bone, muscle, and fat cells (Gabbiani and Rungger-Brändle, 1981). In addition, fibroblasts are in large part responsible for the secretion of the macromolecular constituents of the extracellular matrix (ECM). The ECM in turn plays an active and complex role in regulating the behaviour of the cells that contact it, influencing their development, migration, proliferation, shape, and metabolic functions (Hay, 1981). The process of adipocyte differentiation is regulated by factors that affect cell shape and anchorage (reviewed in Smas and Sul, 1995), demonstrating the importance of appropriate ECM composition and cell-ECM interactions for adipose tissue development. Therefore, it is conceivable that aberrations in fibroblast function that lead to alterations in either differentiation capacity or synthesis and secretion of ECM components may interfere with proper fat cell differentiation, potentially resulting in the abnormalities associated with CGL. Analysis of fibroblast gene expression in both normal and CGL cells may reveal other differences which PPAR $\gamma$  expression may in some way influence. Similar studies of fibroblast cells in which PPAR $\gamma$  function is disrupted, for example by introduction of antisense RNA or expression of a dominant-negative mutant form of the receptor, would also assist in delineating the role of PPAR $\gamma$  in this tissue. Additional assessments of fibroblast tissue *in vivo*, such as in PPAR $\gamma$  knockout mice, may further enable determination of the fibroblast-specific functions of PPAR $\gamma$ .

It is also important to determine if fibroblast cells from other CGL patients exhibit similarly reduced PPAR $\gamma$  mRNA levels compared to normal controls. This would provide information as to whether a low abundance of PPAR $\gamma$  message is a common feature of the disorder, or if it is unique to the case under study.

The implications of the variability in PPAR $\gamma$  expression observed among the normal fibroblast cell cultures examined (Figures 4.10 and 4.11) are also unknown. The method of Northern blotting used for hPPAR $\gamma$  transcript detection does not discriminate between different PPAR $\gamma$  splice variants. It has been postulated that the ratio of the

PPAR $\gamma$ 1 and PPAR $\gamma$ 2 isoforms has possible functional importance (Vidal-Puig *et al.*, 1997). Demonstration of differential transcriptional activation functions between PPAR $\gamma$ 1 and PPAR $\gamma$ 2 further illustrates the significance of their relative expression levels (Werman *et al.*, 1997). The recent suggestion that a third isoform exists adds another potential level of complexity, implying that differential promoter activity at three separate sites within the PPAR $\gamma$  gene is involved in the control of PPAR $\gamma$  function. Therefore it is necessary to determine the amounts of each of the PPAR $\gamma$  transcripts within the normal cells examined, for example through quantitative RT-PCR or sensitive RNase protection procedures, in order to compare PPAR $\gamma$  expression among them more effectively.

It is important to determine the level of PPAR $\gamma$  protein present in the fibroblast cells in order to understand the significance of the differences in mRNA levels observed between the CGL cells and normal fibroblasts, and also among the individual normal cell cultures examined. The availability of specific antibodies is crucial for such analyses. The potential unreliability of raising antibodies against synthetic peptide epitopes was illustrated in the present study (Figures 4.12 and 4.13). Recognition of the peptide immunogen does not guarantee recognition of the full-length protein. Differences in binding of the antibodies may be attributable to the conformation adopted by the full-length molecule, or perhaps post-translational modifications that might prohibit access of the antibodies to the immunogenic site. PPAR $\gamma$  has been shown to be phosphorylated under certain conditions (Zhang *et al.*, 1996a; Hu *et al.*, 1996; Camp and Tafuri, 1997; Adams *et al.*, 1997; Reginato *et al.*, 1998), and this may contribute to the lack of antibody binding observed.

It is unclear why the commercial anti-PPAR $\gamma$  antibody preparation used for immunoblot analysis recognizes multiple species within the fibroblast protein extracts (Figure 4.14). The low level of protein detected at the expected molecular weight may be due to insufficient amounts of total protein loaded. Indeed the low level of PPAR $\gamma$  mRNA present in the fibroblast cells would likely result in correspondingly low amounts of protein synthesized. Human PPAR $\gamma$  protein may also be relatively unstable in fibroblast cells, and therefore would not be efficiently detected in the lysates. Pulse-chase experiments to determine the half-life of the hPPAR $\gamma$  protein in fibroblast cells would address this question.

The nature of the higher molecular weight species recognized by the commercial antibodies is unknown. It may represent a covalently modified form of the hPPAR $\gamma$

protein. Alternatively, it may correspond to a protein unrelated to PPAR $\gamma$  that contains an epitope similar to the peptide antigen used for generation of the antibodies. Competition experiments using the antigenic peptide would assess the specificity of antibody binding. In any case, expression of this molecule appears to vary widely among the different cell types studied, with no clear distinction between normal and CGL fibroblasts. Thus it is unlikely that its expression plays a role in the progression of this disease.

An additional method that may be employed to detect and study PPAR $\gamma$  protein in the human fibroblasts is immunoprecipitation from cell lysates using specific antibodies. Examination of the phosphorylation state of the receptor would also be useful for further analysis of its possible function in these cells.

The ability of several mouse fibroblast cell lines to undergo conversion to adipocytes is well documented (reviewed in Hwang *et al.*, 1997). The process of adipogenesis has been observed in cell types at various stages of development, including multipotent stem cells, non-determined fibroblasts, preadipocytes, and committed myoblasts. Thus it seemed reasonable to hypothesize that similar phenotypic conversion may be possible within human fibroblast cells, with the potential of affecting the course of CGL. *In vitro* culture studies demonstrate that the exogenous agents required to induce differentiation vary for the different established mouse cell lines, likely dependent on the particular stage of adipocyte development at which the cells were arrested at the time of cloning. The finding that ectopic PPAR $\gamma$  expression and/or treatment with PPAR $\gamma$  activators circumvents the need for the typical hormonal stimuli in a number of these cell lines, and also specifies fat cell conversion in those which are non-committed or alternately committed with respect to lineage, suggested that culturing human fibroblasts under similar conditions might accordingly result in adipogenesis. However, neither normal nor CGL human fibroblasts displayed the characteristic features of differentiated fat cells when culture conditions mimicking those described for adipocytic conversion of 3T3-L1 preadipocytes or non-determined NIH 3T3 fibroblasts were used (Figure 4.15). A number of explanations could account for these observations.

It is possible that the human fibroblasts examined do not express sufficient amounts of PPAR $\gamma$  to promote efficient adipogenesis. This has been observed for cultures of NIH 3T3 cells, which do not normally express detectable levels of PPAR $\gamma$  and do not undergo adipocyte conversion when treated with a peroxisome proliferator unless

exogenous PPAR $\gamma$  is introduced (Tontonoz *et al.*, 1994c). Although PPAR $\gamma$  expression is detected in the human fibroblasts (Figure 4.10), the mRNA levels are observed to be quite low considering the amount of poly(A)<sup>+</sup> RNA and long exposure times required in Northern blotting procedures. As proposed for C/EBP $\alpha$ -mediated stimulation of adipogenesis in fibroblasts (Freytag *et al.*, 1994), there may be a requirement of a minimum threshold level of PPAR $\gamma$  expression in order for the adipocyte differentiation program to proceed. Studies performed on CGL cells stably transfected with a retroviral vector encoding PPAR $\gamma$  show some degree of differentiation above that of control cultures (G. Castillo and B. Spiegelman, personal communication), however it is not known if the human fibroblast cultures tested consist of a homogeneous population of cells.

The requirements for stimulation of fat cell development in the human fibroblasts under study may also be distinct from established adipogenic cell lines. This would necessitate the development of unique *in vitro* culture parameters for human fibroblast cultures, as has been demonstrated for the individual mouse lines. Consequently, the lack of adipocyte conversion observed for the normal and CGL cells may be due to the use of inappropriate cell culture conditions. An example of this might be the absence of methylisobutylxanthine (MIX) as a hormonal stimulant in the culture media used, observed to be required for adipogenesis in certain murine cultures (Hwang *et al.*, 1997). MIX is an inducer of C/EBP $\beta$  gene expression, a transcription factor shown to regulate PPAR $\gamma$  expression, and cultures deprived of this hormone exhibit considerable delays in the differentiation process (Yeh *et al.*, 1995). The absence of MIX and other unknown required components might be responsible for preventing adipogenesis in the CGL and normal human fibroblasts.

The amount and type of PPAR $\gamma$  activator used in the cell culture experiments may also be insufficient for adipogenic conversion of the fibroblasts. Titrations of 15-d-PGJ<sub>2</sub> and wy-14,643 could be performed to determine whether optimal concentrations of these activators required for efficient adipocyte differentiation of the human fibroblasts differ from those tested. Alternatively, more potent PPAR $\gamma$  ligands, such as the thiazolidinedione compound BRL49653, may have a greater stimulatory effect. Confirmation of effective PPAR $\gamma$  activation may also be made by assessing the expression of target genes shown to be involved in the differentiation process, such as lipoprotein lipase. This gene might be particularly useful for analysis as it is expressed

early in the adipogenic program (Tontonoz *et al.*, 1994a) and has been shown to be directly regulated by PPAR $\gamma$  (Schoonjans *et al.*, 1996).

All the mouse fibroblast cell lines that have been shown to undergo conversion to adipocytes are homogeneous populations of cells that possess inherent adipogenic potential (Hwang *et al.*, 1997). This may not be true of the normal and CGL fibroblasts analyzed. Evidence exists to suggest that fibroblasts in different parts of the body are intrinsically different (Conrad *et al.*, 1977), and it is also uncertain whether fibroblasts in a given region are equivalent. Several distinct fibroblast populations may exist in a given sample of connective tissue, including those committed to particular lineages as well as those incapable of further differentiation, and in various proportions, as opposed to a homogeneous clonal population of one type of cell with multiple developmental capabilities. Furthermore, the developmental state of the host cells from which the fibroblast cultures were derived may dictate their adipogenic capacity. The extent of adipose conversion in cell strains obtained from rat tissues has been shown to vary with parameters such as age of the donor rat and anatomical site of extraction (Ailhaud, 1982). Another study demonstrates the ability to induce the differentiation program in fibroblast cells derived from mouse embryos, while human fibroblasts obtained from fetal lung tissue were unable to undergo similar conversion (Freytag *et al.*, 1994). It is possible that embryonic and fetal tissues differ in their complement of particular types of fibroblasts, consisting of differentiation-competent (with varying degrees of developmental potential) or differentiation-incompetent cells. Thus adult tissues, from which the CGL and normal human cells used in this study were derived, may be comprised of fibroblasts that exhibit an even greater degree of resistance to fat cell conversion. Embryonic fibroblasts may be more suitable for *in vitro* studies of adipogenesis in human systems.

Species differences may also contribute to the observed ability of mouse fibroblasts to become adipocytes and lack thereof for human fibroblasts. Certain rat and human preadipocyte and adipose-converted cells display characteristics not shared by several murine adipogenic cell lines (Ailhaud, 1982), indicating that different processes may be responsible for fat tissue development in each of these species.

An aberrant coding sequence in the PPAR $\gamma$  gene within the CGL patient would imply alterations in PPAR $\gamma$  function compared to normal individuals. The 4-nucleotide deletion identified in exon 2 would result in the synthesis of unstable mRNA transcripts owing to the presence of premature stop codons (reviewed in Maquat, 1995), effectively

reducing the translation-competent PPAR $\gamma$  message pool, and thereby decreasing the amount of normal PPAR $\gamma$  protein produced. This mutation may be the cause of or contribute to the reduced level of PPAR $\gamma$  mRNA observed within the CGL fibroblasts (Figures 4.10 and 4.11). Additionally, mRNA molecules evading such decay mechanisms might lead to the production of a dysfunctional protein, which could also have significant consequences for a variety of processes in which PPAR $\gamma$  is involved. These might include effects on PPAR $\gamma$  function in adipose tissue, which may lead to defects in fat development and possibly the CGL phenotype. It is necessary to determine whether this PPAR $\gamma$  coding region abnormality is expressed in order to address its functional significance. This may be done through an analysis of RNA samples from the CGL patient for detection of the corresponding sequence in hPPAR $\gamma$  mRNA molecules within various tissues.

The presence of a similar exon 2 sequence anomaly in the patient's father's PPAR $\gamma$  gene suggests paternal inheritance of the variant allele. However the additional detection of normal PPAR $\gamma$  exon 2 coding regions in DNA from the CGL patient, as well as the absence of the deletion in the mother's gene, implies heterozygosity for this aberration. This abnormality by itself is likely not responsible for CGL since the patient's father is not afflicted with the disorder. Nonconsanguinity of the parents also implies that homozygous recessive transmission of a mutant allele may not be the causative determinant of development of the disease in this case. It is possible that multiple genetic alterations in the patient may act in concert to bring about the observed phenotype. Mutations elsewhere within the hPPAR $\gamma$  gene, such as in regulatory promoter regions, or in other genes that are involved in the process of adipogenesis, perhaps which affect PPAR $\gamma$  expression and/or function, may have been inherited from the mother or may have arisen spontaneously. Absence of such additional genetic defects in the father would explain the failure to develop CGL while harboring the deletion within the PPAR $\gamma$  exon 2 sequence. Thus studies of the non-coding gene sequences of PPAR $\gamma$  and also of the sequences and function of other adipogenic regulatory proteins within tissues of the CGL patient may reveal additional abnormalities that contribute to the diseased state.

It is unclear why three products are generated in amplifications of hPPAR $\gamma$  exon 2 from the patient's and patient's father's genomic DNA. This observation might be the result of promiscuous binding of the primers to intron DNA sequences upstream and

downstream of exon 2. Alternatively, it may reflect the existence of multiple copies of hPPAR $\gamma$  gene sequences within these individuals, perhaps as a result of genetic rearrangement and recombination events creating duplicated sequences, or due to the presence of pseudogene sequences within the genomic DNA. The intron DNA normally found upstream of exon 2 might differ in some way from these additional loci and thus might result in the generation of the different sizes of PCR products observed (Figure 4.16). Elucidation of the DNA sequences at the termini of these products would help to distinguish between these possibilities.

Two reports have recently emerged detailing the analysis of PPAR $\gamma$  coding sequences within several individuals diagnosed with CGL (Okazawa *et al.*, 1997; Vigouroux *et al.*, 1998). One of these studies finds no coding mutations within the PPAR $\gamma$  gene in twelve Japanese patients (Okazawa *et al.*, 1997). The second report describes the occurrence of a heterozygous CCA $\rightarrow$ GCA (alanine $\rightarrow$ proline) substitution at codon 12 in some cases, although the polymorphism was not detected in the majority of patients analyzed (7/33 heterozygotes identified) and was also found among unaffected individuals (Vigouroux *et al.*, 1998). No other instances of abnormalities in PPAR $\gamma$  sequence appear in the literature for studies of CGL or other human disorders. The lack of detection among all of these cases of the 4-nucleotide deletion identified in this study suggests that it is not a general genetic defect in CGL. Therefore its existence may be unique to this particular case or a limited number of cases as yet not investigated. The possibility that the sequence anomaly is not implicated in the disorder also cannot be discounted. Nevertheless, given the dramatic change in amino acid sequence of all PPAR $\gamma$  isoforms that would be induced upon its expression, assessment of its physiological significance would be of interest.

*In vivo* studies that would provide information on the role of PPAR $\gamma$  in the etiology and potential treatment of CGL include the development and analysis of PPAR $\gamma$  knockout and transgenic mice. If alteration of normal PPAR $\gamma$  expression and function is indeed important for the origin or progression of the disorder, mice with a disruption in the PPAR $\gamma$  gene would be expected to exhibit the features characteristic of CGL. This could also be assessed using transgenic mice that express a dominant-negative form of this nuclear hormone receptor. Mice in which adipose tissue has been genetically ablated through targeted expression of the diphtheria toxin A chain have been described and appear to mimic the acquired form of generalized lipodystrophy (Burant *et al.*, 1997).

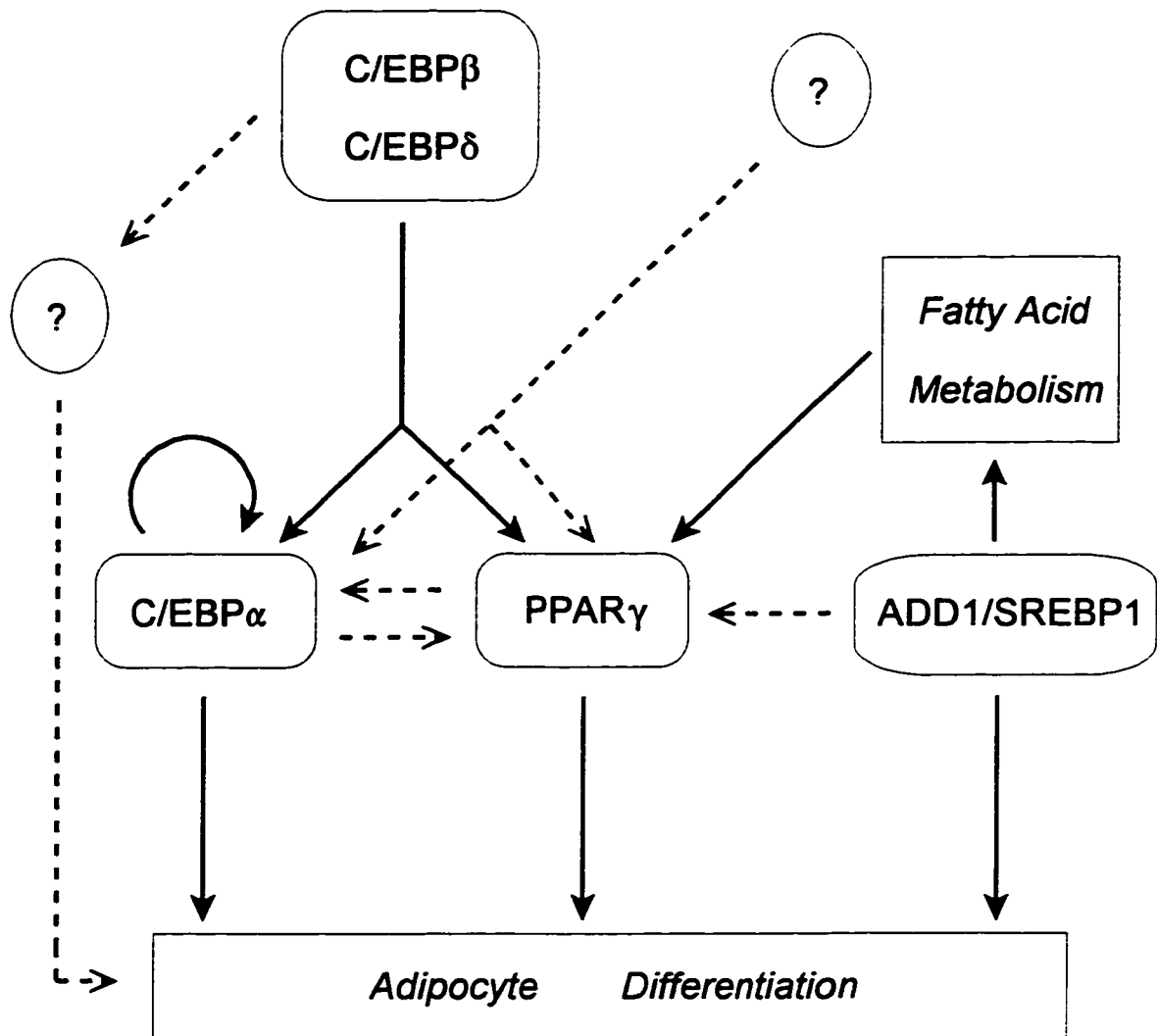
Consistent with the lipoatrophy observed, PPAR $\gamma$  mRNA levels were dramatically reduced in remnant tissues compared to fat pads of wild-type mice (Burant *et al.*, 1997). Treatment of these mice with troglitazone, a known PPAR $\gamma$  ligand, alleviates their diabetic condition and also normalizes the hyperlipidemia observed, suggesting that a significant amount of adipose tissue is not required for the action of thiazolidinedione drugs (Burant *et al.*, 1997). Furthermore, studies of obese rats demonstrate that troglitazone is able to increase the number of small adipocytes, which display greater insulin sensitivity, and reduce the number of large adipocytes, which secrete inhibitors to adipogenesis including tumor necrosis factor  $\alpha$  (TNF $\alpha$ ) (Okuno *et al.*, 1998). Thus overall fat mass does not appear to be critical for the action of troglitazone, presumably through PPAR $\gamma$  activation, in improving insulin resistance. These agents may therefore also prove beneficial in the treatment of the metabolic disorders characteristic of CGL.

Factors other than PPAR $\gamma$  may play a greater causative role in the development of CGL, such as the aforementioned cytokine, TNF $\alpha$ . TNF $\alpha$  has been observed to have a number of effects on adipose tissue physiology, including inhibition of preadipocyte differentiation, stimulation of adipocyte de-differentiation, promotion of adipocyte apoptosis, induction of insulin resistance, production of leptin, stimulation of lipolysis, and suppression of lipogenesis (reviewed in Spiegelman and Hotamisligil, 1993; Prins *et al.*, 1997). In addition, this molecule is able to downregulate PPAR $\gamma$  expression in both preadipocytes and adipocytes (Zhang *et al.*, 1996b; Xing *et al.*, 1997). Thus TNF $\alpha$  may be considered a more likely candidate gene whose dysregulation may result in the defects observed in CGL.

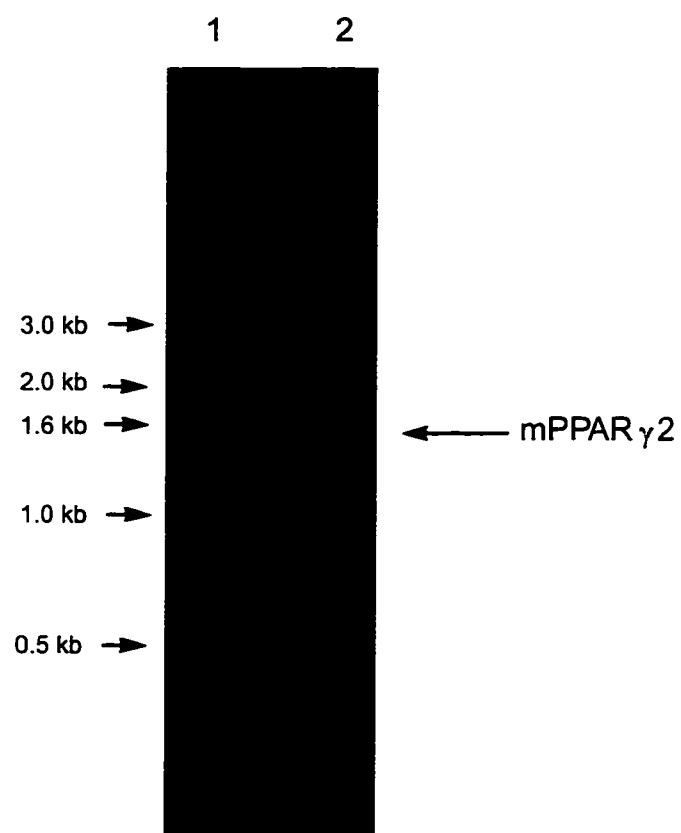
Additional methods that could be employed to isolate the gene(s) responsible for CGL include genetic linkage analysis in affected families, for which studies performed to date have not revealed the CGL locus (Gedde-Dahl *et al.*, 1996), positional cloning techniques, and molecular scanning of the numerous other genes known to be involved in adipocyte differentiation and maintenance. Identification of the genetic factors implicated in this and other cases of CGL will assist in developing an understanding of the pathophysiology of this disease. It will also provide insight into metabolic abnormalities such as insulin resistance and dyslipidemia that are common features of more frequent disorders such as obesity and NIDDM.



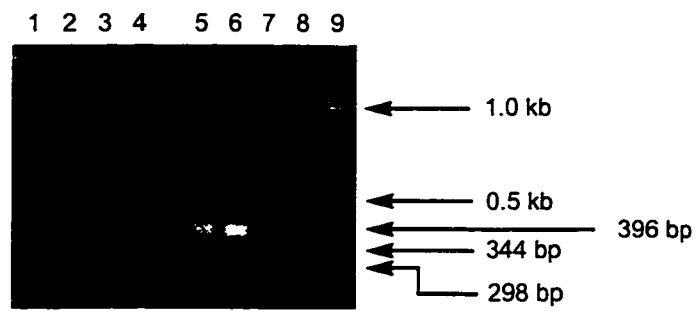
**Figure 4.1 Interactions among transcription factors in the control of adipocyte differentiation.** Solid arrows represent positive regulatory interactions. Less well characterized interactions are indicated with broken arrows. See text for details. (Adapted from Hwang *et al.*, 1997)



**Figure 4.2 Isolation of mPPAR $\gamma$ 2 cDNA from a 14-day mouse whole embryo cDNA library.** A 14-day mouse whole embryo cDNA plasmid library (Chevray and Nathans, 1992) was screened by PCR using the oligonucleotide primers mPPAR $\gamma$ 2-for2 and mPPAR $\gamma$ 2-rev2 (see Table 2.2) to amplify the ~1.6 kb full-length coding region of mPPAR $\gamma$ 2. Library screening was performed as described (section 2.4.2.1) and the PCR reaction contained approximately 380 ng of the library plasmid DNA as template, 200 pmol of each primer, and 2.5 mM MgCl<sub>2</sub>. An annealing temperature of 64°C was used in 30 amplification cycles. The expected product spans nucleotides +30 to +1572 of the mPPAR $\gamma$ 2 cDNA. Shown is a photograph of the 1% agarose gel stained with ethidium bromide on which an aliquot of the PCR reaction was run (lane 2). DNA size markers were also run on the gel as indicated (lane 1).



**Figure 4.3** An internal fragment of hPPAR $\gamma$  can be amplified from RNA of normal human fibroblasts and CGL fibroblasts. RT-PCR was performed to detect the presence of hPPAR $\gamma$  transcripts within normal and CGL primary human fibroblasts. Reverse transcription of total RNA preparations was performed as described (section 2.5.3) at a temperature of 55°C for the cDNA synthesis reaction. cDNAs were primed using the uHPPARG-r primer for PPAR $\gamma$  sequence amplification and the HBACTIN-r primer for  $\beta$ -actin sequence amplification. PCR was performed using the uHPPARG-f and HPPARG-rev2 primers for hPPAR $\gamma$  amplification (to yield a 371-bp product) and the HBACTIN-for3 and HBACTIN-rev3 primers for human  $\beta$ -actin amplification (to yield a 415-bp product). 35 amplification cycles and an annealing temperature of 60°C was used for the PCRs. Shown is a photograph of the ethidium bromide-stained 1% agarose gel on which the RT-PCR products from duplicate reactions using two independent RNA preparations were run. *Lanes 1 and 5*, hPPAR $\gamma$  fragment amplified from normal fibroblast cells; *lanes 2 and 6*, hPPAR $\gamma$  fragment amplified from CGL cells; *lanes 3 and 7*,  $\beta$ -actin fragment amplified from normal fibroblasts; *lanes 4 and 8*,  $\beta$ -actin fragment amplified from CGL fibroblasts; *lane 9*, DNA size markers.

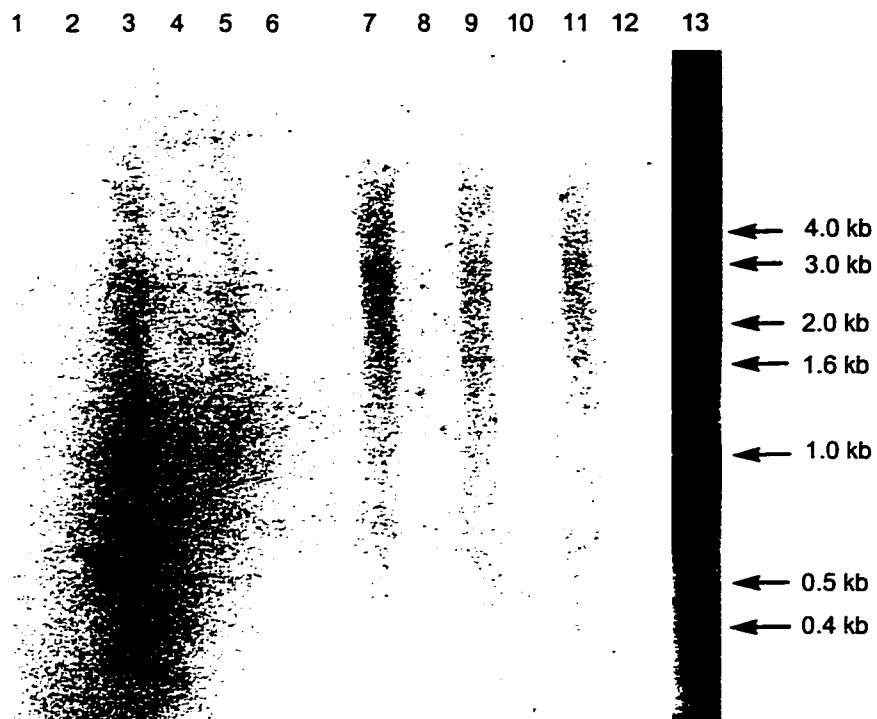
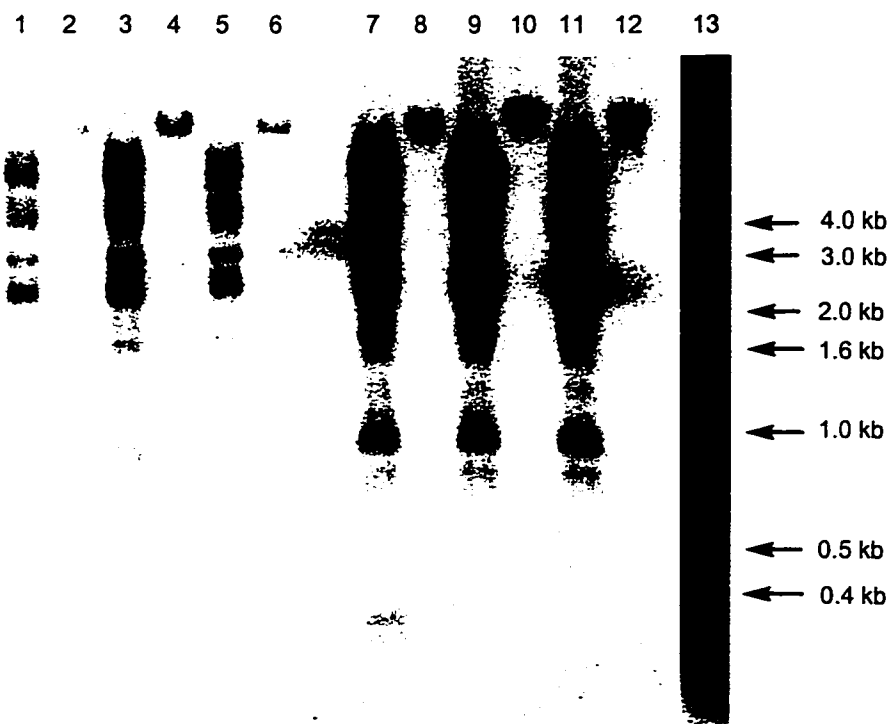


**Figure 4.4 Nucleotide sequence of the 5' RACE product obtained from RNA of CGL fibroblasts encoding an aberrant form of hPPAR $\gamma$ .** 5' RACE was performed as described (section 2.5.4.1) using total RNA extracted from CGL cells for the cDNA synthesis, and using the 5' RACE anchor subprimer and HPPARG-rev2 hPPAR $\gamma$  gene-specific primer for the PCR amplification of synthesized cDNA. Reamplifications were performed using the 5' RACE anchor subprimer and the nested HPPARG-r4 (GSP2) hPPAR $\gamma$  gene-specific primer. Subcloning and manual DNA sequencing resulted in the identification of the hybrid RACE product whose sequence is shown (CGL-RACE). Alignment with the normal hPPAR $\gamma$  cDNA sequence (from Elbrecht *et al.*, 1996) is given. Vertical lines between nucleotides of the two sequences indicate sequence identity. 3-letter abbreviations for encoded amino acids are given above and below the two sequences. Amino acids specifically encoded by the hybrid RACE product are shown above the CGL-RACE sequence (stop codons in italics) while the unlabelled codons correspond to shared protein sequence with hPPAR $\gamma$ , given below the normal hPPAR $\gamma$  nucleotide sequence. Vertical dotted lines indicate the boundaries between domains A/B (transactivation domain) and C (DNA-binding domain), and between domains C and D (hinge region) of the hPPAR $\gamma$  protein. Known positions of exon boundaries within the hPPAR $\gamma$  sequence are shown in boldface and the normal length of each exon is given in brackets. A consensus intron/exon boundary sequence identified within the hybrid RACE product is underlined.





**Figure 4.5** Distinct signals corresponding to the unknown 5' sequence of the hybrid RACE product do not appear on Southern blots of human genomic DNA from normal fibroblasts or from blood samples of CGL-associated individuals. Duplicate aliquots of 10 µg of genomic DNA extracted from cultured human fibroblast cells or from human blood samples was digested with *EcoRI/HindIII*. The DNA fragments generated were electrophoresed on two 1% agarose gels, transferred to nitrocellulose, and analyzed by Southern blotting. Blots were probed with radiolabelled DNA fragments corresponding to the unknown 103-bp 5' sequence of the hybrid RACE product (Panel A) or a full-length human cytoplasmic β-actin cDNA (Panel B). Shown are autoradiographs of the probed Southern blots (3-day exposures). Odd-numbered lanes contain digested genomic DNA samples while even-numbered lanes contain approximately 1 µg of undigested genomic DNA. The samples from which DNA was extracted for Southern analysis are as follows: *lanes 1 and 2*, normal human fibroblast cell line 986; *lanes 3 and 4*, normal human fibroblast cell line 1056; *lanes 5 and 6*, human CGL primary fibroblasts; *lanes 7 and 8*, blood samples from the CGL patient; *lanes 9 and 10*, blood samples from the CGL patient's mother; *lanes 11 and 12*, blood samples from the CGL patient's father. Lane 13 in Panel A corresponds to linearized positive control plasmid DNA containing the hybrid RACE product sequence. Lane 13 in Panel B corresponds to linearized positive control plasmid DNA containing the human β-actin cDNA sequence. Migration of DNA size markers on the gels is indicated.

**A****B**

**Figure 4.6** The hybrid RACE product sequence is found in genomic DNA from normal and CGL human fibroblasts. Approximately 800 ng of genomic DNA isolated from normal or CGL cultured human fibroblasts or from human blood samples was used as the template in PCR reactions. Amplification of the hybrid RACE product sequence was attempted using 25 pmol of each of the oligonucleotide primers 9-6c2 for-2 and HPPARG ex3-rev in a reaction using Ready-To-Go® PCR beads (Pharmacia Biotech). Control PCRs involved the use of ~50 ng of plasmid DNA or no DNA as the template. 36 amplification cycles were performed using an annealing temperature of 65°C. Shown is a photograph of a 3% NuSieve® GTG agarose gel containing ethidium bromide on which the PCR products were run. DNA templates used were extracted from the following samples: *lane 2*, normal human fibroblast cell line 986; *lane 3*, CGL fibroblasts; *lane 4*, blood sample of CGL patient's mother; *lane 5*, blood sample of CGL patient's father. Control reactions: *lane 6*, human  $\beta$ -actin cDNA in pGEM5Zf (negative control plasmid) as template; *lane 7*, hybrid RACE product in pGEM5Zf (positive control plasmid) as template; *lane 8*, no DNA template. *Lane 1*, 1kb-Plus DNA size markers.

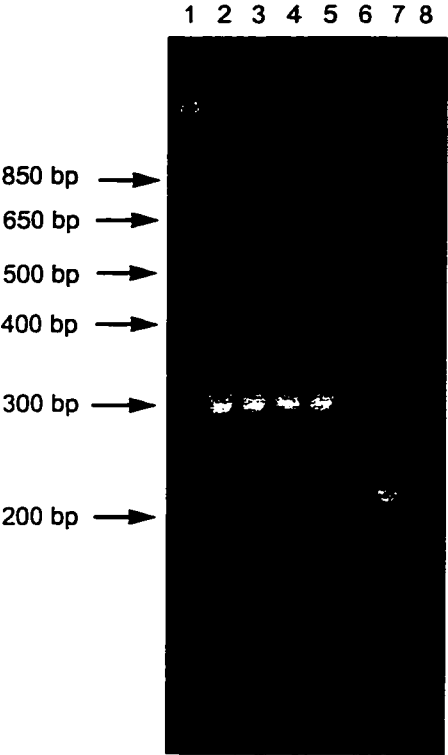


**Figure 4.7** The unknown 5' sequence of the hybrid RACE product consists of normal hPPAR $\gamma$  intron DNA. The PCR products shown in Figure 4.6 were purified and subjected to automated DNA sequencing using the same oligonucleotide primers used for the amplification reactions. Shown is a portion of the sequence corresponding to PCR products obtained from the genomic DNA of both normal and CGL cells (top), a representation of the hybrid RACE product aligned with the genomic DNA sequence (middle), and the consensus sequences found at exon-intron junctions and lariat branch sites of eukaryotic pre-mRNAs (bottom; adapted from Voet and Voet, 1995). The nucleotide sequences shown in the top and middle panels correspond to published sequences for normal hPPAR $\gamma$  intron DNA (Okazawa *et al.*, 1997). In the top panel, putative 5' splice donor, intron lariat branch, and 3' splice acceptor sites within the genomic DNA are underlined in succession. Indicated with an asterisk is the proposed site of C→U conversion in the RNA transcript. A partial mooring element sequence required for RNA editing is given in boldface and labelled. The 81 nucleotides missing from the hybrid RACE product are shown as a broken line in the middle panel. The subscripts in the bottom panel indicate the percentage of eukaryotic pre-mRNAs in which the specified bases have been found to occur, where R, Y, and N denote, respectively, purine, pyrimidine, and any nucleotides.

**Genomic DNA:**

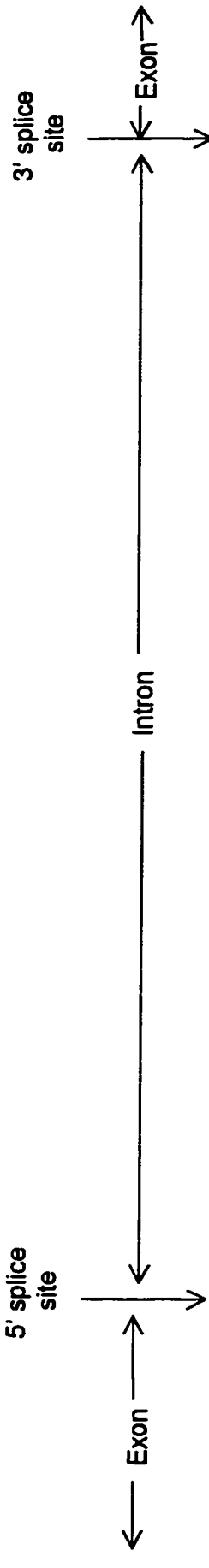
5'-...98 bp-CCCAGGCCAGTATACCTTTCGCTGTAGGTTGCTGCTCCATGTGTCTATAAGACTTAAATTTGCTTCTTTTATCCCTTTGCAG-exon 3...3'

\*  partial mooring element sequence

**Hybrid RACE product:**

5'- 98 bp-CCCAG -----exon 3...3'

**Consensus exon-intron boundary and lariat branch site sequences:**



5'-.....(A/C)A<sub>62</sub>R<sub>>77</sub> | G<sub>100</sub>U<sub>100</sub>A<sub>80</sub>A<sub>74</sub>G<sub>84</sub>U<sub>50</sub>.....CURA<sub>100</sub>Y.....11(Y)<sub>77-81</sub>NC<sub>78</sub>A<sub>100</sub>G<sub>100</sub> | R<sub>>55</sub>...-3'

**Figure 4.8 The hybrid RACE product sequence is detected in poly(A)<sup>+</sup> RNA pools from normal and CGL human fibroblasts.** RT-PCR was performed using 2 µg of poly(A)<sup>+</sup> RNA extracted from cultured human fibroblasts and the HPPARG-r4 (GSP2) oligonucleotide to prime cDNA synthesis. The reverse transcription reaction was carried out at 52°C. PCR amplification of the hybrid RACE product sequence from the partial cDNAs synthesized was performed using 25 pmol of each of the primers 9-6c2 for-2 and 9-6c2 rev in reactions using the Ready-To-Go<sup>®</sup> PCR beads. 37 amplification cycles with an annealing temperature of 60°C were performed for the PCRs. Shown is a photograph of a 3% NuSieve<sup>®</sup> GTG agarose gel stained with ethidium bromide on which the RT-PCR products were run. The cultured cells from which the poly(A)<sup>+</sup> RNA starting material was isolated were as follows: *lane 2*, CGL fibroblasts; *lane 3*, normal human primary fibroblasts; *lane 4*, normal human fibroblast cell line 986. *Lane 5* contains products of a negative control PCR reaction in which no template DNA was included. *Lane 1*, 1kb DNA size markers.





**Figure 4.9 Human PPAR $\gamma$  message is specifically detected in a variety of human tissues using a hPPAR $\gamma$  cDNA fragment probe.** A human multiple tissue Northern blot containing 2  $\mu$ g of poly(A)<sup>+</sup> RNA per lane (CLONTECH Laboratories) was analyzed as described (section 2.5.5.5) using a 288-bp radiolabelled DNA fragment corresponding to the region of the hybrid RACE product identical to the normal hPPAR $\gamma$  cDNA sequence (nucleotides +567 to +854) as a probe. Shown is the resulting autoradiograph of the probed blot (3-day exposure). The human tissues from which the RNA samples contained on the blot were derived are as follows: *lane 1*, pancreas; *lane 2*, kidney; *lane 3*, skeletal muscle; *lane 4*, liver; *lane 5*, lung; *lane 6*, placenta; *lane 7*, brain; *lane 8*, heart. The position of RNA size markers (given in kilobases) is indicated.

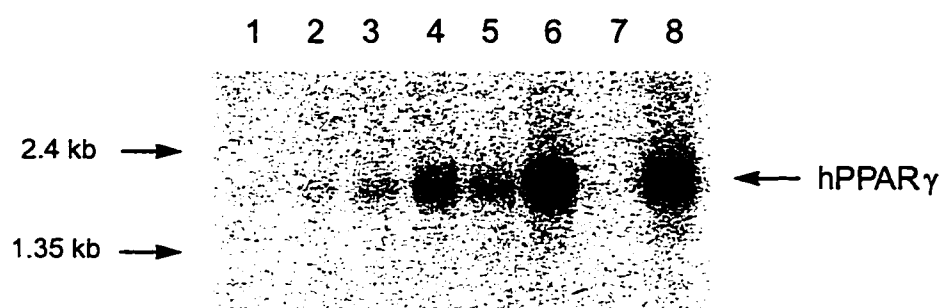


**Figure 4.10 Human PPAR $\gamma$  message is found in normal human fibroblasts while is virtually undetectable in CGL fibroblasts.** 5  $\mu$ g of poly(A)<sup>+</sup> RNA was isolated from cultured human fibroblasts as described (sections 2.5.1-2.5.2). RNA preparations were electrophoresed on 1% agarose-formaldehyde gels, transferred to nitrocellulose, and analyzed by Northern blotting as described (section 2.5.5). Blots were probed sequentially with radiolabelled DNA fragments corresponding to a 288-bp sequence within the normal hPPAR $\gamma$  cDNA sequence (Panels A1 and A2) and a full-length human  $\beta$ -actin cDNA (Panels B1 and B2). Shown are autoradiographs of two separate Northern blots generated and processed identically. Panel A1 shows a 5-day exposure of the hPPAR $\gamma$  fragment-probed blot, while Panel B1 shows a 1-day exposure of the same blot stripped once and reprobed with the  $\beta$ -actin cDNA probe. Panel A2 shows a 7-day exposure of a separate blot probed with the hPPAR $\gamma$  cDNA fragment, while Panel B2 shows a 1-day exposure of the same blot stripped once and reprobed with the  $\beta$ -actin cDNA probe. Cultured cells from which the RNA samples were extracted are as follows: *lane 1*, normal human fibroblast cell line 1059; *lane 2*, normal human fibroblast cell line 1056; *lane 3*, normal human fibroblast cell line 986; *lane 4*, normal human primary fibroblasts; *lane 5*, CGL primary fibroblasts. Hybridization signals corresponding to hPPAR $\gamma$  and  $\beta$ -actin mRNAs are indicated.



**Figure 4.11 Densitometric analysis of hPPAR $\gamma$  mRNA levels in normal and CGL fibroblasts detected by Northern blotting.** Northern blots shown in Figure 4.10 were subjected to densitometry as described (section 2.5.5.4). Normalized densitometric values for hPPAR $\gamma$  autoradiographic signals were calculated as a percentage of the corresponding  $\beta$ -actin signal appearing on the same blot. Plotted are the average values obtained from the two blots  $\pm$  standard error of the mean.

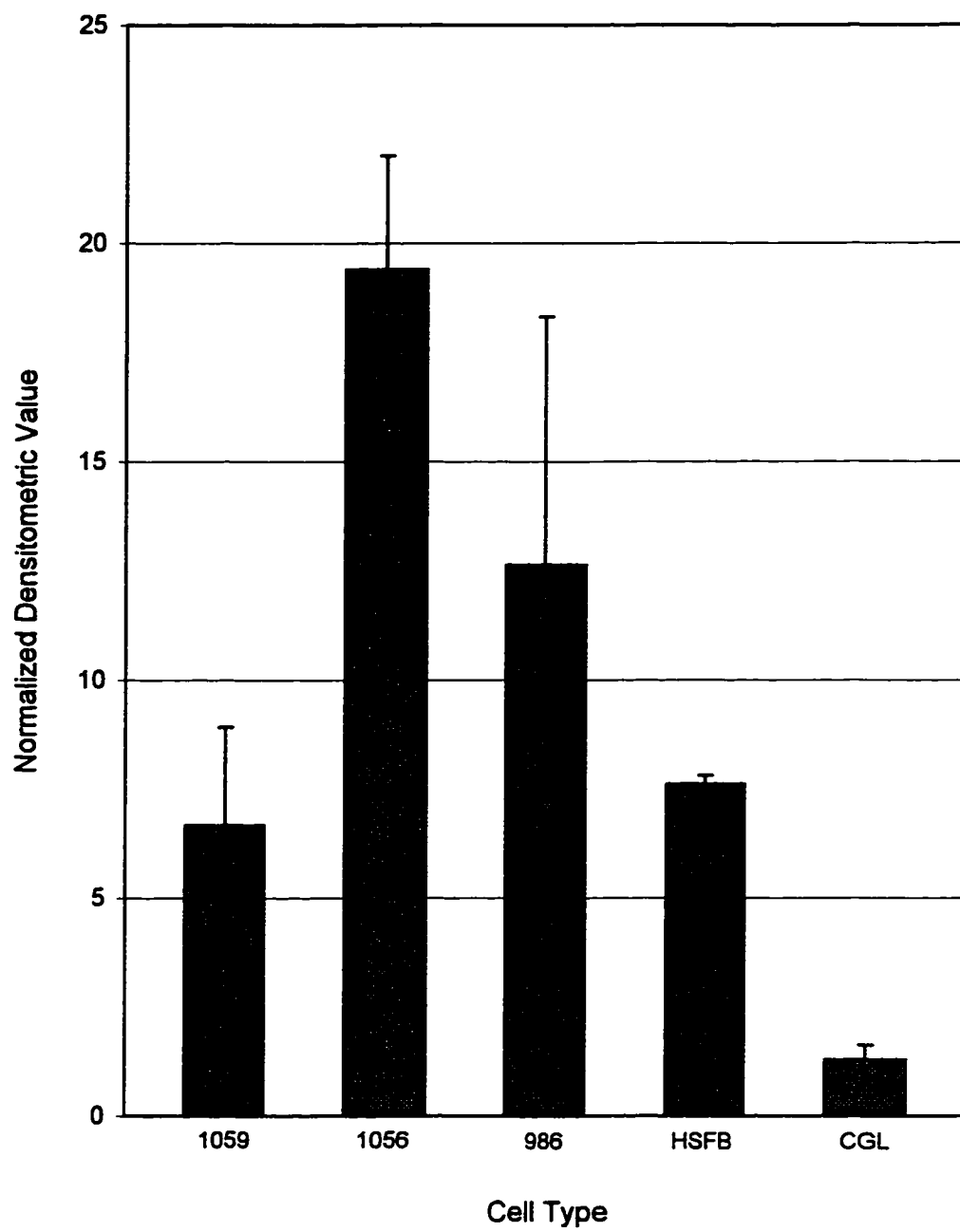


**Figure 4.12 Specificity test for rabbit serum containing antibodies raised against a hPPAR $\gamma$  synthetic peptide.** Serum was prepared from test bleeds collected prior to injection and following the second injection of rabbits with a hPPAR $\gamma$  synthetic peptide-KLH conjugate (section 2.6.6.3). Dilutions of the serum samples were prepared and analyzed for immunoreactivity with the hPPAR $\gamma$  synthetic peptide by Western blotting. Shown are autoradiographs (1-minute exposures) of a series of Western blots containing 10  $\mu$ g of the hPPAR $\gamma$  synthetic peptide-BSA conjugate (odd-numbered lanes) run alongside 10  $\mu$ g of pure BSA (even-numbered lanes) in SDS-PAGE gels and transferred to nitrocellulose. Serum dilutions used for probing the blots are given below each blot. The mobility of protein molecular weight markers is indicated. *PI*, pre-immune serum.

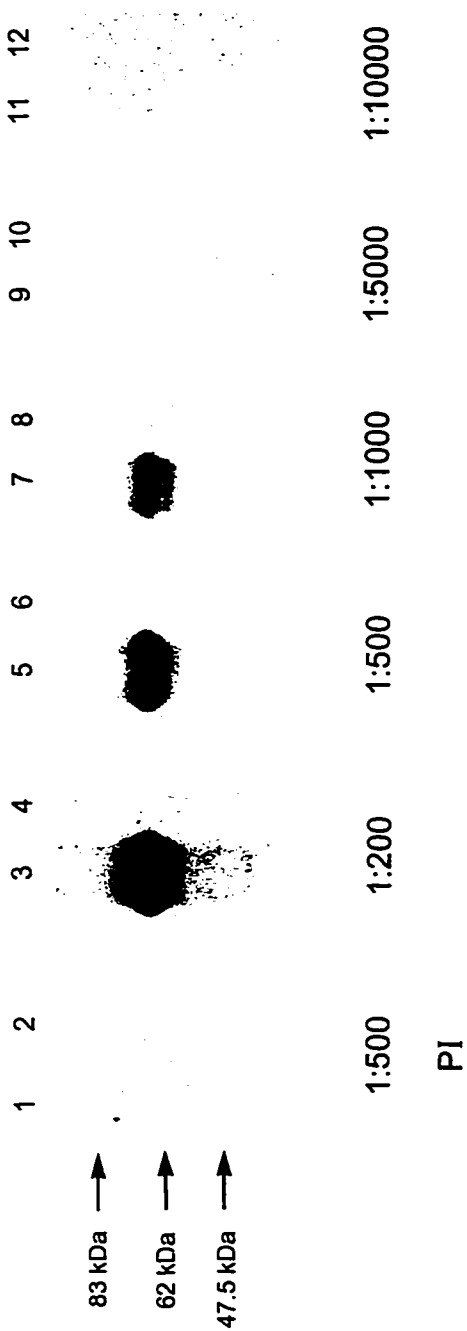




**Figure 4.13 Rabbit polyclonal antibodies raised against a hPPAR $\gamma$ -specific synthetic peptide do not recognize human PPAR $\gamma$  protein.** Shown is an autoradiograph (10-minute exposure) of a Western blot containing positive and negative control protein samples probed with a 1:500 dilution of serum extracted from rabbits injected with a hPPAR $\gamma$  synthetic peptide. *Lane 1*, protein extract from mock-transfected COS cells (negative control); *lane 2*, protein extract from COS cells transfected with an expression plasmid encoding hPPAR $\gamma$ ; *lane 3*, a sample of *in vitro* transcribed/translated mPPAR $\gamma$ 2 protein. The migration of protein molecular weight markers is indicated.

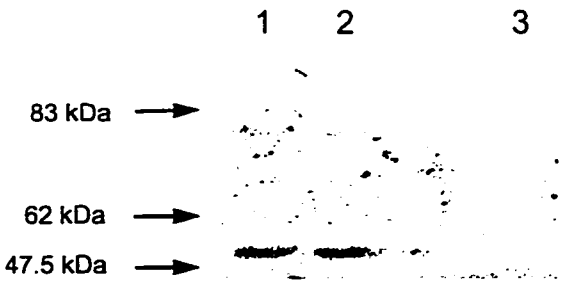


**Figure 4.14 Detection of hPPAR $\gamma$  protein in extracts of normal human fibroblasts and CGL cells.** Proteins were extracted from cultured normal fibroblasts and CGL cells using the TRI-Reagent<sup>®</sup> as described (section 2.6.1.1). Protein samples were subjected to SDS-PAGE on 7.5% mini-gels, followed by Western blotting with a commercial PPAR $\gamma$ -specific goat polyclonal antibody preparation (Santa Cruz Biotechnology, Inc.). Detection of immunoreactive species was performed by ECL followed by autoradiography. Two separate autoradiographs are shown, representing a 30-minute exposure (lanes 1-5) and a 15-minute exposure (lanes 6-8) of Western blots to film. Lanes 1-5 contain 60  $\mu$ g of total protein per lane extracted from the following cell types: *lane 1*, human fibroblast cell line 986; *lane 2*, human fibroblast cell line 1056; *lane 3*, human fibroblast cell line 1059; *lane 4*, normal human primary fibroblasts; *lane 5*, CGL primary fibroblasts. Lane 6 contains a negative control protein extract obtained from mock-transfected COS cells. Lane 7 contains a positive control protein extract obtained from COS cells transfected with an expression plasmid encoding hPPAR $\gamma$ . Lane 8 contains a sample of *in vitro* transcribed/translated mPPAR $\gamma$ 2. The migration of protein size markers was the same for each blot, with positions as indicated.

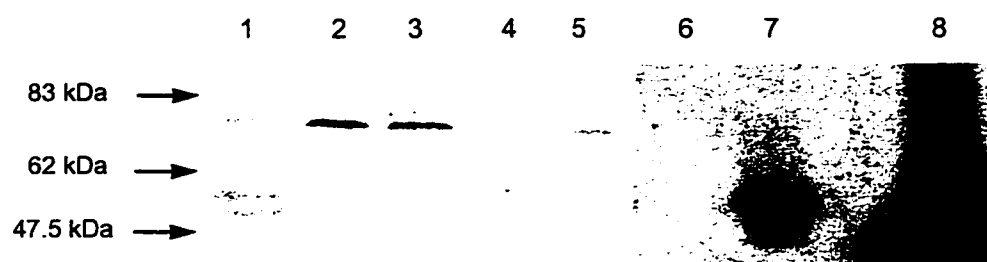


**Figure 4.15 Treatment of normal or CGL fibroblasts with PPAR $\gamma$  activators does not induce hPPAR $\gamma$  expression.** Cultured normal human primary fibroblasts (HSFB cells) or CGL primary fibroblasts were treated with the PPAR $\gamma$  activators wy-14,643 or 15-d-PGJ<sub>2</sub>, or with DMSO as a control compound, in a preadipocyte differentiation assay (Panels A1 and B1, section 2.2.3.1) or by a procedure for stimulation of adipogenesis in non-determined fibroblasts (Panels A2 and B2, section 2.2.3.2). Total RNA was extracted from the treated cells and assessed for hPPAR $\gamma$  and human  $\beta$ -actin expression by Northern blotting as described (section 2.5.5). Shown are autoradiographs of the Northern blots sequentially probed with the hPPAR $\gamma$  and  $\beta$ -actin probes as described in Figure 4.8. Panels A1 and B1 represent the same blot, containing 8  $\mu$ g of total RNA per lane. Panels A2 and B2 are autoradiographs of a blot containing 20  $\mu$ g of total RNA per lane. The hPPAR $\gamma$ -probed blots were exposed to film for 5 days, while 1-day exposures of the  $\beta$ -actin-probed blots are shown. PPAR $\gamma$  activator treatments to the different cell types were as follows: *lanes 1 and 5*, HSFB cells + DMSO; *lane 2*, HSFB cells + 15-d-PGJ<sub>2</sub>; *lane 6*, HSFB cells + wy-14,643; *lanes 3 and 7*, CGL cells + DMSO; *lane 4*, CGL cells + 15-d-PGJ<sub>2</sub>; *lane 8*, CGL cells + wy-14,643. Positions of hPPAR $\gamma$  and  $\beta$ -actin transcripts on each blot are indicated.

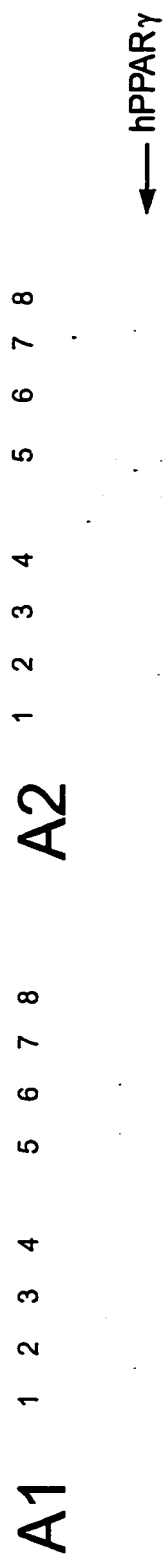


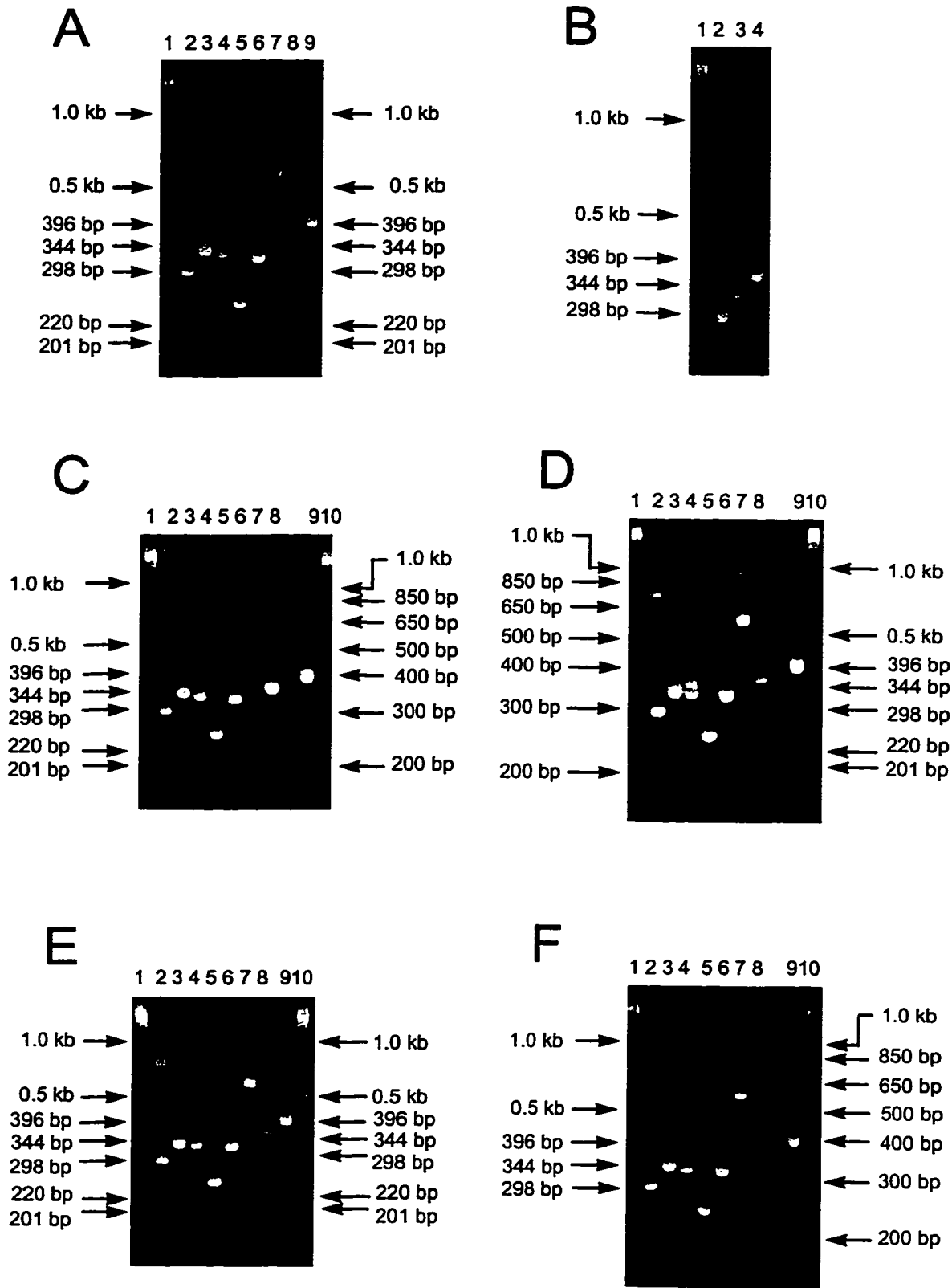
Table 4.1 Oligonucleotide primer sets<sup>a</sup> used for hPPAR $\gamma$  exon and  $\beta$ -actin fragment amplification from genomic DNA samples

product specificity	forward primer name	reverse primer name	expected size of PCR product (bp)
hPPAR $\gamma$ exons:			
$\gamma$ 2	hPPAR $\gamma$ 2 Ex $\gamma$ 2-for	hPPAR $\gamma$ 2 Ex $\gamma$ 2-rev	299
1	hPPAR $\gamma$ 2 Ex1-for	hPPAR $\gamma$ 2 Ex1-rev	346
2	hPPAR $\gamma$ 2 Ex2-for	hPPAR $\gamma$ 2 Ex2-rev	335
3	hPPAR $\gamma$ 2 Ex3-for	hPPAR $\gamma$ 2 Ex3-rev	253
4	hPPAR $\gamma$ 2 Ex4-for	hPPAR $\gamma$ 2 Ex4-rev	331
5	hPPAR $\gamma$ 2 Ex5-for	hPPAR $\gamma$ 2 Ex5-rev	601
6	hPPAR $\gamma$ 2 Ex6-for	hPPAR $\gamma$ 2 Ex6-rev	369
human $\beta$ -actin:	HBACTIN-for3	HBACTIN-rev3	415

<sup>a</sup> primer sequences, descriptions, and estimated melting temperatures are given in Table 2.2.

**Figure 4.16 PCR amplification of hPPAR $\gamma$  exons from genomic DNA samples.** Approximately 800 ng of genomic DNA extracted from cultured human fibroblast cells or from human blood samples was used as the template in PCR reactions performed to amplify hPPAR $\gamma$  exon sequences. Positive control reactions to amplify a fragment of human cytoplasmic  $\beta$ -actin were also performed. The oligonucleotide primer sets used for the PCRs are given in Table 4.1. All reactions performed involved the use of 25 pmol of each primer, Ready-To-Go<sup>®</sup> PCR beads, and 35 amplification cycles. Shown are photographs of ethidium bromide-stained 3% NuSieve<sup>®</sup> GTG agarose gels in which the PCR products were electrophoresed. Panels A and B show the products of reactions performed using genomic DNA isolated from CGL primary fibroblasts as template. The products in Panel A were generated using an annealing temperature of 50°C. A higher annealing temperature of 57°C was used to eliminate any nonspecific bands observed for the reactions performed at 50°C, and the products of these secondary PCRs are shown in Panel B. Panels C-F show the PCR products generated in reactions using an annealing temperature of 50°C and genomic DNA templates from the following sources: *Panel C*, blood from the CGL patient's mother; *Panel D*, blood from the CGL patient's father; *Panel E*, normal human fibroblast cell line 986; *Panel F*, normal human fibroblast cell line 1056. The individual reactions performed in Panels A-F were as follows (variations in Panel B are described in brackets): *lane 2*, hPPAR $\gamma$  exon  $\gamma$ 2 amplification; *lanes 3-8*, hPPAR $\gamma$  exons 1-6 amplifications, respectively (*Panel B*, *lane 2*, hPPAR $\gamma$  exon 2 amplification; *Panel B*, *lane 3*, hPPAR $\gamma$  exon 6 amplification); *lane 9*, human  $\beta$ -actin fragment amplification. Lanes 1 and 10 contain either 1kb or 1kb-Plus DNA size markers as indicated.

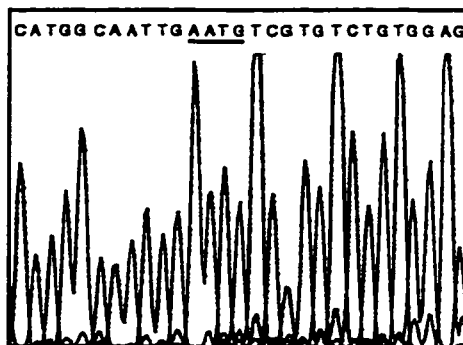
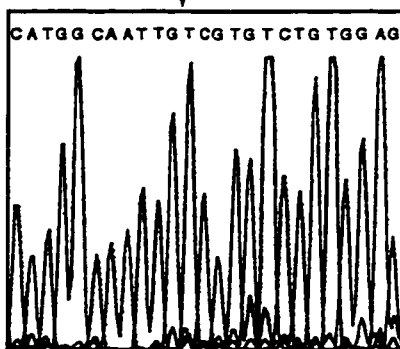
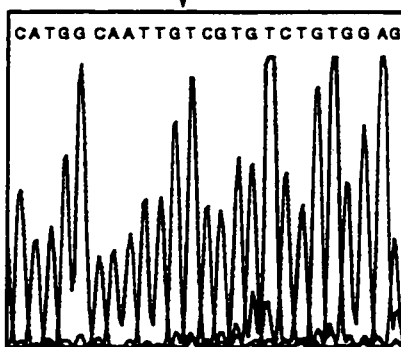




**Figure 4.17 Amplification of an aberrant hPPAR $\gamma$  exon 2 sequence from genomic DNA of the CGL patient and the patient's father.** PCR products corresponding to exon 2 sequences of hPPAR $\gamma$  obtained in the reactions described in Figure 4.13 were purified and subjected to automated DNA sequencing (sections 2.3.14.2 and 2.3.15.2). Shown are portions of the electrophoretograms obtained for three of the sequencing reactions performed. The corresponding nucleotide is given above each individual peak. The sequences shown are those for hPPAR $\gamma$  exon 2 PCR products generated from genomic DNA isolated from the following sources: *Panel A*, normal human fibroblast cell line 986; *Panel B*, CGL fibroblasts; *Panel C*, blood sample from the CGL patient's father. The arrows in Panels B and C indicate the position of the 4-nucleotides missing from the normal hPPAR $\gamma$  exon 2 sequence shown underlined in Panel A. The numbers given above Panel A correspond to nucleotide positions within the normal hPPAR $\gamma$  cDNA sequence (Greene *et al.*, 1995).

+491

+516

**A****B****C**

## **Chapter 5**

### **Summary and Conclusions**

PPARs are important regulatory proteins involved in the control of transcriptional events implicated in a variety of biological processes. The work described in this thesis was performed to further characterize the actions of PPAR family members in mammalian systems, with a particular emphasis on the effects and modulation of receptor activity under altered environmental and genetic conditions.

The influence of peroxisome proliferators on normal physiology has been extensively studied and consequently has expanded our knowledge of the mechanisms underlying normal metabolic function and responsiveness to environmental and pharmacological agents. It is important to fully characterize the molecular events induced by these chemicals in order to understand how they bring about their wide ranging effects, both advantageous and deleterious. Influences on peroxisome biology, most notably lipid metabolism, are of significance in determining their benefits to human health, for example regarding the therapeutic actions of hypolipidemic drugs. Conversely, it is crucial to outline the molecular basis of the negative risks associated with exposure to this class of compounds, such as tumorigenesis.

To these ends, investigation into the mode of action of PPARs, the proteins mediating the effects of peroxisome proliferators, has enabled a more detailed analysis of the cellular and biochemical events that define peroxisome proliferation. The most intensively studied of the peroxisomal processes characterizing this phenomenon is that of straight-chain fatty acid  $\beta$ -oxidation. The coordinate transcriptional activation of the genes encoding the three enzymes of this lipolytic pathway upon peroxisome proliferator exposure is well established. The mechanism of regulation of the first two enzymes of the fatty acid degradation cycle have been elucidated, however details regarding the transcriptional control of the third enzyme, peroxisomal 3-ketoacyl-CoA thiolase, are unknown. The studies described in Chapter 3 demonstrate that the PPRE for the inducible peroxisomal thiolase gene is not located within two kilobases of the transcriptional start site. This finding is contrary to reports of the existence of a responsive element located at -681 to -669 of the thiolase B gene promoter region, defined as such based on sequence prediction and PPAR $\alpha$ -binding assays. It is important to identify the functional PPRE for this gene to gain a more complete understanding of the mechanisms that control fatty acid  $\beta$ -oxidation occurring as a normal physiological process and as a series of biochemical reactions that can be dramatically induced in response to specific stimuli.

In recent years, PPARs have been shown to play a variety of specialized roles in a number of different tissues. The name given to these receptors is therefore somewhat outdated, reflecting solely the function identified at the time of their discovery and unrepresentative of the plethora of actions they have more recently demonstrated. Among the most significant of findings pertaining to PPAR function is the identification of an involvement in the process of adipogenesis. Several landmark studies now establish the PPAR $\gamma$  isoform as a central regulator of fat cell differentiation. Such a claim clearly has far-reaching implications regarding the pathogenesis of diseases characterized by excessive or deficient adipose tissue mass. Chapter 4 describes work performed in an effort to study the role of this nuclear hormone receptor in the development and possible treatment of one such disorder, congenital generalized lipodystrophy, in which body fat is virtually absent.

Analysis of PPAR $\gamma$  expression in human skin fibroblasts reveals that processing of PPAR $\gamma$  transcripts yields multiple mRNA species resulting from both correct and aberrant splicing events. This is likely a common phenomenon occurring for several genes following their transcription, as such molecules were detected in both normal and CGL cells. The mechanisms in place in mammalian cells to compensate for such errors in RNA transcript processing presumably function to prevent the harmful consequences which may result from translation of abnormal protein-encoding mRNA molecules.

A clear difference was observed in the level of PPAR $\gamma$  expression between normal human fibroblast cells and fibroblasts derived from a CGL patient. The significantly reduced amount of PPAR $\gamma$  message in CGL cells suggests that this may contribute to the abnormalities associated with the disorder. Further analysis of PPAR $\gamma$  protein within these tissues is required to investigate the relevance of the low message levels to overall PPAR $\gamma$  function in CGL cells. Determination of the impact of deficient PPAR $\gamma$  expression in skin fibroblast cells on CGL awaits the characterization of PPAR $\gamma$  function in this tissue.

Activation of PPAR $\gamma$  in several experimental fibroblast cell lines has been observed to effectively promote adipocyte differentiation. Attempts to stimulate the adipogenic program in both normal and CGL human fibroblasts with PPAR $\gamma$  activators were not successful. This may be attributed to inappropriate cell culture conditions or activator potency, or to limited adipogenic potential of the particular cells examined. The behaviour of human fibroblast cells *in vitro* and *in vivo* needs to more carefully assessed

before adipocytic conversion can be addressed as a possible treatment for the lack of body fat observed in CGL.

Molecular scanning of the PPAR $\gamma$  gene within normal and CGL fibroblasts was performed to detect the presence of coding sequence abnormalities that may be responsible for or contribute to the diseased state. A novel sequence anomaly was detected in the CGL patient's and patient's father's genomic DNA that would yield reduced PPAR $\gamma$  message levels or a dysfunctional protein if expressed, suggesting a possible involvement of the PPAR $\gamma$  gene in the particular case of CGL under study. Additional analysis of the implications of this PPAR $\gamma$  coding sequence aberration is required to determine if it does indeed play a role in the etiology of CGL.

Continued investigation of the actions of PPARs in the variety of tissues in which their expression has been detected will enable a more complete understanding of the biological processes under their transcriptional control. Identification of instances of PPAR dysfunction in human disorders will reveal the physiological importance of this subfamily of nuclear hormone receptors in humans and may lead to improved therapeutic strategies.

## **Chapter 6**

### **Bibliography**



- Adams, M., Reginato, M. J., Shao, D., Lazar, M. A., and Chatterjee, V. K. (1997) Transcriptional activation by peroxisome proliferator-activated receptor  $\gamma$  is inhibited by phosphorylation at a consensus mitogen-activated protein kinase site. *J. Biol. Chem.* **272**(8):5128-32.
- Ailhaud, G. (1982) Adipose cell differentiation in culture. *Mol. Cell. Biochem.* **49**(1):17-31.
- Aldridge, T. C., Tugwood, J. D., and Green, S. (1995) Identification and characterization of DNA elements implicated in the regulation of CYP4A1 transcription. *Biochem. J.* **306**(Pt 2):473-9.
- Altioik, S., Xu, M., and Spiegelman, B. M. (1997) PPAR $\gamma$  induces cell cycle withdrawal: inhibition of E2F/DP DNA-binding activity via down-regulation of PP2A. *Genes Dev.* **11**(15):1987-98.
- Altschul, S. F., Gish, W., Miller, W., Myers, E. W., and Lipman, D. J. (1990) Basic local alignment search tool. *J. Mol. Biol.* **215**(3):403-10.
- Antonenkov, V. D., Van Veldhoven, P. P., Waelkens, E., and Mannaerts, G. P. (1997) Substrate specificities of 3-oxoacyl-CoA thiolase A and sterol carrier protein 2/3-oxoacyl-CoA thiolase purified from normal rat liver peroxisomes. *J. Biol. Chem.* **272**(41):26023-31.
- Aoyama, T., Peters, J. M., Iritani, N., Nakajima, T., Furihata, K., Hashimoto, T., and Gonzalez, F. J. (1998) Altered constitutive expression of fatty acid-metabolizing enzymes in mice lacking the peroxisome proliferator-activated receptor  $\alpha$  (PPAR $\alpha$ ). *J. Biol. Chem.* **273**(10):5678-84.
- Arnold, C., and Hodgson, I. J. (1991) Vectorette PCR: a novel approach to genomic walking. *PCR Methods Appl.* **1**(1):39-42.
- Ashby, J., Brady, A., Elcombe, C. R., Elliott, B. M., Ishmael, J., Odum, J., Tugwood, J. D., Kettle, S., and Purchase, I. F. (1994) Mechanistically-based human hazard assessment of peroxisome proliferator-induced hepatocarcinogenesis. *Hum. Exp. Toxicol.* **13** Suppl 2:S1-S117.
- Ashkenas, J. (1997) Gene regulation by mRNA editing. *Am. J. Hum. Genet.* **60**(2):278-83.
- Auboeuf, D., Rieusset, J., Fajas, L., Vallier, P., Frering, V., Riou, J. P., Staels, B., Auwerx, J., Laville, M., and Vidal, H. (1997) Tissue distribution and quantification of the expression of mRNAs of peroxisome proliferator-activated receptors and liver X receptor- $\alpha$  in humans: no alteration in adipose tissue of obese and NIDDM patients. *Diabetes* **46**(8):1319-27.
- Ausubel, F. M., Brent, R., Kingston, R. E., Moore, D. D., Seidman, J. G., Smith, J. A., and Struhl, K., eds. (1996) *Current Protocols in Molecular Biology* (New York, NY: John Wiley & Sons, Inc.).

Backus, J. W., and Smith, H. C. (1991) Apolipoprotein B mRNA sequences 3' of the editing site are necessary and sufficient for editing and editosome assembly. *Nucleic Acids Res.* **19**(24):6781-6.

Bardot, O., Aldridge, T. C., Latruffe, N., and Green, S. (1993) PPAR-RXR heterodimer activates a peroxisome proliferator response element upstream of the bifunctional enzyme gene. *Biochem. Biophys. Res. Commun.* **192**(1):37-45.

Berger, J., Bailey, P., Biswas, C., Cullinan, C. A., Doebber, T. W., Hayes, N. S., Saperstein, R., Smith, R. G., and Leibowitz, M. D. (1996) Thiazolidinediones produce a conformational change in peroxisomal proliferator-activated receptor- $\gamma$ : binding and activation correlate with antidiabetic actions in db/db mice. *Endocrinology* **137**(10):4189-95.

Blaauboer, B. J., van Holsteijn, C. W., Bleumink, R., Mennes, W. C., van Pelt, F. N., Yap, S. H., van Pelt, J. F., van Iersel, A. A., Timmerman, A., and Schmid, B. P. (1990) The effect of becloric acid and clofibrilic acid on peroxisomal  $\beta$ -oxidation and peroxisome proliferation in primary cultures of rat, monkey and human hepatocytes. *Biochem. Pharmacol.* **40**(3):521-8.

Bodnar, A. G., and Rachubinski, R. A. (1990) Cloning and sequence determination of cDNA encoding a second rat liver peroxisomal 3-ketoacyl-CoA thiolase. *Gene* **91**(2):193-9.

Bogazzi, F., Hudson, L. D., and Nikodem, V. M. (1994) A novel heterodimerization partner for thyroid hormone receptor. *J. Biol. Chem.* **269**(16):11683-6.

Bout, A., Franse, M. M., Collins, J., Blonden, L., Tager, J. M., and Benne, R. (1991) Characterization of the gene encoding human peroxisomal 3-oxoacyl-CoA thiolase (ACAA). No large DNA rearrangement in a thiolase-deficient patient. *Biochim. Biophys. Acta* **1090**(1):43-51.

Bradford, M. M. (1976) A rapid and sensitive method for the quantitation of microgram quantities of protein utilizing the principle of protein-dye binding. *Anal. Biochem.* **72**:248-54.

Braissant, O., Fougelle, F., Scotto, C., Dauca, M., and Wahli, W. (1996) Differential expression of peroxisome proliferator-activated receptors (PPARs): tissue distribution of PPAR- $\alpha$ , - $\beta$ , and - $\gamma$  in the adult rat. *Endocrinology* **137**(1):354-66.

Braissant, O., and Wahli, W. (1998) Differential expression of peroxisome proliferator-activated receptor- $\alpha$ , - $\beta$ , and - $\gamma$  during rat embryonic development. *Endocrinology* **139**(6):2748-54.

Brun, R. P., Tontonoz, P., Forman, B. M., Ellis, R., Chen, J., Evans, R. M., and Spiegelman, B. M. (1996a) Differential activation of adipogenesis by multiple PPAR isoforms. *Genes Dev.* **10**(8):974-84.

Brun, R. P., Kim, J. B., Hu, E., Altiock, S., and Spiegelman, B. M. (1996b) Adipocyte differentiation: a transcriptional regulatory cascade. *Curr. Opin. Cell. Biol.* **8**(6):826-32.

Burant, C. F., Sreenan, S., Hirano, K., Tai, T. A., Lohmiller, J., Lukens, J., Davidson, N. O., Ross, S., and Graves, R. A. (1997) Troglitazone action is independent of adipose tissue. *J. Clin. Invest.* **100**(11):2900-8.

Cameron, R. G., De la Iglesia, F. A., and Feuer, G. (1996) Hepatotoxicity of cardiovascular drugs. *In* Drug-Induced Hepatotoxicity. R. G. Cameron, G. Feuer and F. A. De la Iglesia, eds. (Heidelberg: Springer-Verlag) pp.477-513.

Camp, H. S., and Tafuri, S. R. (1997) Regulation of peroxisome proliferator-activated receptor  $\gamma$  activity by mitogen-activated protein kinase. *J. Biol. Chem.* **272**(16):10811-6.

Cao, Z., Umek, R. M., and McKnight, S. L. (1991) Regulated expression of three C/EBP isoforms during adipose conversion of 3T3-L1 cells. *Genes Dev.* **5**(9):1538-52.

Chawla, A., Schwarz, E. J., Dimaculangan, D. D., and Lazar, M. A. (1994) Peroxisome proliferator-activated receptor (PPAR)  $\gamma$ : adipose-predominant expression and induction early in adipocyte differentiation. *Endocrinology* **135**(2):798-800.

Chawla, A., and Lazar, M. A. (1994) Peroxisome proliferator and retinoid signaling pathways co-regulate preadipocyte phenotype and survival. *Proc. Natl. Acad. Sci. USA* **91**(5):1786-90.

Chevray, P. M., and Nathans, D. (1992) Protein interaction cloning in yeast: identification of mammalian proteins that react with the leucine zipper of Jun. *Proc. Natl. Acad. Sci. USA* **89**(13):5789-93.

Chu, R., Lin, Y., Rao, M. S., and Reddy, J. K. (1995a) Cooperative formation of higher order peroxisome proliferator-activated receptor and retinoid X receptor complexes on the peroxisome proliferator responsive element of the rat hydratase-dehydrogenase gene. *J. Biol. Chem.* **270**(50):29636-9.

Chu, R., Madison, L. D., Lin, Y., Kopp, P., Rao, M. S., Jameson, J. L., and Reddy, J. K. (1995b) Thyroid hormone (T3) inhibits ciprofibrate-induced transcription of genes encoding  $\beta$ -oxidation enzymes: cross talk between peroxisome proliferator and T3 signaling pathways. *Proc. Natl. Acad. Sci. USA* **92**(25):11593-7.

Coligan, J. E., Dunn, B. M., Ploegh, H. L., Speicher, D. W., and Wingfield, P. T., eds. (1995) Current Protocols in Protein Science (New York, NY: John Wiley & Sons, Inc.).

Conrad, G. W., Hart, G. W., and Chen, Y. (1977) Differences *in vitro* between fibroblast-like cells from cornea, heart, and skin of embryonic chicks. *J. Cell Sci.* **26**:119-37.

Cullingford, T. E., Bhakoo, K., Peuchen, S., Dolphin, C. T., Patel, R., and Clark, J. B. (1998) Distribution of mRNAs encoding the peroxisome proliferator-activated receptor  $\alpha$ ,  $\beta$ , and  $\gamma$  and the retinoid X receptor  $\alpha$ ,  $\beta$ , and  $\gamma$  in rat central nervous system. *J. Neurochem.* **70**(4):1366-75.

de Duve, C., and Baudhuin, P. (1966) Peroxisomes (microbodies and related particles). *Physiol. Rev.* **46**(2):323-57.

De Vos, P., Lefebvre, A. M., Miller, S. G., Guerre-Millo, M., Wong, K., Saladin, R., Hamann, L. G., Staels, B., Briggs, M. R., and Auwerx, J. (1996) Thiazolidinediones repress *ob* gene expression in rodents via activation of peroxisome proliferator-activated receptor  $\gamma$ . *J. Clin. Invest.* **98**(4):1004-9.

de Wet, J. R., Wood, K. V., DeLuca, M., Helinski, D. R., and Subramani, S. (1987) Firefly luciferase gene: structure and expression in mammalian cells. *Mol. Cell. Biol.* **7**(2):725-37.

Desbois-Mouthon, C., Magre, J., Amselem, S., Reynet, C., Blivet, M. J., Goossens, M., Capeau, J., and Besmond, C. (1995) Lipoatrophic diabetes: genetic exclusion of the insulin receptor gene. *J. Clin. Endocrinol. Metab.* **80**(1):314-9.

Devchand, P. R., Keller, H., Peters, J. M., Vazquez, M., Gonzalez, F. J., and Wahli, W. (1996) The PPAR $\alpha$ -leukotriene B<sub>4</sub> pathway to inflammation control. *Nature* **384**(6604):39-43.

Devon, R. S., Porteous, D. J., and Brookes, A. J. (1995) Splinkerettes—improved vectorettes for greater efficiency in PCR walking. *Nucleic Acids Res.* **23**(9):1644-5.

Diczfalusy, U., and Alexson, S. E. (1988) Peroxisomal chain-shortening of prostaglandin F<sub>2</sub>  $\alpha$ . *J. Lipid Res.* **29**(12):1629-36.

Dreyer, C., Krey, G., Keller, H., Givel, F., Helftenbein, G., and Wahli, W. (1992) Control of the peroxisomal  $\beta$ -oxidation pathway by a novel family of nuclear hormone receptors. *Cell* **68**(5):879-87.

Driscoll, D. M., and Zhang, Q. (1994) Expression and characterization of p27, the catalytic subunit of the apolipoprotein B mRNA editing enzyme. *J. Biol. Chem.* **269**(31):19843-7.

DuBois, R. N., Gupta, R., Brockman, J., Reddy, B. S., Krakow, S. L., and Lazar, M. A. (1998) The nuclear eicosanoid receptor, PPAR $\alpha$ , is aberrantly expressed in colonic cancers. *Carcinogenesis* **19**(1):49-53.

Elbrecht, A., Chen, Y., Cullinan, C. A., Hayes, N., Leibowitz, M. D., Moller, D. E., and Berger, J. (1996) Molecular cloning, expression and characterization of human peroxisome proliferator activated receptors  $\gamma$ 1 and  $\gamma$ 2. *Biochem. Biophys. Res. Commun.* **224**(2):431-7.

Fajas, L., Auboeuf, D., Raspe, E., Schoonjans, K., Lefebvre, A. M., Saladin, R., Najib, J., Laville, M., Fruchart, J. C., Deeb, S., Vidal-Puig, A., Flier, J., Briggs, M. R., Staels, B., Vidal, H., and Auwerx, J. (1997) The organization, promoter analysis, and expression of the human PPAR $\gamma$  gene. *J. Biol. Chem.* **272**(30):18779-89.

Fajas, L., Fruchart, J. C., and Auwerx, J. (1998) Transcriptional control of adipogenesis. *Curr. Opin. Cell Biol.* **10**(2):165-73.

Fan, C. Y., Pan, J., Usuda, N., Yeldandi, A. V., Rao, M. S., and Reddy, J. K. (1998)

Steatohepatitis, spontaneous peroxisome proliferation and liver tumors in mice lacking peroxisomal fatty acyl-CoA oxidase. *J. Biol. Chem.* **273**(25):15639-45.

Forman, B. M., Tontonoz, P., Chen, J., Brun, R. P., Spiegelman, B. M., and Evans, R. M. (1995) 15-Deoxy- $\Delta^{12,14}$ -prostaglandin  $J_2$  is a ligand for the adipocyte determination factor PPAR $\gamma$ . *Cell* **83**(5):803-12.

Forman, B. M., Chen, J., and Evans, R. M. (1997a) Hypolipidemic drugs, polyunsaturated fatty acids, and eicosanoids are ligands for peroxisome proliferator-activated receptors  $\alpha$  and  $\delta$ . *Proc. Natl. Acad. Sci. USA* **94**(9):4312-7.

Forman, B. M., Ruan, B., Chen, J., Schroeffer, G. J., Jr., and Evans, R. M. (1997b) The orphan nuclear receptor LXR $\alpha$  is positively and negatively regulated by distinct products of mevalonate metabolism. *Proc. Natl. Acad. Sci. USA* **94**(20):10588-93.

Foster, D. W. (1998) The lipodystrophies and other rare disorders of adipose tissue. *In* Harrison's Principles of Internal Medicine, 14th Edition. A. S. Fauci, E. Braunwald, K. J. Isselbacher, J. D. Wilson, J. B. Martin, D. L. Kasper, S. L. Hauser and D. L. Longo, eds. (New York, NY: McGraw-Hill, Inc.) pp.2209-14.

Freytag, S. O., Paielli, D. L., and Gilbert, J. D. (1994) Ectopic expression of the CCAAT/enhancer-binding protein  $\alpha$  promotes the adipogenic program in a variety of mouse fibroblastic cells. *Genes Dev.* **8**(14):1654-63.

Frohman, M. A., Dush, M. K., and Martin, G. R. (1988) Rapid production of full-length cDNAs from rare transcripts: amplification using a single gene-specific oligonucleotide primer. *Proc. Natl. Acad. Sci. USA* **85**(23):8998-9002.

Gabbiani, G., and Rungger-Brändle, E. (1981) The fibroblast. *In* Tissue Repair and Regeneration. L. E. Glynn, ed. (Amsterdam:Elsevier) pp.1-50.

Ganning, A. E., Brunk, U., and Dallner, G. (1984) Phthalate esters and their effect on the liver. *Hepatology* **4**(3):541-7.

Gearing, K. L., Gottlicher, M., Teboul, M., Widmark, E., and Gustafsson, J. A. (1993) Interaction of the peroxisome-proliferator-activated receptor and retinoid X receptor. *Proc. Natl. Acad. Sci. USA* **90**(4):1440-4.

Gedde-Dahl, T., Jr., Trygstad, O., Van Maldergem, L., Magré, J., van der Hagen, C. B., Olaisen, B., Stenersen, M., and Mevåg, B. (1996) Genetics of the Berardinelli-Seip syndrome (congenital generalized lipodystrophy) in Norway: epidemiology and gene mapping. *Acta Paediatr. Suppl.* **413**:52-8.

Gharbi-Chihi, J., Teboul, M., Bismuth, J., Bonne, J., and Torresani, J. (1993) Increase of adipose differentiation by hypolipidemic fibrate drugs in Ob17 preadipocytes: requirement for thyroid hormones. *Biochim. Biophys. Acta* **1177**(1):8-14.

Gimble, J. M., Robinson, C. E., Wu, X., Kelly, K. A., Rodriguez, B. R., Kliewer, S. A., Lehmann, J. M., and Morris, D. C. (1996) Peroxisome proliferator-activated receptor- $\gamma$  activation by thiazolidinediones induces adipogenesis in bone marrow stromal cells. *Mol.*

*Pharmacol.* **50**(5):1087-94.

Glass, C. K. (1994) Differential recognition of target genes by nuclear receptor monomers, dimers, and heterodimers. *Endocr. Rev.* **15**(3):391-407.

Glauert, H. P., Reddy, J. K., Kennan, W. S., Sattler, G. L., Rao, V. S., and Pitot, H. C. (1984) Effect of hypolipidemic peroxisome proliferators on unscheduled DNA synthesis in cultured hepatocytes and on mutagenesis in *Salmonella*. *Cancer Lett.* **24**(2):147-56.

Göttlicher, M., Widmark, E., Li, Q., and Gustafsson, J. Å. (1992) Fatty acids activate a chimera of the clofibril acid-activated receptor and the glucocorticoid receptor. *Proc. Natl. Acad. Sci. USA* **89**(10):4653-7.

Granneman, J., Skoff, R., and Yang, X. (1998) Member of the peroxisome proliferator-activated receptor family of transcription factors is differentially expressed by oligodendrocytes. *J. Neurosci. Res.* **51**(5):563-73.

Gray, R. H., and de la Iglesia, F. A. (1984) Quantitative microscopy comparison of peroxisome proliferation by the lipid-regulating agent gemfibrozil in several species. *Hepatology* **4**(3):520-30.

Green, H., and Kehinde, O. (1975) An established preadipose cell line and its differentiation in culture. II. Factors affecting the adipose conversion. *Cell* **5**(1):19-27.

Greene, M. E., Blumberg, B., McBride, O. W., Yi, H. F., Kronquist, K., Kwan, K., Hsieh, L., Greene, G., and Nimer, S. D. (1995) Isolation of the human peroxisome proliferator activated receptor gamma cDNA: expression in hematopoietic cells and chromosomal mapping. *Gene Expr.* **4**(4-5):281-99.

Gulick, T., Cresci, S., Caira, T., Moore, D. D., and Kelly, D. P. (1994) The peroxisome proliferator-activated receptor regulates mitochondrial fatty acid oxidative enzyme gene expression. *Proc. Natl. Acad. Sci. USA* **91**(23):11012-6.

Gupta, R. C., Goel, S. K., Earley, K., Singh, B., and Reddy, J. K. (1985) <sup>32</sup>P-postlabeling analysis of peroxisome proliferator-DNA adduct formation in rat liver *in vivo* and hepatocytes *in vitro*. *Carcinogenesis* **6**(6):933-6.

Hadjiagapiou, C., Giannoni, F., Funahashi, T., Skarosi, S. F., and Davidson, N. O. (1994) Molecular cloning of a human small intestinal apolipoprotein B mRNA editing protein. *Nucleic Acids Res.* **22**(10):1874-9.

Hajra, A. K., and Bishop, J. E. (1982) Glycerolipid biosynthesis in peroxisomes via the acyl dihydroxyacetone phosphate pathway. *Ann. N.Y. Acad. Sci.* **386**:170-82.

Halaas, J. L., Gajiwala, K. S., Maffei, M., Cohen, S. L., Chait, B. T., Rabinowitz, D., Lallone, R. L., Burley, S. K., and Friedman, J. M. (1995) Weight-reducing effects of the plasma protein encoded by the *obese* gene. *Science* **269**(5223):543-6.

Hallakou, S., Doare, L., Foufelle, F., Kergoat, M., Guerre-Millo, M., Berthault, M. F., Dugail, I., Morin, J., Auwerx, J., and Ferre, P. (1997) Pioglitazone induces *in vivo* adipocyte differentiation in the obese Zucker *fa/fa* rat. *Diabetes* **46**(9):1393-9.

Hanefeld, M., Kemmer, C., and Kadner, E. (1983) Relationship between morphological changes and lipid-lowering action of p-chlorophenoxyisobutyric acid (CPIB) on hepatic mitochondria and peroxisomes in man. *Atherosclerosis* **46**(2):239-46.

Hanish, J., and McClelland, M. (1988) Activity of DNA modification and restriction enzymes in KGB, a potassium glutamate buffer. *Gene Anal. Tech.* **5**(5):105-7.

Harlow, E. and Lane, D., eds. (1988) *Antibodies: A Laboratory Manual* (Cold Spring Harbor, NY: Cold Spring Harbor Laboratory).

Hashimoto, T. (1982) Individual peroxisomal  $\beta$ -oxidation enzymes. *Ann. N.Y. Acad. Sci.* **386**:5-12.

Hauner, H., Entenmann, G., Wabitsch, M., Gaillard, D., Ailhaud, G., Negrel, R., and Pfeiffer, E. F. (1989) Promoting effect of glucocorticoids on the differentiation of human adipocyte precursor cells cultured in a chemically defined medium. *J. Clin. Invest.* **84**(5):1663-70.

Hay, E. D., ed. (1981) *Cell Biology of Extracellular Matrix* (New York, NY: Plenum).

Hengen, P. N. (1995) Vectors, splinkerettes and boomerang DNA amplification. *Trends Biochem. Sci.* **20**(9):372-3.

Hertz, R., Amon, J., Hoter, A., Shouval, D., and Bar-Tana, J. (1987) Clofibrate does not induce peroxisomal proliferation in human hepatoma cell lines PLC/PRF/5 and SK-HEP-1. *Cancer Lett.* **34**(3):263-72.

Hertz, R., Kalderon, B., and Bar-Tana, J. (1993) Thyromimetic effect of peroxisome proliferators. *Biochimie* **75**(3-4):257-61.

Hijikata, M., Wen, J. K., Osumi, T., and Hashimoto, T. (1990) Rat peroxisomal 3-ketoacyl-CoA thiolase gene. *J. Biol. Chem.* **265**(8):4600-6.

Hofmann, C., Lorenz, K., and Colca, J. R. (1991) Glucose transport deficiency in diabetic animals is corrected by treatment with the oral antihyperglycemic agent pioglitazone. *Endocrinology* **129**(4):1915-25.

Hofmann, C. A., Edwards, C. W., III, Hillman, R. M., and Colca, J. R. (1992) Treatment of insulin-resistant mice with the oral antidiabetic agent pioglitazone: evaluation of liver GLUT2 and phosphoenolpyruvate carboxykinase expression. *Endocrinology* **130**(2):735-40.

Hollenberg, A. N., Susulic, V. S., Madura, J. P., Zhang, B., Moller, D. E., Tontonoz, P., Sarraf, P., Spiegelman, B. M., and Lowell, B. B. (1997) Functional antagonism between CCAAT/Enhancer binding protein- $\alpha$  and peroxisome proliferator-activated receptor- $\gamma$  on the leptin promoter. *J. Biol. Chem.* **272**(8):5283-90.

Horwitz, K. B., Jackson, T. A., Bain, D. L., Richer, J. K., Takimoto, G. S., and Tung, L. (1996) Nuclear receptor coactivators and corepressors. *Mol. Endocrinol.* **10**(10):1167-77.

- Hu, E., Tontonoz, P., and Spiegelman, B. M. (1995) Transdifferentiation of myoblasts by the adipogenic transcription factors PPAR $\gamma$  and C/EBP $\alpha$ . *Proc. Natl. Acad. Sci. USA* **92**(21):9856-60.
- Hu, E., Kim, J. B., Sarraf, P., and Spiegelman, B. M. (1996) Inhibition of adipogenesis through MAP kinase-mediated phosphorylation of PPAR $\gamma$ . *Science* **274**(5295):2100-3.
- Hunter, J., Kassam, A., Winrow, C. J., Rachubinski, R. A., and Capone, J. P. (1996) Crosstalk between the thyroid hormone and peroxisome proliferator-activated receptors in regulating peroxisome proliferator-responsive genes. *Mol. Cell. Endocrinol.* **116**(2):213-21.
- Hwang, J. J., Hsia, M. T., and Jirtle, R. L. (1993) Induction of sister chromatid exchange and micronuclei in primary cultures of rat and human hepatocytes by the peroxisome proliferator, Wy-14,643. *Mutat. Res.* **286**(2):123-33.
- Hwang, C. S., Loftus, T. M., Mandrup, S., and Lane, M. D. (1997) Adipocyte differentiation and leptin expression. *Annu. Rev. Cell Dev. Biol.* **13**:231-59.
- Ijpenberg, A., Jeannin, E., Wahli, W., and Desvergne, B. (1997) Polarity and specific sequence requirements of peroxisome proliferator-activated receptor (PPAR)/retinoid X receptor heterodimer binding to DNA. *J. Biol. Chem.* **272**(32):20108-17.
- Imai, E., Stromstedt, P. E., Quinn, P. G., Carlstedt-Duke, J., Gustafsson, J. Å., and Granner, D. K. (1990) Characterization of a complex glucocorticoid response unit in the phosphoenolpyruvate carboxykinase gene. *Mol. Cell. Biol.* **10**(9):4712-9.
- Imai, E., Miner, J. N., Mitchell, J. A., Yamamoto, K. R., and Granner, D. K. (1993) Glucocorticoid receptor-cAMP response element-binding protein interaction and the response of the phosphoenolpyruvate carboxykinase gene to glucocorticoids. *J. Biol. Chem.* **268**(8):5353-6.
- Innis, M. A., Gelfand, D. H., Sninsky, J. J., and White, T. J., eds. (1990) PCR Protocols: A Guide to Methods and Applications (San Diego, CA: Academic Press, Inc.).
- Issemann, I., and Green, S. (1990) Activation of a member of the steroid hormone receptor superfamily by peroxisome proliferators. *Nature* **347**(6294):645-50.
- Issemann, I., Prince, R., Tugwood, J., and Green, S. (1992) A role for fatty acids and liver fatty acid binding protein in peroxisome proliferation? *Biochem. Soc. Trans.* **20**(4):824-7.
- Jedlitschky, G., Huber, M., Volkl, A., Muller, M., Leier, I., Muller, J., Lehmann, W. D., Fahimi, H. D., and Keppler, D. (1991) Peroxisomal degradation of leukotrienes by  $\beta$ -oxidation from the  $\omega$ -end. *J. Biol. Chem.* **266**(36):24763-72.
- Jiang, C., Ting, A. T., and Seed, B. (1998) PPAR- $\gamma$  agonists inhibit production of monocyte inflammatory cytokines. *Nature* **391**(6662):82-6.



Johansson, M., and Karlsson, A. (1997) Cloning of the cDNA and chromosome localization of the gene for human thymidine kinase 2. *J. Biol. Chem.* **272**(13):8454-8.

Jones, D. H., and Winistorfer, S. C. (1992) Sequence specific generation of a DNA panhandle permits PCR amplification of unknown flanking DNA. *Nucleic Acids Res.* **20**(3):595-600.

Jones, P. S., Savory, R., Barratt, P., Bell, A. R., Gray, T. J., Jenkins, N. A., Gilbert, D. J., Copeland, N. G., and Bell, D. R. (1995) Chromosomal localisation, inducibility, tissue-specific expression and strain differences in three murine peroxisome-proliferator-activated-receptor genes. *Eur. J. Biochem.* **233**(1):219-26.

Jones, D. H., and Winistorfer, S. C. (1997) Amplification of 4-9-kb human genomic DNA flanking a known site using a panhandle PCR variant. *Biotechniques* **23**(1):132-8.

Jow, L., and Mukherjee, R. (1995) The human peroxisome proliferator-activated receptor (PPAR) subtype NUC1 represses the activation of hPPAR $\alpha$  and thyroid hormone receptors. *J. Biol. Chem.* **270**(8):3836-40.

Juge-Aubry, C. E., Gorla-Bajszczak, A., Pemin, A., Lemberger, T., Wahli, W., Burger, A. G., and Meier, C. A. (1995) Peroxisome proliferator-activated receptor mediates cross-talk with thyroid hormone receptor by competition for retinoid X receptor. *J. Biol. Chem.* **270**(30):18117-22.

Juge-Aubry, C., Pemin, A., Favez, T., Burger, A. G., Wahli, W., Meier, C. A., and Desvergne, B. (1997) DNA binding properties of peroxisome proliferator-activated receptor subtypes on various natural peroxisome proliferator response elements. *J. Biol. Chem.* **272**(40):25252-9.

Kaikaus, R. M., Chan, W. K., Lysenko, N., Ray, R., Ortiz de Montellano, P. R., and Bass, N. M. (1993) Induction of peroxisomal fatty acid  $\beta$ -oxidation and liver fatty acid-binding protein by peroxisome proliferators. *J. Biol. Chem.* **268**(13):9593-603.

Kallen, C. B., and Lazar, M. A. (1996) Antidiabetic thiazolidinediones inhibit leptin (*ob*) gene expression in 3T3-L1 adipocytes. *Proc. Natl. Acad. Sci. USA* **93**(12):5793-6.

Karpichev, I. V., Luo, Y., Marians, R. C., and Small, G. M. (1997) A complex containing two transcription factors regulates peroxisome proliferation and the coordinate induction of  $\beta$ -oxidation enzymes in *Saccharomyces cerevisiae*. *Mol. Cell. Biol.* **17**(1):69-80.

Keller, E. B., and Noon, W. A. (1984) Intron splicing: a conserved internal signal in introns of animal pre- mRNAs. *Proc. Natl. Acad. Sci. USA* **81**(23):7417-20.

Keller, H., Givel, F., Perroud, M., and Wahli, W. (1995) Signaling cross-talk between peroxisome proliferator-activated receptor/retinoid X receptor and estrogen receptor through estrogen response elements. *Mol. Endocrinol.* **9**(7):794-804.

Kim, J. B., and Spiegelman, B. M. (1996) ADD1/SREBP1 promotes adipocyte differentiation and gene expression linked to fatty acid metabolism. *Genes Dev.* **10**(9):1096-107.

Kim, J. B., Wright, H. M., Wright, M., and Spiegelman, B. M. (1998) ADD1/SREBP1 activates PPAR $\gamma$  through the production of endogenous ligand. *Proc. Natl. Acad. Sci. USA* 95(8):4333-7.

Kliwer, S. A., Umesono, K., Noonan, D. J., Heyman, R. A., and Evans, R. M. (1992) Convergence of 9-*cis* retinoic acid and peroxisome proliferator signalling pathways through heterodimer formation of their receptors. *Nature* 358(6389):771-4.

Kliwer, S. A., Forman, B. M., Blumberg, B., Ong, E. S., Borgmeyer, U., Mangelsdorf, D. J., Umesono, K., and Evans, R. M. (1994) Differential expression and activation of a family of murine peroxisome proliferator-activated receptors. *Proc. Natl. Acad. Sci. USA* 91(15):7355-9.

Kliwer, S. A., Lenhard, J. M., Willson, T. M., Patel, I., Morris, D. C., and Lehmann, J. M. (1995) A prostaglandin J<sub>2</sub> metabolite binds peroxisome proliferator-activated receptor  $\gamma$  and promotes adipocyte differentiation. *Cell* 83(5):813-9.

Kliwer, S. A., Sundseth, S. S., Jones, S. A., Brown, P. J., Wisely, G. B., Koble, C. S., Devchand, P., Wahli, W., Willson, T. M., Lenhard, J. M., and Lehmann, J. M. (1997) Fatty acids and eicosanoids regulate gene expression through direct interactions with peroxisome proliferator-activated receptors  $\alpha$  and  $\gamma$ . *Proc. Natl. Acad. Sci. USA* 94(9):4318-23.

Kobayashi, M., Iwanishi, M., Egawa, K., and Shigeta, Y. (1992) Pioglitazone increases insulin sensitivity by activating insulin receptor kinase. *Diabetes* 41(4):476-83.

Krey, G., Braissant, O., L'Horsset, F., Kalkhoven, E., Perroud, M., Parker, M. G., and Wahli, W. (1997) Fatty acids, eicosanoids, and hypolipidemic agents identified as ligands of peroxisome proliferator-activated receptors by coactivator-dependent receptor ligand assay. *Mol. Endocrinol.* 11(6):779-91.

Krisans, S. K., Thompson, S. L., Pena, L. A., Kok, E., and Javitt, N. B. (1985) Bile acid synthesis in rat liver peroxisomes: metabolism of 26-hydroxycholesterol to 3- $\beta$ -hydroxy-5-cholenoic acid. *J. Lipid Res.* 26(11):1324-32.

Krisans, S. K. (1992) The role of peroxisomes in cholesterol metabolism. *Am. J. Respir. Cell Mol. Biol.* 7(4):358-64.

Kruszynska, Y. T., Mukherjee, R., Jow, L., Dana, S., Paterniti, J. R., and Olefsky, J. M. (1998) Skeletal muscle peroxisome proliferator-activated receptor- $\gamma$  expression in obesity and non-insulin-dependent diabetes mellitus. *J. Clin. Invest.* 101(3):543-8.

Laemmli, U. K. (1970) Cleavage of structural proteins during the assembly of the head of bacteriophage T4. *Nature* 227(259):680-5.

Lambe, K. G., and Tugwood, J. D. (1996) A human peroxisome-proliferator-activated receptor- $\gamma$  is activated by inducers of adipogenesis, including thiazolidinedione drugs. *Eur. J. Biochem.* 239(1):1-7.

Laudet, V., Hanni, C., Coll, J., Catzeflis, F., and Stehelin, D. (1992) Evolution of the

nuclear receptor gene superfamily. *EMBO J.* 11(3):1003-13.

Laudet, V. (1997) Evolution of the nuclear receptor superfamily: early diversification from an ancestral orphan receptor. *J. Mol. Endocrinol.* 19(3):207-26.

Lazarow, P. B., and De Duve, C. (1976) A fatty acyl-CoA oxidizing system in rat liver peroxisomes; enhancement by clofibrate, a hypolipidemic drug. *Proc. Natl. Acad. Sci. USA* 73(6):2043-6.

Lazarow, P. B. (1977) Three hypolipidemic drugs increase hepatic palmitoyl-coenzyme A oxidation in the rat. *Science* 197(4303):580-1.

Lazarow, P. B., Fujiki, Y., Mortensen, R., and Hashimoto, T. (1982) Identification of  $\beta$ -oxidation enzymes among peroxisomal polypeptides. *FEBS Lett.* 150(2):307-10.

Lazarow, P. B., and Fujiki, Y. (1985) Biogenesis of peroxisomes. *Annu. Rev. Cell Biol.* 1:489-530.

Lee, S. S., Pineau, T., Drago, J., Lee, E. J., Owens, J. W., Kroetz, D. L., Fernandez-Salguero, P. M., Westphal, H., and Gonzalez, F. J. (1995) Targeted disruption of the  $\alpha$  isoform of the peroxisome proliferator-activated receptor gene in mice results in abolishment of the pleiotropic effects of peroxisome proliferators. *Mol. Cell. Biol.* 15(6):3012-22.

Lehmann, J. M., Moore, L. B., Smith-Oliver, T. A., Wilkison, W. O., Willson, T. M., and Kliewer, S. A. (1995) An antidiabetic thiazolidinedione is a high affinity ligand for peroxisome proliferator-activated receptor  $\gamma$  (PPAR $\gamma$ ). *J. Biol. Chem.* 270(22):12953-6.

Lehmann, J. M., Lenhard, J. M., Oliver, B. B., Ringold, G. M., and Kliewer, S. A. (1997a) Peroxisome proliferator-activated receptors  $\alpha$  and  $\gamma$  are activated by indomethacin and other non-steroidal anti-inflammatory drugs. *J. Biol. Chem.* 272(6):3406-10.

Lehmann, J. M., Kliewer, S. A., Moore, L. B., Smith-Oliver, T. A., Oliver, B. B., Su, J. L., Sundseth, S. S., Winegar, D. A., Blanchard, D. E., Spencer, T. A., and Willson, T. M. (1997b) Activation of the nuclear receptor LXR by oxysterols defines a new hormone response pathway. *J. Biol. Chem.* 272(6):3137-40.

Lemberger, T., Staels, B., Saladin, R., Desvergne, B., Auwerx, J., and Wahli, W. (1994) Regulation of the peroxisome proliferator-activated receptor  $\alpha$  gene by glucocorticoids. *J. Biol. Chem.* 269(40):24527-30.

Lemberger, T., Desvergne, B., and Wahli, W. (1996) Peroxisome proliferator-activated receptors: a nuclear receptor signaling pathway in lipid physiology. *Annu. Rev. Cell Dev. Biol.* 12:335-63.

Lin, F. T., and Lane, M. D. (1992) Antisense CCAAT/enhancer-binding protein RNA suppresses coordinate gene expression and triglyceride accumulation during differentiation of 3T3-L1 preadipocytes. *Genes Dev.* 6(4):533-44.

Lin, F. T., MacDougald, O. A., Diehl, A. M., and Lane, M. D. (1993) A 30-kDa alternative

translation product of the CCAAT/enhancer binding protein  $\alpha$  message: transcriptional activator lacking antimitotic activity. *Proc. Natl. Acad. Sci. USA* **90**(20):9606-10.

Lin, F. T., and Lane, M. D. (1994) CCAAT/enhancer binding protein  $\alpha$  is sufficient to initiate the 3T3-L1 adipocyte differentiation program. *Proc. Natl. Acad. Sci. USA* **91**(19):8757-61.

Lock, E. A., Mitchell, A. M., and Elcombe, C. R. (1989) Biochemical mechanisms of induction of hepatic peroxisome proliferation. *Annu. Rev. Pharmacol. Toxicol.* **29**:145-63.

Maas, S., Melcher, T., and Seeburg, P. H. (1997) Mammalian RNA-dependent deaminases and edited mRNAs. *Curr. Opin. Cell Biol.* **9**(3):343-9.

MacDougald, O. A., and Lane, M. D. (1995) Transcriptional regulation of gene expression during adipocyte differentiation. *Annu. Rev. Biochem.* **64**:345-73.

Mangelsdorf, D. J., and Evans, R. M. (1995) The RXR heterodimers and orphan receptors. *Cell* **83**(6):841-50.

Maniatis, T., Fritsch, E. F., and Sambrook, J., eds. (1989) *Molecular Cloning: A Laboratory Manual* (Cold Spring Harbor, NY: Cold Spring Harbor Laboratory).

Mannaerts, G. P., and Debeer, L. J. (1982) Mitochondrial and peroxisomal  $\beta$ -oxidation of fatty acids in rat liver. *Ann. N.Y. Acad. Sci.* **386**:30-9.

Mannaerts, G. P., and van Veldhoven, P. P. (1996) Functions and organization of peroxisomal  $\beta$ -oxidation. *Ann. N.Y. Acad. Sci.* **804**:99-115.

Maquat, L. E. (1995) When cells stop making sense: effects of nonsense codons on RNA metabolism in vertebrate cells. *RNA* **1**(5):453-65.

Maquat, L. E. (1996) Defects in RNA splicing and the consequence of shortened translational reading frames. *Am. J. Hum. Genet.* **59**(2):279-86.

Marcus, S. L., Miyata, K. S., Zhang, B., Subramani, S., Rachubinski, R. A., and Capone, J. P. (1993) Diverse peroxisome proliferator-activated receptors bind to the peroxisome proliferator-responsive elements of the rat hydratase/dehydrogenase and fatty acyl-CoA oxidase genes but differentially induce expression. *Proc. Natl. Acad. Sci. USA* **90**(12):5723-7.

Marcus, S. L., Capone, J. P., and Rachubinski, R. A. (1996) Identification of COUP-TFII as a peroxisome proliferator response element binding factor using genetic selection in yeast: COUP-TFII activates transcription in yeast but antagonizes PPAR signaling in mammalian cells. *Mol. Cell. Endocrinol.* **120**(1):31-9.

Meier-Heusler, S. C., Zhu, X., Juge-Aubry, C., Pernin, A., Burger, A. G., Cheng, S. Y., and Meier, C. A. (1995) Modulation of thyroid hormone action by mutant thyroid hormone receptors, c-erbA  $\alpha 2$  and peroxisome proliferator-activated receptor: evidence for different mechanisms of inhibition. *Mol. Cell. Endocrinol.* **107**(1):55-66.

Miyamoto, T., Kaneko, A., Kakizawa, T., Yajima, H., Kamijo, K., Sekine, R., Hiramatsu, K., Nishii, Y., Hashimoto, T., and Hashizume, K. (1997) Inhibition of peroxisome proliferator signaling pathways by thyroid hormone receptor. *J. Biol. Chem.* **272**(12):7752-8.

Miyata, K. S., Zhang, B., Marcus, S. L., Capone, J. P., and Rachubinski, R. A. (1993) Chicken ovalbumin upstream promoter transcription factor (COUP-TF) binds to a peroxisome proliferator-responsive element and antagonizes peroxisome proliferator-mediated signaling. *J. Biol. Chem.* **268**(26):19169-72.

Miyata, K. S., McCaw, S. E., Marcus, S. L., Rachubinski, R. A., and Capone, J. P. (1994) The peroxisome proliferator-activated receptor interacts with the retinoid X receptor *in vivo*. *Gene* **148**(2):327-30.

Miyata, K. S., McCaw, S. E., Patel, H. V., Rachubinski, R. A., and Capone, J. P. (1996) The orphan nuclear hormone receptor LXR $\alpha$  interacts with the peroxisome proliferator-activated receptor and inhibits peroxisome proliferator signaling. *J. Biol. Chem.* **271**(16):9189-92.

Moller, D. E., and O'Rahilly, S. (1993) Syndromes of severe insulin resistance: clinical and pathophysiological features. *In* Insulin Resistance. D. E. Moller, ed. (New York, NY: John Wiley & Sons Ltd.) pp.49-81.

Moody, D. E., Reddy, J. K., Lake, B. G., Popp, J. A., and Reese, D. H. (1991) Peroxisome proliferation and nongenotoxic carcinogenesis: commentary on a symposium. *Fundam. Appl. Toxicol.* **16**(2):233-48.

Moser, H. W. (1993) Peroxisomal diseases. *Adv. Hum. Genet.* **21**:1-106.

Mueller, E., Sarraf, P., Tontonoz, P., Evans, R. M., Martin, K. J., Zhang, M., Fletcher, C., Singer, S., and Spiegelman, B. M. (1998) Terminal differentiation of human breast cancer through PPAR $\gamma$ . *Mol. Cell* **1**(3):465-70.

Muerhoff, A. S., Griffin, K. J., and Johnson, E. F. (1992) The peroxisome proliferator-activated receptor mediates the induction of CYP4A6, a cytochrome P450 fatty acid  $\omega$ -hydroxylase, by clofibrate. *J. Biol. Chem.* **267**(27):19051-3.

Mukherjee, R., Jow, L., Croston, G. E., and Paterniti, J. R., Jr. (1997) Identification, characterization, and tissue distribution of human peroxisome proliferator-activated receptor (PPAR) isoforms PPAR $\gamma$ 2 *versus* PPAR $\gamma$ 1 and activation with retinoid X receptor agonists and antagonists. *J. Biol. Chem.* **272**(12):8071-6.

Mullis, K. B., and Faloona, F. A. (1987) Specific synthesis of DNA *in vitro* via a polymerase-catalyzed chain reaction. *Methods Enzymol.* **155**:335-50.

Nagy, L., Tontonoz, P., Alvarez, J. G., Chen, H., and Evans, R. M. (1998) Oxidized LDL regulates macrophage gene expression through ligand activation of PPAR $\gamma$ . *Cell* **93**(2):229-40.

Nakajima-Iijima, S., Hamada, H., Reddy, P., and Kakunaga, T. (1985) Molecular

structure of the human cytoplasmic  $\beta$ -actin gene: interspecies homology of sequences in the introns. *Proc. Natl. Acad. Sci. USA* 82(18):6133-7.

Nakamuta, M., Oka, K., Krushkal, J., Kobayashi, K., Yamamoto, M., Li, W. H., and Chan, L. (1995) Alternative mRNA splicing and differential promoter utilization determine tissue-specific expression of the apolipoprotein B mRNA-editing protein (ApoBec1) gene in mice. *J. Biol. Chem.* 270(22):13042-56.

Nakshatri, H., and Bhat-Nakshatri, P. (1998) Multiple parameters determine the specificity of transcriptional response by nuclear receptors HNF-4, ARP-1, PPAR, RAR and RXR through common response elements. *Nucleic Acids Res.* 26(10):2491-9.

Niwa, M., and Berget, S. M. (1991) Polyadenylation precedes splicing *in vitro*. *Gene Expr.* 1(1):5-14.

Ochman, H., Gerber, A. S., and Hartl, D. L. (1988) Genetic applications of an inverse polymerase chain reaction. *Genetics* 120(3):621-3.

Oda, T., Funai, T., and Ichiyama, A. (1997) Induction by peroxisome proliferators and triiodothyronine of serine:pyruvate/alanine:glyoxylate aminotransferase of rat liver. *FEBS Lett.* 418(3):265-8.

Okazawa, H., Mori, H., Tamori, Y., Araki, S., Niki, T., Masugi, J., Kawanishi, M., Kubota, T., Shinoda, H., and Kasuga, M. (1997) No coding mutations are detected in the peroxisome proliferator-activated receptor- $\gamma$  gene in Japanese patients with lipotrophic diabetes. *Diabetes* 46(11):1904-6.

Okuno, A., Tamemoto, H., Tobe, K., Ueki, K., Mori, Y., Iwamoto, K., Umesono, K., Akanuma, Y., Fujiwara, T., Horikoshi, H., Yazaki, Y., and Kadowaki, T. (1998) Troglitazone increases the number of small adipocytes without the change of white adipose tissue mass in obese Zucker rats. *J. Clin. Invest.* 101(6):1354-61.

Osmundsen, H. (1982) Peroxisomal  $\beta$ -oxidation of long fatty acids: effects of high fat diets. *Ann. N.Y. Acad. Sci.* 386:13-29.

Osumi, T., and Hashimoto, T. (1984) The inducible fatty acid oxidation system in mammalian peroxisomes. *Trends Biochem. Sci.* 9(7):317-9.

Osumi, T., Yokota, S., and Hashimoto, T. (1990) Proliferation of peroxisomes and induction of peroxisomal  $\beta$ -oxidation enzymes in rat hepatoma H4IIEC3 by ciprofibrate. *J. Biochem.* 108(4):614-21.

Osumi, T., Wen, J. K., and Hashimoto, T. (1991) Two *cis*-acting regulatory sequences in the peroxisome proliferator-responsive enhancer region of rat acyl-CoA oxidase gene. *Biochem. Biophys. Res. Commun.* 175(3):866-71.

Padgett, R. A., Grabowski, P. J., Konarska, M. M., Seiler, S., and Sharp, P. A. (1986) Splicing of messenger RNA precursors. *Annu. Rev. Biochem.* 55:1119-50.

Palmer, C. N., Hsu, M. H., Griffin, H. J., and Johnson, E. F. (1995) Novel sequence

determinants in peroxisome proliferator signaling. *J. Biol. Chem.* **270**(27):16114-21.

Park, K. S., Ciaraldi, T. P., Abrams-Carter, L., Mudaliar, S., Nikoulina, S. E., and Henry, R. R. (1997) PPAR- $\gamma$  gene expression is elevated in skeletal muscle of obese and type II diabetic subjects. *Diabetes* **46**(7):1230-4.

Pedersen, J. I. (1993) Peroxisomal oxidation of the steroid side chain in bile acid formation. *Biochimie* **75**(3-4):159-65.

Pelleymounter, M. A., Cullen, M. J., Baker, M. B., Hecht, R., Winters, D., Boone, T., and Collins, F. (1995) Effects of the *obese* gene product on body weight regulation in *ob/ob* mice. *Science* **269**(5223):540-3.

Peters, J. M., Hennuyer, N., Staels, B., Fruchart, J. C., Fievet, C., Gonzalez, F. J., and Auwerx, J. (1997) Alterations in lipoprotein metabolism in peroxisome proliferator-activated receptor  $\alpha$ -deficient mice. *J. Biol. Chem.* **272**(43):27307-12.

Ponte, P., Ng, S. Y., Engel, J., Gunning, P., and Kedes, L. (1984) Evolutionary conservation in the untranslated regions of actin mRNAs: DNA sequence of a human  $\beta$ -actin cDNA. *Nucleic Acids Res.* **12**(3):1687-96.

Prins, J. B., and O'Rahilly, S. (1997) Regulation of adipose cell number in man. *Clin. Sci.* **92**(1):3-11.

Prins, J. B., Niesler, C. U., Winterford, C. M., Bright, N. A., Siddle, K., O'Rahilly, S., Walker, N. I., and Cameron, D. P. (1997) Tumor necrosis factor- $\alpha$  induces apoptosis of human adipose cells. *Diabetes* **46**(12):1939-44.

Rao, M. S., and Reddy, J. K. (1987) Peroxisome proliferation and hepatocarcinogenesis. *Carcinogenesis* **8**(5):631-6.

Reddy, J. K., Rao, S., and Moody, D. E. (1976) Hepatocellular carcinomas in acatalasemic mice treated with nafenopin, a hypolipidemic peroxisome proliferator. *Cancer Res.* **36**(4):1211-7.

Reddy, J. K., Azamoff, D. L., and Hignite, C. E. (1980) Hypolipidaemic hepatic peroxisome proliferators form a novel class of chemical carcinogens. *Nature* **283**(5745):397-8.

Reddy, J. K., and Lalwani, N. D. (1983) Carcinogenesis by hepatic peroxisome proliferators: evaluation of the risk of hypolipidemic drugs and industrial plasticizers to humans. *CRC Crit. Rev. Toxicol.* **12**:1-58.

Reddy, J. K., Lalwani, N. D., Qureshi, S. A., Reddy, M. K., and Moehle, C. M. (1984a) Induction of hepatic peroxisome proliferation in nonrodent species, including primates. *Am. J. Pathol.* **114**(1):171-83.

Reddy, J. K., Jirtle, R. L., Watanabe, T. K., Reddy, N. K., Michalopoulos, G., and Qureshi, S. A. (1984b) Response of hepatocytes transplanted into syngeneic hosts and heterotransplanted into athymic nude mice to peroxisome proliferators. *Cancer Res.*

44(6):2582-9.

Reddy, J. K., Goel, S. K., Nemali, M. R., Carrino, J. J., Laffler, T. G., Reddy, M. K., Sperbeck, S. J., Osumi, T., Hashimoto, T., Lalwani, N. D., and al., e. (1986) Transcription regulation of peroxisomal fatty acyl-CoA oxidase and enoyl-CoA hydratase/3-hydroxyacyl-CoA dehydrogenase in rat liver by peroxisome proliferators. *Proc. Natl. Acad. Sci. USA* 83(6):1747-51.

Reddy, J. K., and Mannaerts, G. P. (1994) Peroxisomal lipid metabolism. *Annu. Rev. Nutr.* 14:343-70.

Reddy, J. K., and Chu, R. (1996) Peroxisome proliferator-induced pleiotropic responses: pursuit of a phenomenon. *Ann. N.Y. Acad. Sci.* 804:176-201.

Reginato, M. J., Krakow, S. L., Bailey, S. T., and Lazar, M. A. (1998) Prostaglandins promote and block adipogenesis through opposing effects on peroxisome proliferator-activated receptor  $\gamma$ . *J. Biol. Chem.* 273(4):1855-8.

Reisenbichler, H., and Eckl, P. M. (1993) Genotoxic effects of selected peroxisome proliferators. *Mutat. Res.* 286(2):135-44.

Ricote, M., Li, A. C., Willson, T. M., Kelly, C. J., and Glass, C. K. (1998a) The peroxisome proliferator-activated receptor- $\gamma$  is a negative regulator of macrophage activation. *Nature* 391(6662):79-82.

Ricote, M., Huang, J., Fajas, L., Li, A., Welch, J., Najib, J., Witztum, J. L., Auwerx, J., Palinski, W., and Glass, C. K. (1998b) Expression of the peroxisome proliferator-activated receptor  $\gamma$  (PPAR $\gamma$ ) in human atherosclerosis and regulation in macrophages by colony stimulating factors and oxidized low density lipoprotein. *Proc. Natl. Acad. Sci. USA* 95(13):7614-9.

Riley, J., Butler, R., Ogilvie, D., Finniear, R., Jenner, D., Powell, S., Anand, R., Smith, J. C., and Markham, A. F. (1990) A novel, rapid method for the isolation of terminal sequences from yeast artificial chromosome (YAC) clones. *Nucleic Acids Res.* 18(10):2887-90.

Roberts, R. A., James, N. H., Woodyatt, N. J., Macdonald, N., and Tugwood, J. D. (1998) Evidence for the suppression of apoptosis by the peroxisome proliferator activated receptor  $\alpha$  (PPAR $\alpha$ ). *Carcinogenesis* 19(1):43-8.

Rosenthal, A., and Jones, D. S. (1990) Genomic walking and sequencing by oligo-cassette mediated polymerase chain reaction. *Nucleic Acids Res.* 18(10):3095-6.

Saiki, R. K., Scharf, S., Faloona, F., Mullis, K. B., Horn, G. T., Erlich, H. A., and Amheim, N. (1985) Enzymatic amplification of  $\beta$ -globin genomic sequences and restriction site analysis for diagnosis of sickle cell anemia. *Science* 230(4732):1350-4.

Sanger, F., Nicklen, S., and Coulson, A. R. (1977) DNA sequencing with chain-terminating inhibitors. *Proc. Natl. Acad. Sci. USA* 74(12):5463-7.



Schoonjans, K., Watanabe, M., Suzuki, H., Mahfoudi, A., Krey, G., Wahli, W., Grimaldi, P., Staels, B., Yamamoto, T., and Auwerx, J. (1995) Induction of the acyl-coenzyme A synthetase gene by fibrates and fatty acids is mediated by a peroxisome proliferator response element in the C promoter. *J. Biol. Chem.* **270**(33):19269-76.

Schoonjans, K., Peinado-Onsurbe, J., Lefebvre, A. M., Heyman, R. A., Briggs, M., Deeb, S., Staels, B., and Auwerx, J. (1996) PPAR $\alpha$  and PPAR $\gamma$  activators direct a distinct tissue-specific transcriptional response via a PPRE in the lipoprotein lipase gene. *EMBO J.* **15**(19):5336-48.

Scott, D. K., Mitchell, J. A., and Granner, D. K. (1996) The orphan receptor COUP-TF binds to a third glucocorticoid accessory factor element within the phosphoenolpyruvate carboxykinase gene promoter. *J. Biol. Chem.* **271**(50):31909-14.

Sears, I. B., MacGinnitie, M. A., Kovacs, L. G., and Graves, R. A. (1996) Differentiation-dependent expression of the brown adipocyte uncoupling protein gene: regulation by peroxisome proliferator-activated receptor  $\gamma$ . *Mol. Cell. Biol.* **16**(7):3410-9.

Seip, M., and Trygstad, O. (1996) Generalized lipodystrophy, congenital and acquired (lipoatrophy). *Acta Paediatr. Suppl.* **413**:2-28.

Shao, D., and Lazar, M. A. (1997) Peroxisome proliferator activated receptor  $\gamma$ , CCAAT/enhancer-binding protein  $\alpha$ , and cell cycle status regulate the commitment to adipocyte differentiation. *J. Biol. Chem.* **272**(34):21473-8.

Sharma, R. K., Lake, B. G., Makowski, R., Bradshaw, T., Earnshaw, D., Dale, J. W., and Gibson, G. G. (1989) Differential induction of peroxisomal and microsomal fatty acid-oxidizing enzymes by peroxisome proliferators in rat liver and kidney. *Eur. J. Biochem.* **184**(1):69-78.

Silver, K., Walston, J., Plotnick, L., Taylor, S. I., Kahn, C. R., and Shuldiner, A. R. (1997) Molecular scanning of  $\beta$ -3-adrenergic receptor gene in total congenital lipotrophic diabetes mellitus. *J. Clin. Endocrinol. Metab.* **82**(10):3395-8.

Skuse, G. R., Cappione, A. J., Sowden, M., Metheny, L. J., and Smith, H. C. (1996) The neurofibromatosis type I messenger RNA undergoes base-modification RNA editing. *Nucleic Acids Res.* **24**(3):478-85.

Smas, C. M., and Sul, H. S. (1995) Control of adipocyte differentiation. *Biochem. J.* **309**(Pt 3):697-710.

Spiegelman, B. M., and Hotamisligil, G. S. (1993) Through thick and thin: wasting, obesity, and TNF $\alpha$ . *Cell* **73**(4):625-7.

Spiegelman, B. M., and Flier, J. S. (1996) Adipogenesis and obesity: rounding out the big picture. *Cell* **87**(3):377-89.

Spiegelman, B. M. (1998) PPAR- $\gamma$ : adipogenic regulator and thiazolidinedione receptor. *Diabetes* **47**(4):507-14.

Steinberg, D., Parthasarathy, S., Carew, T. E., Khoo, J. C., and Witztum, J. L. (1989) Beyond cholesterol. Modifications of low-density lipoprotein that increase its atherogenicity. *N. Engl. J. Med.* **320**(14):915-24.

Stoltz, C., Vachon, M. H., Trottier, E., Dubois, S., Paquet, Y., and Anderson, A. (1998) The CYP2B2 phenobarbital response unit contains an accessory factor element and a putative glucocorticoid response element essential for conferring maximal phenobarbital responsiveness. *J. Biol. Chem.* **273**(14):8528-36.

Sundvold, H., Brzozowska, A., and Lien, S. (1997) Characterisation of bovine peroxisome proliferator-activated receptors  $\gamma 1$  and  $\gamma 2$ : genetic mapping and differential expression of the two isoforms. *Biochem. Biophys. Res. Commun.* **239**(3):857-61.

Tanaka, T., Yoshida, N., Kishimoto, T., and Akira, S. (1997) Defective adipocyte differentiation in mice lacking the C/EBP $\beta$  and/or C/EBP $\delta$  gene. *EMBO J.* **16**(24):7432-43.

Teboul, L., Gaillard, D., Staccini, L., Inadera, H., Amri, E. Z., and Grimaldi, P. A. (1995) Thiazolidinediones and fatty acids convert myogenic cells into adipose-like cells. *J. Biol. Chem.* **270**(47):28183-7.

Thompson, S. L., Burrows, R., Laub, R. J., and Krisans, S. K. (1987) Cholesterol synthesis in rat liver peroxisomes. *J. Biol. Chem.* **262**(36):17420-5.

Tokunaga, K., Taniguchi, H., Yoda, K., Shimizu, M., and Sakiyama, S. (1986) Nucleotide sequence of a full-length cDNA for mouse cytoskeletal  $\beta$ -actin mRNA. *Nucleic Acids Res.* **14**(6):2829.

Tolbert, N. E. (1981) Metabolic pathways in peroxisomes and glyoxysomes. *Annu. Rev. Biochem.* **50**:133-57.

Tontonoz, P., Kim, J. B., Graves, R. A., and Spiegelman, B. M. (1993) ADD1: a novel helix-loop-helix transcription factor associated with adipocyte determination and differentiation. *Mol. Cell. Biol.* **13**(8):4753-9.

Tontonoz, P., Hu, E., Graves, R. A., Budavari, A. I., and Spiegelman, B. M. (1994a) mPPAR $\gamma 2$ : tissue-specific regulator of an adipocyte enhancer. *Genes Dev.* **8**(10):1224-34.

Tontonoz, P., Graves, R. A., Budavari, A. I., Erdjument-Bromage, H., Lui, M., Hu, E., Tempst, P., and Spiegelman, B. M. (1994b) Adipocyte-specific transcription factor ARF6 is a heterodimeric complex of two nuclear hormone receptors, PPAR $\gamma$  and RXR $\alpha$ . *Nucleic Acids Res.* **22**(25):5628-34.

Tontonoz, P., Hu, E., and Spiegelman, B. M. (1994c) Stimulation of adipogenesis in fibroblasts by PPAR $\gamma 2$ , a lipid-activated transcription factor. *Cell* **79**(7):1147-56.

Tontonoz, P., Hu, E., Devine, J., Beale, E. G., and Spiegelman, B. M. (1995) PPAR $\gamma 2$  regulates adipose expression of the phosphoenolpyruvate carboxykinase gene. *Mol. Cell. Biol.* **15**(1):351-7.

Tontonoz, P., Singer, S., Forman, B. M., Sarraf, P., Fletcher, J. A., Fletcher, C. D., Brun, R. P., Mueller, E., Altok, S., Oppenheim, H., Evans, R. M., and Spiegelman, B. M. (1997) Terminal differentiation of human liposarcoma cells induced by ligands for peroxisome proliferator-activated receptor  $\gamma$  and the retinoid X receptor. *Proc. Natl. Acad. Sci. USA* **94**(1):237-41.

Tontonoz, P., Nagy, L., Alvarez, J. G., Thomazy, V. A., and Evans, R. M. (1998) PPAR $\gamma$  promotes monocyte/macrophage differentiation and uptake of oxidized LDL. *Cell* **93**(2):241-52.

Torchia, J., Glass, C., and Rosenfeld, M. G. (1998) Co-activators and co-repressors in the integration of transcriptional responses. *Curr. Opin. Cell Biol.* **10**(3):373-83.

Treisman, R., Orkin, S. H., and Maniatis, T. (1983) Specific transcription and RNA splicing defects in five cloned  $\beta$ -thalassaemia genes. *Nature* **302**(5909):591-6.

Tsai, M. J., and O'Malley, B. W. (1994) Molecular mechanisms of action of steroid/thyroid receptor superfamily members. *Annu. Rev. Biochem.* **63**:451-86.

Tsutsui, T., Watanabe, E., and Barrett, J. C. (1993) Ability of peroxisome proliferators to induce cell transformation, chromosome aberrations and peroxisome proliferation in cultured Syrian hamster embryo cells. *Carcinogenesis* **14**(4):611-8.

Tugwood, J. D., Issemann, I., Anderson, R. G., Bundell, K. R., McPheat, W. L., and Green, S. (1992) The mouse peroxisome proliferator activated receptor recognizes a response element in the 5' flanking sequence of the rat acyl CoA oxidase gene. *EMBO J.* **11**(2):433-9.

Tugwood, J. D., Aldridge, T. C., Lambe, K. G., Macdonald, N., and Woodyatt, N. J. (1996) Peroxisome proliferator-activated receptors: structures and function. *Ann. N.Y. Acad. Sci.* **804**:252-65.

Umesono, K., Murakami, K. K., Thompson, C. C., and Evans, R. M. (1991) Direct repeats as selective response elements for the thyroid hormone, retinoic acid, and vitamin D3 receptors. *Cell* **65**(7):1255-66.

van den Bosch, H., Schutgens, R. B., Wanders, R. J., and Tager, J. M. (1992) Biochemistry of peroxisomes. *Annu. Rev. Biochem.* **61**:157-97.

van der Klei, I. J., Harder, W., and Veenhuis, M. (1991) Biosynthesis and assembly of alcohol oxidase, a peroxisomal matrix protein in methylotrophic yeasts: a review. *Yeast* **7**(3):195-209.

van der Vorm, E. R., Kuipers, A., Bonenkamp, J. W., Kleijer, W. J., Van Maldergem, L., Herwig, J., and Maassen, J. A. (1993) Patients with lipodystrophic diabetes mellitus of the Seip-Berardinelli type, express normal insulin receptors. *Diabetologia* **36**(2):172-4.

Varanasi, U., Chu, R., Huang, Q., Castellon, R., Yeldandi, A. V., and Reddy, J. K. (1996) Identification of a peroxisome proliferator-responsive element upstream of the human peroxisomal fatty acyl coenzyme A oxidase gene. *J. Biol. Chem.* **271**(4):2147-55.

Vidal-Puig, A., Jimenez-Linan, M., Lowell, B. B., Hamann, A., Hu, E., Spiegelman, B., Flier, J. S., and Moller, D. E. (1996) Regulation of PPAR $\gamma$  gene expression by nutrition and obesity in rodents. *J. Clin. Invest.* 97(11):2553-61.

Vidal-Puig, A. J., Considine, R. V., Jimenez-Linan, M., Werman, A., Pories, W. J., Caro, J. F., and Flier, J. S. (1997) Peroxisome proliferator-activated receptor gene expression in human tissues. *J. Clin. Invest.* 99(10):2416-22.

Vigouroux, C., Khallouf, E., Bourut, C., Robert, J. J., de Kerdanet, M., Tubiana-Rufi, N., Fauré, S., Weissenbach, J., Capeau, J., and Magré, J. (1997) Genetic exclusion of 14 candidate genes in lipoatrophic diabetes using linkage analysis in 10 consanguineous families. *J. Clin. Endocrinol. Metab.* 82(10):3438-44.

Vigouroux, C., Fajas, L., Khallouf, E., Meier, M., Gyapay, G., Lascols, O., Auwerx, J., Weissenbach, J., Capeau, J., and Magré, J. (1998) Human peroxisome proliferator-activated receptor- $\gamma$ 2: genetic mapping, identification of a variant in the coding sequence, and exclusion as the gene responsible for lipoatrophic diabetes. *Diabetes* 47(3):490-2.

Voet, D., and Voet, J. G. (1995) Biochemistry, 2nd Edition. (New York, NY: John Wiley & Sons, Inc.) p.947.

Wanders, R. J., Denis, S., Wouters, F., Wirtz, K. W., and Seedorf, U. (1997) Sterol carrier protein X (SCPx) is a peroxisomal branched-chain  $\beta$ -ketothiolase specifically reacting with 3-oxo-pristanoyl-CoA: a new, unique role for SCPx in branched-chain fatty acid metabolism in peroxisomes. *Biochem. Biophys. Res. Commun.* 236(3):565-9.

Wang, N. D., Finegold, M. J., Bradley, A., Ou, C. N., Abdelsayed, S. V., Wilde, M. D., Taylor, L. R., Wilson, D. R., and Darlington, G. J. (1995) Impaired energy homeostasis in C/EBP $\alpha$  knockout mice. *Science* 269(5227):1108-12.

Warren, J. R., Simmon, V. F., and Reddy, J. K. (1980) Properties of hypolipidemic peroxisome proliferators in the lymphocyte [ $^3$ H]thymidine and Salmonella mutagenesis assays. *Cancer Res.* 40(1):36-41.

Winrow, C. J., Marcus, S. L., Miyata, K. S., Zhang, B., Capone, J. P., and Rachubinski, R. A. (1994) Transactivation of the peroxisome proliferator-activated receptor is differentially modulated by hepatocyte nuclear factor-4. *Gene Expr.* 4(1-2):53-62.

Winrow, C. J., Capone, J. P., and Rachubinski, R. A. (1998) Crosstalk between orphan nuclear hormone receptor RZR $\alpha$  and peroxisome proliferator-activated receptor  $\alpha$  in regulation of the peroxisomal hydratase-dehydrogenase gene. *J. Biol. Chem.* (submitted).

Wu, Z., Xie, Y., Bucher, N. L., and Farmer, S. R. (1995) Conditional ectopic expression of C/EBP $\beta$  in NIH-3T3 cells induces PPAR $\gamma$  and stimulates adipogenesis. *Genes Dev.* 9(19):2350-63.

Wu, Z., Bucher, N. L., and Farmer, S. R. (1996) Induction of peroxisome proliferator-

activated receptor  $\gamma$  during the conversion of 3T3 fibroblasts into adipocytes is mediated by C/EBP $\beta$ , C/EBP $\delta$ , and glucocorticoids. *Mol. Cell. Biol.* **16**(8):4128-36.

Wu, Z., Xie, Y., Morrison, R. F., Bucher, N. L., and Farmer, S. R. (1998) PPAR $\gamma$  induces the insulin-dependent glucose transporter GLUT4 in the absence of C/EBP $\alpha$  during the conversion of 3T3 fibroblasts into adipocytes. *J. Clin. Invest.* **101**(1):22-32.

Xing, G., Zhang, L., Heynen, T., Yoshikawa, T., Smith, M., Weiss, S., and Detera-Wadleigh, S. (1995) Rat PPAR $\delta$  contains a CGG triplet repeat and is prominently expressed in the thalamic nuclei. *Biochem. Biophys. Res. Commun.* **217**(3):1015-25.

Xing, H., Northrop, J. P., Grove, J. R., Kilpatrick, K. E., Su, J. L., and Ringold, G. M. (1997) TNF $\alpha$ -mediated inhibition and reversal of adipocyte differentiation is accompanied by suppressed expression of PPAR $\gamma$  without effects on Pref-1 expression. *Endocrinology* **138**(7):2776-83.

Yamanaka, S., Poksay, K. S., Balestra, M. E., Zeng, G. Q., and Innerarity, T. L. (1994) Cloning and mutagenesis of the rabbit ApoB mRNA editing protein. *J. Biol. Chem.* **269**(34):21725-34.

Yamanaka, S., Balestra, M. E., Ferrell, L. D., Fan, J., Arnold, K. S., Taylor, S., Taylor, J. M., and Innerarity, T. L. (1995) Apolipoprotein B mRNA-editing protein induces hepatocellular carcinoma and dysplasia in transgenic animals. *Proc. Natl. Acad. Sci. USA* **92**(18):8483-7.

Yamanaka, S., Poksay, K. S., Driscoll, D. M., and Innerarity, T. L. (1996) Hyperediting of multiple cytidines of apolipoprotein B mRNA by APOBEC-1 requires auxiliary protein(s) but not a mooring sequence motif. *J. Biol. Chem.* **271**(19):11506-10.

Yan, Z. H., Karam, W. G., Staudinger, J. L., Medvedev, A., Ghanayem, B. I., and Jetten, A. M. (1998) Regulation of peroxisome proliferator-activated receptor  $\alpha$ -induced transactivation by the nuclear orphan receptor TAK1/TR4. *J. Biol. Chem.* **273**(18):10948-57.

Yeh, W. C., Cao, Z., Classon, M., and McKnight, S. L. (1995) Cascade regulation of terminal adipocyte differentiation by three members of the C/EBP family of leucine zipper proteins. *Genes Dev.* **9**(2):168-81.

Yeldandi, A. V., Chu, R., Pan, J., Zhu, Y., and Usuda, N. (1996) Peroxisomal purine metabolism. *Ann. N.Y. Acad. Sci.* **804**:165-75.

Yokoyama, C., Wang, X., Briggs, M. R., Admon, A., Wu, J., Hua, X., Goldstein, J. L., and Brown, M. S. (1993) SREBP-1, a basic-helix-loop-helix-leucine zipper protein that controls transcription of the low density lipoprotein receptor gene. *Cell* **75**(1):187-97.

Yu, K., Bayona, W., Kallen, C. B., Harding, H. P., Ravera, C. P., McMahon, G., Brown, M., and Lazar, M. A. (1995) Differential activation of peroxisome proliferator-activated receptors by eicosanoids. *J. Biol. Chem.* **270**(41):23975-83.

Zhang, H., Scholl, R., Browse, J., and Somerville, C. (1988) Double stranded DNA

sequencing as a choice for DNA sequencing. *Nucleic Acids Res.* 16(3):1220.

Zhang, B., Marcus, S. L., Sajjadi, F. G., Alvares, K., Reddy, J. K., Subramani, S., Rachubinski, R. A., and Capone, J. P. (1992) Identification of a peroxisome proliferator-responsive element upstream of the gene encoding rat peroxisomal enoyl-CoA hydratase/3-hydroxyacyl-CoA dehydrogenase. *Proc. Natl. Acad. Sci. USA* 89(16):7541-5.

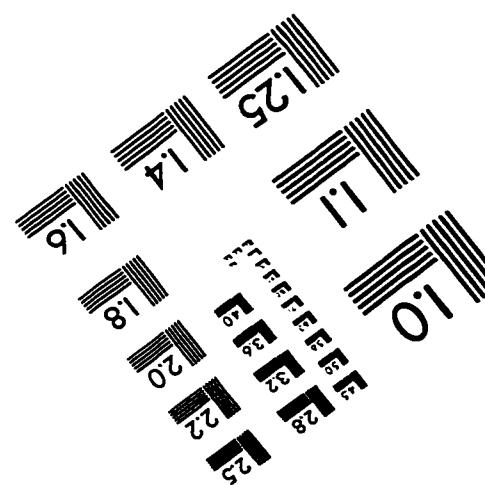
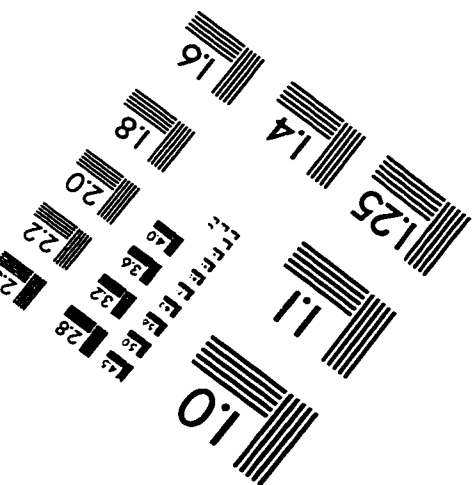
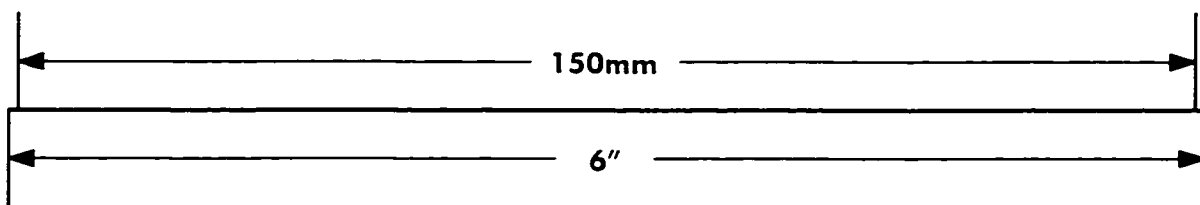
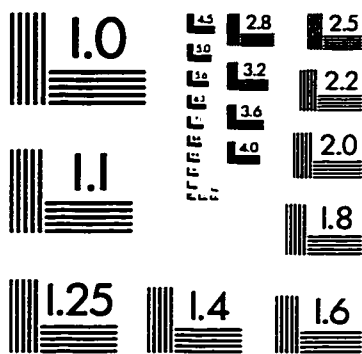
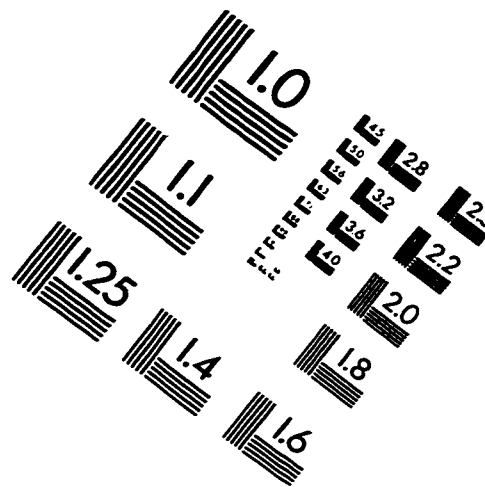
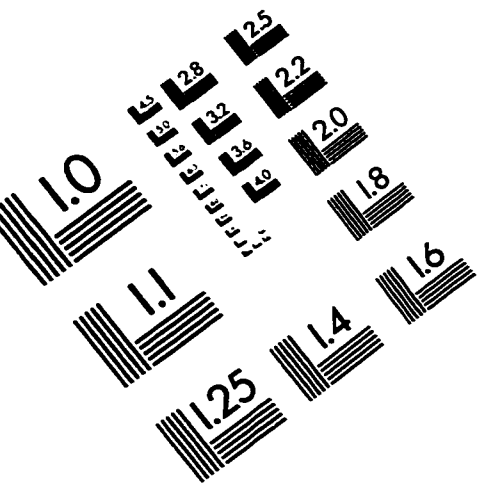
Zhang, B., Berger, J., Zhou, G., Elbrecht, A., Biswas, S., White-Carrington, S., Szalkowski, D., and Moller, D. E. (1996a) Insulin- and mitogen-activated protein kinase-mediated phosphorylation and activation of peroxisome proliferator-activated receptor  $\gamma$ . *J. Biol. Chem.* 271(50):31771-4.

Zhang, B., Berger, J., Hu, E., Szalkowski, D., White-Carrington, S., Spiegelman, B. M., and Moller, D. E. (1996b) Negative regulation of peroxisome proliferator-activated receptor- $\gamma$  gene expression contributes to the antiadipogenic effects of tumor necrosis factor- $\alpha$ . *Mol. Endocrinol.* 10(11):1457-66.

Zhu, Y., Alvares, K., Huang, Q., Rao, M. S., and Reddy, J. K. (1993) Cloning of a new member of the peroxisome proliferator-activated receptor gene family from mouse liver. *J. Biol. Chem.* 268(36):26817-20.

Zhu, Y., Qi, C., Korenberg, J. R., Chen, X. N., Noya, D., Rao, M. S., and Reddy, J. K. (1995) Structural organization of mouse peroxisome proliferator-activated receptor  $\gamma$  (mPPAR $\gamma$ ) gene: alternative promoter use and different splicing yield two mPPAR $\gamma$  isoforms. *Proc. Natl. Acad. Sci. USA* 92(17):7921-5.

# IMAGE EVALUATION TEST TARGET (QA-3)



APPLIED IMAGE, Inc.  
1653 East Main Street  
Rochester, NY 14609 USA  
Phone: 716/482-0300  
Fax: 716/288-5989

© 1993, Applied Image, Inc., All Rights Reserved